

DESIGN OF A POWERED LOWER-LIMB EXOSKELETON
AND CONTROL FOR GAIT ASSISTANCE IN PARAPLEGICS

By

RYAN JAMES FARRIS

Dissertation

Submitted to the Faculty of the
Graduate School of Vanderbilt University
in partial fulfillment of the requirements
for the degree of

DOCTOR OF PHILOSOPHY

in

Mechanical Engineering

May, 2012

Nashville, Tennessee

Approved:

Dr. Michael Goldfarb

Dr. Chris Byrne

Dr. Peter Konrad

Dr. Nilanjan Sarkar

Dr. Eric J. Barth

Dr. Robert J. Webster III

Copyright © 2012 by Ryan James Farris

All Rights Reserved

To my wife, Renee

ACKNOWLEDGEMENTS

I have been privileged to work and study under engineers of the highest caliber during my five years at Vanderbilt. I am grateful for and amazed by the consistently insightful vision with which my advisor, Dr. Michael Goldfarb, has directed our lab. His integrity and humility inspire me. My gratitude also extends to Hugo Quintero for his exceptional engineering, dedication, and camaraderie as we have labored together for the past three years on this common work. I am thankful to the rest of my colleagues at the Center for Intelligent Mechatronics, each of whom I have learned from during our time together. I would also like to express my appreciation to the members of my dissertation committee: Dr. Chris Byrne, Dr. Eric Barth, Dr. Nilanjan Sarkar, Dr. Robert Webster, and Dr. Peter Konrad, for their time and support. Thanks are also due to the National Institutes of Health, grant 1R01HD059832-01A1, for funding this work.

A special thanks goes to the Shepherd Center for providing clinical expertise and supervision during our subject testing. In particular, physical therapist Clare Hartigan and orthosis test subject Michael Gore showed exceptional effort and dedication as they worked with us to evaluate the performance of the Vanderbilt Exoskeleton. Clare's enthusiastic guidance and expertise and Michael's perseverance through the debugging process have been invaluable.

Preparation for this moment began before I ever entered the halls of Vanderbilt and for this I owe a debt of gratitude to Western Kentucky University, and specifically Dr. Chris Byrne. An inspiring teacher, an engineer for all occasions, and a good friend, Chris is a noble guiding light for more than just my career.

I thank my parents and sisters for their constant support and encouragement during my studies. My family taught me the most important principle of all: trust in God.

I give God thanks and praise for His goodness to me. He has provided me with abilities and opportunities and it is to Him that I give the credit for anything good that

He accomplishes through me.

Finally, I thank the one to whom I dedicate this dissertation, my wife, Renee. Her love, support, and patience is cherished more than she knows. I am especially grateful for the balance she has brought to my life during the demanding years of doctoral study. I look forward with excitement to the next adventure that we embark upon together.

TABLE OF CONTENTS

	Page
DEDICATION	iii
ACKNOWLEDGEMENTS	iv
LIST OF FIGURES	viii
LIST OF TABLES	x
CHAPTER I. Overview	1
INTRODUCTION AND MOTIVATION	1
LITERATURE SURVEY.....	1
SCOPE AND SUMMARY OF RESEARCH	3
ORGANIZATION OF THE DOCUMENT	4
REFERENCES	7
CHAPTER II. Manuscript 1: Preliminary Evaluation of a Powered Lower Limb Orthosis to Aid Walking in Paraplegic Individuals	10
ABSTRACT	11
INTRODUCTION	11
THE VANDERBILT POWERED ORTHOSIS	14
ORTHOSIS CONTROL	19
EXPERIMENTAL IMPLEMENTATION	20
DISCUSSION	25
CONCLUSION	26
REFERENCES	27
CHAPTER III. Manuscript 2: A Method for the Autonomous Control of a Lower Limb Exoskeleton for Persons with Paraplegia	30
ABSTRACT	31
INTRODUCTION	31
POWERED ORTHOSIS PROTOTYPE	33
POWERED ORTHOSIS CONTROL ARCHITECTURE	35
EXPERIMENTAL IMPLEMENTATION	42
CONCLUSION	47
REFERENCES	47

CHAPTER IV. Manuscript 3: A Preliminary Assessment of Mobility and Exertion in a Lower Limb Exoskeleton for Persons with Paraplegia	49
ABSTRACT	50
INTRODUCTION	50
A PROPOSED SET OF ASSESSMENT METRICS	51
COMPARATIVE ASSESSMENT OF TWO MOBILITY AIDS	55
RESULTS AND DISCUSSION	63
CONCLUSION	70
REFERENCES	71
CHAPTER V. Manuscript 4: Joint Torque and Power Requirements during Stair Ascent and Descent in a Lower Limb Exoskeleton for Persons with Paraplegia	74
ABSTRACT	75
INTRODUCTION	75
HARDWARE AND IMPLEMENTATION	77
DATA COLLECTION	81
RESULTS AND DISCUSSION	81
CONCLUSION	90
REFERENCES	91
ADDENDUM: CURBS AND SLOPES	93
ADDENDUM REFERENCES	101
CHAPTER VI. Conclusion	102

LIST OF FIGURES

Figure	Page
2-1. Vanderbilt gait restoration orthosis oblique view	15
2-2. Vanderbilt gait restoration orthosis frontal view	16
2-3. Embedded system framework.....	18
2-4. Embedded system circuit board	18
2-5. State-flow diagram	19
2-6. Subject wearing the powered orthosis.....	21
2-7. Measured joint angles during 23 right steps and 23 left steps	22
2-8. Overlaid joint angles for 23 gait cycles	23
2-9. Average measured electrical power at the knee and hip joints.....	24
3-1. Powered lower limb orthosis.....	34
3-2. Functional schematic of embedded system	34
3-3. Finite state machine for sitting, standing, and walking.....	36
3-4. Walking trajectories corresponding to finite states as indicated	37
3-5. Schematic of stride length and center of pressure.....	40
3-6. Schematic indicating use of center of pressure for sitting and standing	41
3-7. Photographic sequence showing standing, a left step, and a right step	44
3-8. Joint angles and controller state during the third TUG test	44
3-9. Data excerpted from Fig. 3-8: States, CoP, CoP threshold, and step length.....	45
3-10. Finite states corresponding to each of the three TUG tests.....	46
4-1. Vanderbilt lower limb exoskeleton	57
4-2. Long-leg braces used in assessments	59
4-3. T10 complete paraplegic subject wearing Vanderbilt exoskeleton	60
4-4. Subject wearing long-leg braces.....	61
4-5. Graph of TUG test completion times in each walking method	65
4-6. Graph of TMWT completion times in each walking method	66
4-7. Graph of user exertion during TUG test in each walking method	68
4-8. Graph of exertion during TMWT in each walking method	68
4-9. Graph of user-perceived exertion during standardized walking tests.....	69
5-1. Vanderbilt lower limb exoskeleton	78
5-2. Stair ascent sequence	80
5-3. Stair descent sequence.....	80
5-4. Joint angles averaged from 12 stair ascent movements	83
5-5. Body-mass-normalized joint torques averaged over 12 stair ascents.....	84
5-6. Body-mass-normalized power averaged over 12 stair ascents	85
5-7. Joint angles averaged from 12 stair descent movements	86
5-8. Body-mass-normalized joint torques averaged over 12 stair descents.....	87
5-9. Body-mass-normalized power averaged over 12 stair descents	88
5-10. Curb ascent sequence.....	94

5-11.	Curb descent sequence	94
5-12.	Setup for sloped TUG test.....	97
5-13.	Graph of sloped TUG test completion times in each walking method.....	99
5-14.	Graph of user exertion during sloped TUG test in each walking method	100
5-15.	Graph of user perceived exertion during sloped TUG test.....	100

LIST OF TABLES

Table	Page
2-1. Mass breakdown of Vanderbilt Orthosis	16
2-2. Vanderbilt Orthosis electrical power consumption.....	25
3-1. Joint controller characteristics within each state.....	38
3-2. Walking trajectories corresponding to finite states as indicated	41
4-1. Summary of assessment data.....	64
5-1. Summary of slope assessment data	99

CHAPTER I

Overview

Introduction and Motivation

There are currently about 262,000 spinal cord injured (SCI) individuals in the United States, with roughly 12,000 new injuries sustained each year at an average age of injury of 40.2 years [1]. Of these, at least 44% (at least 5300 cases per year) result in paraplegia. One of the most significant impairments resulting from paraplegia is the loss of mobility, particularly given the relatively young (average) age at which such injuries occur. Surveys of persons with paraplegia indicate that mobility concerns are among the most prevalent [2], and that chief among mobility desires is the ability to walk and stand [3]. In addition to impaired mobility, the inability to stand and walk entails severe physiological effects, including muscular atrophy, loss of bone mineral content, frequent skin breakdown problems, increased incidence of urinary tract infection, muscle spasticity, impaired lymphatic and vascular circulation, impaired digestive operation, and reduced respiratory and cardiovascular capacities [4].

Literature Survey

In an effort to restore some degree of legged mobility to individuals with paraplegia, several lower limb orthoses have been developed and described in the engineering literature. The following literature review focuses on orthoses that were developed specifically for restoration of mobility in paraplegic individuals. For recent surveys that consider passive and powered exoskeletons in a more general context, the reader is referred to [5-7]. Also, it should be noted that considerable research has been conducted on the use of functional electrical stimulation (FES) to restore legged mobility to paraplegics, although this topic is also not reviewed here. For a recent review of progress in FES-based gait restoration, the reader is referred to [8]. A number of passive

orthoses have been developed to restore legged mobility to paraplegics. The simplest form of passive orthotics are long-leg braces that incorporate a pair of ankle-foot orthoses (AFOs) to provide support at the ankles, which are rigidly coupled to leg braces that lock the knee joints against flexion. The hips are typically stabilized by the tension in the ligaments and musculature on the anterior aspect of the pelvis. Since almost all energy for movement is provided by the upper body, these (passive) orthoses require considerable upper body strength and a high level of physical exertion, and provide very slow walking speeds. A more sophisticated orthosis, the hip guidance orthosis (HGO), is described in [9-11]. The HGO incorporates hip joints that rigidly resist hip adduction and abduction, and rigid shoe plates that provide increased center of gravity elevation at toe-off, thus enabling a greater degree of forward progression per stride. Another variation on the long-leg orthosis, the reciprocating gait orthosis (RGO), incorporates a kinematic constraint that links hip flexion of one leg with hip extension of the other, typically by means of a push-pull cable assembly. As with other passive orthoses, the paraplegic individual leans forward against the stability aid, utilizing gravity to provide hip extension of the stance leg. Since motion of the hip joints is reciprocally coupled, the gravity-induced hip extension also provides contralateral hip flexion (of the swing leg), such that the stride length of gait is increased. Examples of this type of orthosis, and studies of its efficacy, are described in [12-19].

In order to decrease the high level of exertion associated with passive orthoses, some researchers have investigated the use of powered orthoses, which incorporate actuators to assist with locomotion. Historical efforts to develop powered orthoses to aid in paraplegic mobility include [20-22]. More recently, Ruthenberg [23] developed a powered orthosis for evaluating design requirements for paraplegic gait assistance. In [24-26], a powered orthosis was developed by combining three electric motors with an RGO, two of which were located at the knee joints to enabled knee flexion and extension during swing, and one of which assisted the hip coupling, which in essence assisted both stance hip extension and contralateral swing hip flexion. The orthosis was shown to increase gait speed and decrease compensatory motions, relative to walking without powered assistance. In [27-30], the authors describe control methods for providing

assistive maneuvers (sit-to-stand, stand-to-sit, and walking) to paraplegic individuals with the powered lower limb orthosis HAL, which is an emerging commercial device with (in the incarnation utilized in the aforementioned publications) six electric motors (i.e., powered sagittal plane hip, knee, and ankle joints). Like the powered lower limb orthosis HAL, two additional emerging commercial devices include the ReWalk powered orthosis (Argo Medical Technologies) and the eLEGS powered orthosis (Ekso Bionics). Both of these devices were developed specifically for use with paraplegic individuals, although (at this point) no studies have been published characterizing the performance of these devices, or discussing their efficacy.

Described herein is a powered lower limb orthosis that, like the aforementioned devices, is intended to provide gait assistance to paraplegics by providing assistive torques at both hip and knee joints. This document specifically discusses the mechanical, electrical, and control design of the orthosis, describes experimental implementation of the orthosis on a paraplegic subject (T10 complete), and presents data characterizing the ability of the device to provide various forms of mobility including sitting, standing, level ground walking, sloped walking, stair walking, and curb walking.

Scope and Summary of Research

This dissertation represents the first body of work published at Vanderbilt University in the area of powered exoskeletons. This document marks the transition from the author's previous work in passive orthoses to electrically powered devices. In the previous work described in [31, 32], the author designed a hybrid passive lower limb orthosis with mechanical joint coupling and controllable joint brakes to be used in conjunction with functional electrical stimulation of the leg muscles. The author's Master's thesis work was centered on the development of the custom high torque joint brakes [33]. Despite the promising results that were obtained in the development of the joint-coupled orthosis and custom joint brakes, recent advances in technology made the feasibility of fully powered orthosis clear. The researchers hypothesized that a powered orthosis could provide more benefit to the SCI population via increased mobility capabilities and a more flexible

potential user base (i.e., a wider range of injury levels would be able to be accommodated with a powered orthosis). Development of the orthosis included the mechanical design of the device, actuation assemblies, embedded electronics system, and control strategies. The control of the device has been developed as a finite-state combined trajectory/impedance control structure for gait and incorporates non-gait modes such as standing, sitting and the transitions between standing and sitting. Testing of the device was performed on a paraplegic subject (T10 complete), who demonstrated level-ground walking as well as the standing, sitting, sit-to-stand/stand-to-sit transition modes, as well as advanced mobility including slope walking, stair walking, and curb walking.

Organization of the Document

The dissertation is organized in six chapters. Chapter I presents the introduction and scope of the work. The chapters II, III, IV, and V are comprised of the manuscripts that encompass the body of the work completed specifically on the powered orthosis and have been submitted for publication as journal papers. Chapter VI concludes with a summary of the contributions described in this work. Overviews of the manuscripts presented in this document are as follows:

Manuscript 1: Preliminary Evaluation of a Powered Lower Limb Orthosis to Aid Walking in Paraplegic Individuals

Summary: This paper presents the design of the exoskeleton and initial results from testing with a paraplegic subject.

Abstract: This paper describes a powered lower-limb orthosis that is intended to provide gait assistance to spinal cord injured (SCI) individuals by providing assistive torques at both hip and knee joints. The orthosis has a mass of 12 kg and is capable of providing maximum joint torques of 40 Nm with hip and knee joint ranges of motion from 105° flexion to 30° extension and 105° flexion to 10° hyperextension, respectively. A custom distributed embedded system controls the orthosis with power being provided by a lithium polymer battery which provides power for one hour of

continuous walking. In order to demonstrate the ability of the orthosis to assist walking, the orthosis was experimentally implemented on a paraplegic subject with a T10 complete injury. Data collected during walking indicates a high degree of step-to-step repeatability of hip and knee trajectories (as enforced by the orthosis) and an average walking speed of 0.8 km/hr. The electrical power required at each hip and knee joint during gait was approximately 25 W and 27 W, respectively, contributing to the 117 W overall electrical power required by the device during walking. Manuscript 1 is based on the following paper:

R. J. Farris, H. A. Quintero, and M. Goldfarb, "*Preliminary Evaluation of a Powered Lower Limb Orthosis to Aid Walking in Paraplegic Individuals*," Accepted: *Neural Systems and Rehabilitation Engineering, IEEE Transactions on*, 19(6): 652-659, 2011.

Manuscript 2: *A Method for the Autonomous Control of a Lower Limb Exoskeleton for Persons with Paraplegia*

Summary: This paper describes the control methods used in the orthosis to allow a user to autonomously control the exoskeleton based only on his/her postural cues.

Abstract: Efforts have recently been reported by several research groups on the development of computer-controlled lower limb orthoses to enable legged locomotion in persons with paraplegia. Such systems must employ a control framework that provides essential movements to the paraplegic user (i.e., sitting, standing, and walking), and ideally enable the user to autonomously command these various movements in a safe, reliable, and intuitive manner. This paper describes a control method that enables a paraplegic user to perform sitting, standing, and walking movements, which are commanded based on postural information measured by the device. The proposed user interface and control structure was implemented on a powered lower limb orthosis, and the system was tested on a paraplegic subject with a T10 complete injury. Experimental data is presented that indicates the ability of the proposed control architecture to provide appropriate user-initiated control of sitting, standing, and walking. The authors also provide a link to a video that qualitatively demonstrates the user's ability to independently control basic movements via the

proposed control method. Manuscript 2 is based on the following paper:

H. A. Quintero, R. J. Farris, and M. Goldfarb, “*A Method for the Autonomous Control of a Lower Limb Exoskeleton for Persons with Paraplegia*” Submitted to: *Journal of Medical Devices, ASME*, 2011.

Manuscript 3: A Preliminary Assessment of Mobility and Exertion in a Lower Limb Exoskeleton for Persons with Paraplegia

Summary: This paper proposes a set of assessment metrics to standardize performance evaluations of emerging powered mobility-assist devices such that their efficacies may be compared; the assessment is performed on a paraplegic individual and results are presented.

Abstract: This paper describes a functional assessment of a powered lower limb exoskeleton designed to provide gait assistance to persons with paraplegia. The authors propose an assessment protocol for assessing the mobility and exertion associated with systems that provide legged mobility assistance for persons with SCI. The mobility aspect of the assessment protocol is based on two well-established assessment tools in the clinical community, which are the timed-up-and-go test and the ten meter walk test. The exertion aspect of the assessment is based on the change in heart rate entailed in the two standard tests, in addition to the Borg rating of perceived exertion. The proposed assessment protocol was implemented on a single SCI subject, and the mobility and exertion associated with four cases of mobility and stability aids was assessed. The results indicate that the powered exoskeleton affords similar mobility and requires a somewhat lower level of exertion relative to long-leg braces with a swing-through gait, and affords significantly improved mobility with significantly less exertion relative to long-leg braces with a reciprocal gait. Manuscript 3 is based on the following paper:

R. J. Farris, H. A. Quintero, C. Hartigan, and M. Goldfarb, “*A Preliminary Assessment of Mobility and Exertion in a Lower Limb Exoskeleton for Persons with Paraplegia*,” Submitted to: *Neural Systems and Rehabilitation Engineering, IEEE Transactions on*, November, 2011.

Manuscript 4: *Joint Torque and Power Requirements during Stair Ascent and Descent in a Lower Limb Exoskeleton for Persons with Paraplegia.*

Summary: This paper explores the use of the Vanderbilt Exoskeleton for enabling persons with paraplegia to ascend and descend stairs and presents the joint torque and power demands as experimental results.

Abstract: This paper presents experimental data characterizing the joint torque and power required to provide stair ascent and descent functionality to a person with paraplegia. The authors briefly describe stair ascent and descent functionality in a powered lower limb exoskeleton, and present hip and knee joint angles resulting from (multiple trials of) stair ascent and descent maneuvers, in addition to the hip and knee joint torque and power required to perform this functionality. Joint torque and power requirements are summarized, including peak hip and knee joint torque requirements of 0.75 Nm/kg and 0.87 Nm/kg, respectively, and peak hip and knee joint power requirements of approximately 0.65 W/kg and 0.85 W/kg, respectively. Manuscript 4 is based on the following paper:

R. J. Farris, H. A. Quintero, and M. Goldfarb, "*Joint Torque and Power Requirements during Stair Ascent and Descent in a Lower Limb Exoskeleton for Persons with Paraplegia*" Submitted to: *Journal of Medical Devices, ASME, February, 2012.*

References

- [1] (2011). *Spinal Cord Injury Facts and Figures at a Glance*. Available: <https://www.nscisc.uab.edu>
- [2] R. W. Hanson and M. R. Franklin, "Sexual loss in relation to other functional losses for spinal cord injured males," *Archives of Physical Medicine and Rehabilitation*, vol. 57, pp. 291-293, 1976.
- [3] D. L. Brown-Triolo, M. J. Roach, K. Nelson, and R. J. Triolo, "Consumer perspectives on mobility: implications for neuroprosthesis design," presented at the Journal of Rehabilitation Research and Development, 2002.
- [4] L. Phillips, M. Ozer, P. Axelson, and J. Fonseca, *Spinal cord injury: A guide for patient and family*: Raven Press, 1987.
- [5] A. M. Dollar and H. Herr, "Lower Extremity Exoskeletons and Active Orthoses: Challenges and State-of-the-Art," *Robotics, IEEE Transactions on*, vol. 24, pp. 144-158, 2008.

- [6] H. Herr, "Exoskeletons and orthoses: classification, design challenges and future directions," *Journal of NeuroEngineering and Rehabilitation*, vol. 6, p. 21, 2009.
- [7] R. Bogue, "Exoskeletons and robotic prosthetics: a review of recent developments," *Industrial Robot: An International Journal*, vol. 36, pp. 421-427, 2009.
- [8] K. T. Ragnarsson, "Functional electrical stimulation after spinal cord injury: current use, therapeutic effects and future directions," *Spinal Cord*, vol. 46, pp. 255-274, April 2008.
- [9] P. B. Butler, R. E. Major, and J. H. Patrick, "The technique of reciprocal walking using the hip guidance orthosis (hgo) with crutches," *Prosthetics and Orthotics International*, vol. 8, pp. 33-38, 1984.
- [10] R. E. Major, J. Stallard, and G. K. Rose, "The dynamics of walking using the hip guidance orthosis (hgo) with crutches," *Prosthetics and Orthotics International*, vol. 5, pp. 19-22, 1981.
- [11] G. K. Rose, "The principles and practice of hip guidance articulations," *Prosthetics and Orthotics International*, vol. 3, pp. 37-43, 1979.
- [12] G. Baardman, M. J. Ijzerman, H. J. Hermen, P. H. Veltink, H. B. K. Boom, and G. Zilvold, "The influence of the reciprocal hip joint link in the Advanced Reciprocating Gait Orthosis on standing performance in paraplegia," *Prosthetics and Orthotics International*, vol. 21, pp. 210-221, 1997.
- [13] J. Beillot, F. Carré, G. Le Claire, P. Thoumie, B. Perruoin-Verbe, A. Cormerais, A. Courtillon, E. Tanguy, G. Nadeau, P. Rochcongar, and J. Dassonville, "Energy consumption of paraplegic locomotion using reciprocating gait orthosis," *European Journal of Applied Physiology and Occupational Physiology*, vol. 73, pp. 376-381, 1996.
- [14] M. Bernardi, I. Canale, L. D. F. Castellano, F. Felici, and M. Marchetti, "The efficiency of walking of paraplegic patients using a reciprocating gait orthosis.," *Paraplegia*, vol. 33, pp. 409-415, 1995.
- [15] L. A. Harvey, G. M. Davis, M. B. Smith, and S. Engel, "Energy expenditure during gait using the walkabout and isocentric reciprocal gait orthoses in persons with paraplegia," *Archives of Physical Medicine and Rehabilitation*, vol. 79, pp. 945-949, 1999.
- [16] L. A. Harvey, T. Newton-John, G. M. Davis, M. B. Smith, and S. Engel, "A comparison of the attitude of paraplegic individuals to the walkabout orthosis and the isocentric reciprocal gait orthosis," *Spinal Cord*, vol. 35, pp. 580-584, 1997.
- [17] M. J. Ijzerman, G. Baardman, H. J. Hermens, P. H. Veltink, H. B. K. Boom, and G. Zilvold, "The influence of the reciprocal cable linkage in the advanced reciprocating gait orthosis on paraplegic gait performance," *Prosthetics and Orthotics International*, vol. 21, pp. 52-61, 1997.
- [18] C. Scivoletto, M. I. Mancini, B. Fiorelli, B. Morganti, and M. Molinari, "A prototype of an adjustable advanced reciprocating gait orthosis (ARGO) for spinal cord injury (SCI)," *Spinal Cord*, vol. 41, pp. 187-191, 2003.
- [19] S. Tashman, F. E. Zajac, and I. Perakash, "Modeling and Simulation of Paraplegic Ambulation in a Reciprocating Gait Orthosis," *Journal of Biomechanical Engineering*, vol. 117, pp. 300-308, 1995.

- [20] J. E. Beard, J. C. Conwell, D. S. Rogers, and H. Lamousin, "Design of a powered orthotic device to aid individuals with a loss of bipedal locomotion," in *Second National Applied Mechanisms and Robotics*, 1991.
- [21] M. Townsend and R. Lepofsky, "Powered walking machine prosthesis for paraplegics," *Medical and Biological Engineering and Computing*, vol. 14, pp. 436-444, 1976.
- [22] M. Vukobratovic, D. Hristic, and Z. Stojiljkovic, "Development of active anthropomorphic exoskeletons," *Medical and Biological Engineering and Computing*, vol. 12, pp. 66-80, 1974.
- [23] B. J. Ruthenberg, N. A. Wasylewski, and J. E. Beard, "An experimental device for investigating the force and power requirements of a powered gait orthosis," *Journal of Rehabilitation Research and Development*, vol. 34, pp. 203-213, 1997.
- [24] N. Kawashima, Y. Sone, K. Nakazawa, M. Akai, and H. Yano, "Energy expenditure during walking with weight-bearing control (WBC) orthosis in thoracic level of paraplegic patients," *Spinal Cord*, vol. 41, pp. 506-510, 2003.
- [25] Y. Ohta, H. Yano, R. Suzuki, M. Yoshida, N. Kawashima, and K. Nakazawa, "A two-degree-of-freedom motor-powered gait orthosis for spinal cord injury patients," *Proceedings of the Institution of Mechanical Engineers, Part H: Journal of Engineering in Medicine*, vol. 221, pp. 629-639, 2007.
- [26] H. Yano, S. Kaneko, K. Nakazawa, S.-I. Yamamoto, and A. Bettouh, "A new concept of dynamic orthosis for paraplegia: The weight bearing control (WBC) orthosis," *Prosthetics and Orthotics International*, vol. 21, pp. 222-228, 1997.
- [27] Y. Hasegawa, J. Jang, and Y. Sankai, "Cooperative walk control of paraplegia patient and assistive system," presented at the IEEE/RSJ International Conference on Intelligent Robots and Systems, St. Louis, USA, 2009.
- [28] K. Suzuki, G. Mito, H. Kawamoto, Y. Hasegawa, and Y. Sankai, "Intention-based walking support for paraplegia patients with Robot Suit HAL," *Advanced Robotics*, vol. 21, pp. 1441-1469, 2007.
- [29] A. Tsukahara, Y. Hasegawa, and Y. Sankai, "Standing-up motion support for paraplegic patient with Robot Suit HAL," presented at the IEEE 11th International Conference on Rehabilitation Robotics, Kyoto, Japan, 2009.
- [30] A. Tsukahara, R. Kawanishi, Y. Hasegawa, and Y. Sankai, "Sit-to-Stand and Stand-to-Sit Transfer Support for Complete Paraplegic Patients with Robot Suit HAL," *Advanced Robotics*, vol. 24, pp. 1615-1638, 2010.
- [31] R. J. Farris, H. A. Quintero, T. J. Withrow, and M. Goldfarb, "Design of a joint-coupled orthosis for FES-aided gait," in *Rehabilitation Robotics, 2009. ICORR 2009. IEEE International Conference on*, 2009, pp. 246-252.
- [32] H. A. Quintero, R. J. Farris, W. K. Durfee, and M. Goldfarb, "Feasibility of a hybrid-FES system for gait restoration in paraplegics," in *Engineering in Medicine and Biology Society (EMBC), 2010 Annual International Conference of the IEEE*, 2010, pp. 483-486.
- [33] R. J. Farris and M. Goldfarb, "Design of a Multidisc Electromechanical Brake," *Mechatronics, IEEE/ASME Transactions on*, vol. PP, pp. 1-9, 2010.

CHAPTER II

Manuscript 1: Preliminary Evaluation of a Powered Lower Limb Orthosis to Aid Walking in Paraplegic Individuals

Ryan J. Farris, Hugo A. Quintero, and Michael Goldfarb

Vanderbilt University

Nashville, TN

Accepted as a Regular Paper to the

IEEE/ASME Transactions on Neural Systems and Rehabilitation Engineering

Abstract

This paper describes a powered lower-limb orthosis that is intended to provide gait assistance to spinal cord injured (SCI) individuals by providing assistive torques at both hip and knee joints. The orthosis has a mass of 12 kg and is capable of providing maximum joint torques of 40 Nm with hip and knee joint ranges of motion from 105° flexion to 30° extension and 105° flexion to 10° hyperextension, respectively. A custom distributed embedded system controls the orthosis with power being provided by a lithium polymer battery which provides power for one hour of continuous walking. In order to demonstrate the ability of the orthosis to assist walking, the orthosis was experimentally implemented on a paraplegic subject with a T10 complete injury. Data collected during walking indicates a high degree of step-to-step repeatability of hip and knee trajectories (as enforced by the orthosis) and an average walking speed of 0.8 km/hr. The electrical power required at each hip and knee joint during gait was approximately 25 W and 27 W, respectively, contributing to the 117 W overall electrical power required by the device during walking. A video of walking corresponding to the aforementioned data is included in the supplemental material.

Introduction

There are currently about 262,000 spinal cord injured (SCI) individuals in the United States, with roughly 12,000 new injuries sustained each year at an average age of injury of 40.2 years [1]. Of these, approximately 44% (5300 cases per year) result in paraplegia. One of the most significant impairments resulting from paraplegia is the loss of mobility, particularly given the relatively young age at which such injuries occur. Surveys of persons with paraplegia indicate that mobility concerns are among the most prevalent [2], and that chief among mobility desires is the ability to walk and stand [3]. In addition to impaired mobility, the inability to stand and walk entails severe physiological effects, including muscular atrophy, loss of bone mineral content, frequent skin breakdown problems, increased incidence of urinary tract infection, muscle spasticity, impaired lymphatic and vascular circulation, impaired digestive operation, and reduced respiratory and cardiovascular capacities [4].

In an effort to restore some degree of legged mobility to individuals with paraplegia, several lower limb orthoses have been developed and described in the literature. The following literature review focuses on orthoses that were developed specifically for restoration of mobility in paraplegic individuals. For recent surveys that consider passive and powered exoskeletons in a more general context, the reader is referred to [5-7]. Also, it should be noted that considerable research has been conducted on the use of functional electrical stimulation (FES) to restore legged mobility to paraplegics, although this topic is also not reviewed here. For a recent review of progress in FES-based gait restoration, the reader is referred to [8]. A number of passive orthoses have been developed to restore legged mobility to paraplegics. The simplest form of passive orthotics are long-leg braces that incorporate a pair of ankle-foot orthoses (AFOs) to provide support at the ankles, which are coupled with leg braces that lock the knee joints in full extension. The hips are typically stabilized by the tension in the ligaments and musculature on the anterior aspect of the pelvis. Since almost all energy for movement is provided by the upper body, these (passive) orthoses require considerable upper body strength and a high level of physical exertion, and provide very slow walking speeds. The hip guidance orthosis (HGO), which is a variation on long-leg braces, is described in [9-11]. The HGO incorporates hip joints that rigidly resist hip adduction and abduction, and rigid shoe plates that provide increased center of gravity elevation at toe-off, thus enabling a greater degree of forward progression per stride. Another variation on the long-leg orthosis, the reciprocating gait orthosis (RGO), incorporates a kinematic constraint that links hip flexion of one leg with hip extension of the other, typically by means of a push-pull cable assembly. As with other passive orthoses, the user leans forward against the stability aid while unweighting the swing leg and utilizing gravity to provide hip extension of the stance leg. Since motion of the hip joints is reciprocally coupled through the reciprocating mechanism, the gravity-induced hip extension also provides contralateral hip flexion (of the swing leg), such that the stride length of gait is increased. Examples of this type of orthosis, and studies of its efficacy, are described in [12-19]. In [20, 21], the authors describe a variation on the RGO, which incorporates a hydraulic-circuit-based variable coupling between the left and right hip joints. Experiments

presented in [21] indicate improved hip kinematics with the modulated hydraulic coupling.

In order to decrease the high level of exertion associated with passive orthoses, some researchers have investigated the use of powered orthoses, which incorporate actuators and an associated power supply to assist with locomotion. Historical efforts to develop powered orthoses to aid in paraplegic mobility include [22-24]. More recently, [25] developed a powered orthosis for evaluating design requirements for paraplegic gait assistance. In [26-28], a powered orthosis was developed by combining three electric motors with an RGO, two of which are located at the knee joints to enable knee flexion and extension during swing, and one of which assists the hip coupling, which in essence assists both stance hip extension and contralateral swing hip flexion. The orthosis was shown to increase gait speed and decrease compensatory motions, relative to walking without powered assistance. In [29-32], the authors describe control methods for providing assistive maneuvers (sit-to-stand, stand-to-sit, and walking) to paraplegic individuals with the powered lower limb orthosis HAL, which is an emerging commercial device with (in the incarnation utilized in the aforementioned publications) six electric motors (i.e., powered sagittal plane hip, knee, and ankle joints). Like the powered lower limb orthosis HAL, two additional emerging commercial devices include the ReWalk powered orthosis (Argo Medical Technologies) and the eLEGS powered orthosis (Berkeley Bionics). Both of these devices were developed specifically for use with paraplegic individuals, although no studies have been published characterizing the performance of these devices, or discussing their efficacy.

This paper describes a powered lower limb orthosis that, like the devices already mentioned, is intended to provide gait assistance to paraplegics by providing sagittal plane assistive torques at both hip and knee joints. Although as previously stated, studies have yet to be published providing technical information on ReWalk and eLEGS, the device described here is at minimum different in the fact that it neither includes a portion that is worn over the shoulders, nor a portion that is worn under the shoes. Also, the device described here has a significantly lower mass relative to the respective masses reported for the other two devices to date in the popular media. This paper describes the salient features and characteristics of the orthosis, and discusses the experimental

implementation of the orthosis on a paraplegic subject (T10 complete). Data is presented characterizing the (hip and knee) joint angle trajectories during walking, the step-to-step repeatability of these trajectories (as enforced by the orthosis), and the average walking speed resulting from these trajectories. Additional data characterizes the electrical power consumption and corresponding battery life associated with the walking trials.

The Vanderbilt Powered Orthosis

The powered lower limb orthosis, shown in Figs. 2-1 and 2-2, was designed to provide powered assistance in the sagittal plane at both hip and knee joints. Each joint is powered by a brushless DC motor through a 24:1 gear reduction, which provides each joint with a maximum continuous joint torque of 12 Nm, and shorter duration maximum torques of approximately 40 Nm. The knee motors are additionally equipped with electrically controllable normally locked brakes, such that the knee joints remain locked in the event of a power failure. Each brake consists of a spring-loaded solenoid which, in the absence of power, provides torsional resistance in a drum brake configuration. The brake remains locked during the stance phase of gait and is released during the swing phase of gait and also during sit-to-stand and stand-to-sit transitions by energizing the solenoid. The range of motion for the hip joints is 105° in flexion and 30° in extension, while the range of motion for the knee joints is 105° in flexion and 10° in hyperextension. Hip ab/adduction is accommodated by compliance embedded into the hip segment. Such compliance is intended to provide stability to the wearer, while disallowing excessive adduction during swing, in order to prevent scissoring during walking. The orthosis is intended to be worn in conjunction with a standard ankle foot orthosis (AFO), which provides support at the ankle and prevents foot drop during swing. The structure of the orthosis is a composite of thermoplastic reinforced and supplemented with aluminum inserts. Sensors in the orthosis include potentiometers in both hip and knee joints, in addition to accelerometers located in each thigh link. As shown in Figs. 2-1 and 2-2, hook-and-loop straps on the hip segment, thigh segments, and shank segments secure the orthosis to the user with integrated padding in place to distribute pressure from the straps and

protect the wearer from skin abrasion. The total orthosis mass is 12 kg (26.5 lbs). The orthosis is prevented from sliding down the body primarily by the two thigh straps immediately above the knee joints, and by the orthosis hip segment, which affixed around the subject's waist, just above the gluteal musculature. A mass breakdown showing individual component masses of the orthosis is given in Table 2-1.



Figure 2-1. Vanderbilt gait restoration orthosis oblique view.



Figure 2-2. Vanderbilt gait restoration orthosis frontal view.

Component	Mass (kg)	Mass Distribution
Joint Actuation	3.57	30%
Thigh Frames	4.08	34%
Hip Brace	2.10	17%
Shank Frames	1.09	9%
Battery	0.68	6%
Electronics	0.50	4%
Total	12.02	100%

Table 2-1. Mass breakdown of Vanderbilt Orthosis.

The powered orthosis additionally includes a custom distributed embedded system (DES), the components of which are located in the hip and both thigh segments. A functional diagram of the DES is given in Fig. 2-3. The DES is powered by a 29.6 V, 3.9 A•hr lithium polymer battery, and as indicated in Fig. 2-3, includes a power management module, a computation module, electronic signal conditioning and sensor interface module, power electronics, and communication electronics to interface components within the DES and between the DES and a host computer. The power management module provides, from the battery, linearly regulated ± 12 and $+3.3$ V, which are used for signal conditioning and computation, and are derived from intermediate ± 12.5 and $+5$ V switching regulators for efficient conversion. The main computational modules consist of two 80 MHz PIC32 microcontrollers, each with 512 kB flash memory and 32 kB RAM, and each of which consume approximately 400 mW of power. The microcontrollers are programmed in C using MPLAB IDE and the MP32 C Compiler (both from Microchip Technology, Inc.). A control tether connects the microcontrollers on the orthosis to a laptop computer via an RS-232 interface, such that the orthosis control can be supervised by the laptop host via the real-time interface provided by MATLAB Simulink RealTime Workshop. The two microcontrollers drive the brushless motors via four-quadrant switching servoamplifiers, and also drive the knee brakes via pulse-width-modulated (PWM) power transistors. One of the two main (twin) DES boards is shown mounted within the thigh link in Fig. 2-4.

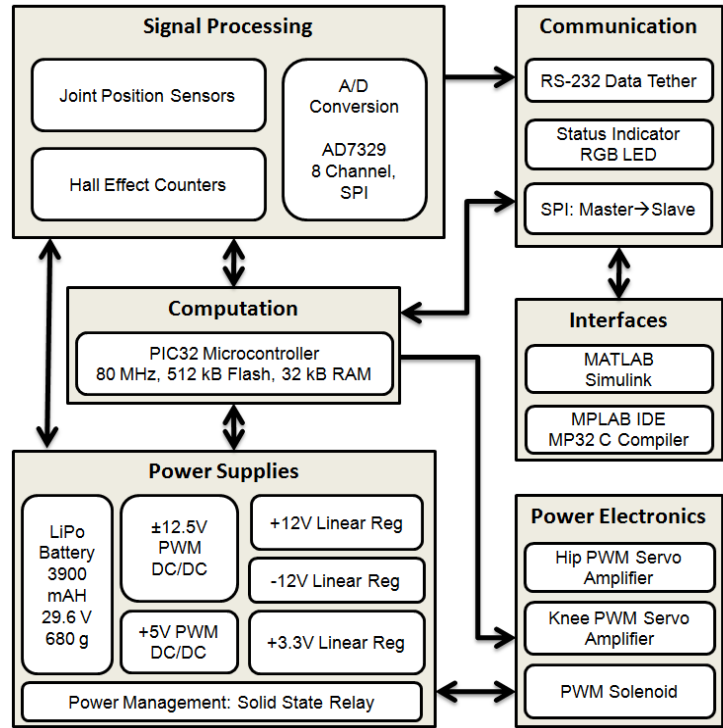


Figure 2-3. Embedded system framework.

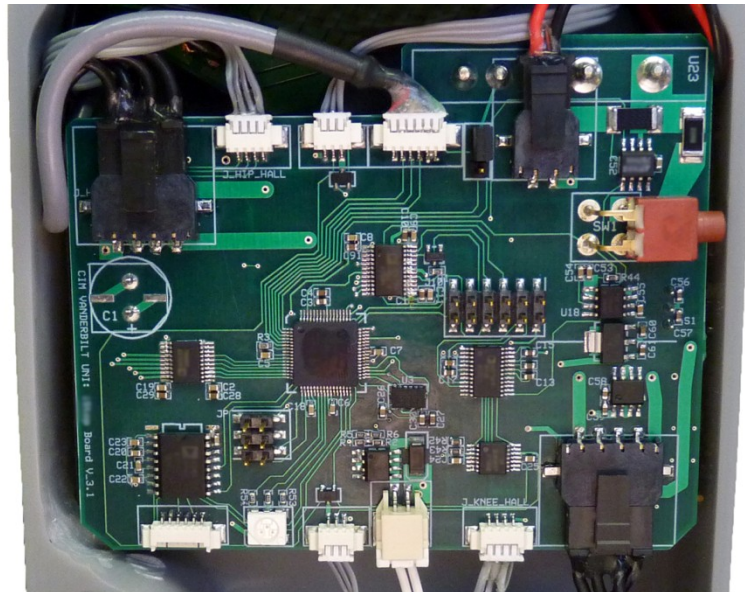


Figure 2-4. Embedded system circuit board.

Orthosis Control

The orthosis controller consists of a state-flow system with four states, as shown in Fig. 2-5. Each state is defined by a set of joint angle trajectories, which are enforced by high-gain proportional-derivative (PD) control loops. Joint angle trajectories were preprogrammed for each motion based on normal biomechanical walking trajectories, obtained from a recording of the joint angle trajectories generated by a healthy subject while wearing the orthosis. For the data presented herein, switching between states was initiated by voice command of the user. The voice commands were keyed into the laptop host computer via an operator, which moved the state machine from one state to the next.

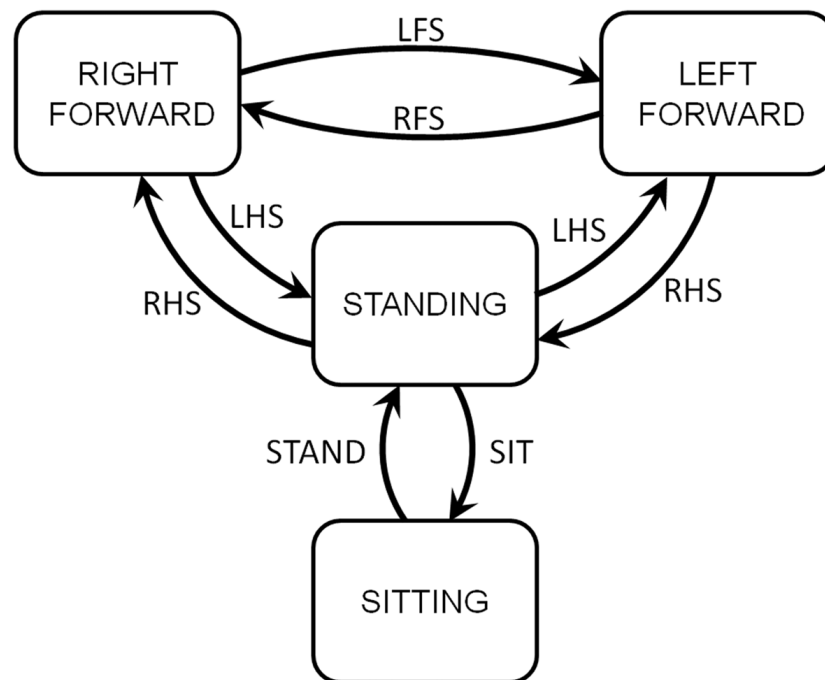


Figure 2-5. State-flow diagram. Boxes represent static states. Transitions are labeled between states, where LFS = left full-step, LHS = left half-step, RFS = right full-step, RHS = right half-step.

Experimental Implementation

In order to substantiate the ability of the powered orthosis to provide gait assistance, the previously described orthosis and controller was implemented on a paraplegic subject. The subject was a 35-year-old male (1.85 m, 73 kg) with a T10 complete injury, 8 years post injury. The evaluations were conducted at the Shepherd Center (Atlanta GA, USA), a rehabilitation hospital specializing in spinal cord injury. The testing was approved by both the respective Vanderbilt University and Shepherd Center Institutional Review Boards. All evaluations described herein were conducted within a standard set of parallel bars. Figure 2-6 shows the test subject wearing the orthosis while standing and walking, respectively, in the parallel bars. For the data presented in the subsequent sections, the evaluation protocol was as follows. The subject stood from a wheelchair with footrests removed by issuing a “stand” voice command. Note that the footrests, if not removed, would obstruct the subject’s ability to bring his feet close to the chair, and therefore would impede his ability to transition from sitting to standing. Once comfortable standing, the subject issued either a “left-step” or “right-step” voice command, and subsequently, a “step” voice command to initiate subsequent steps. Once near the end of the parallel bars, the subject issued a “half-step” command, which returned him to the standing configuration. The subject then turned in place in the parallel bars by lifting his weight with his arms and incrementally twisting around in order to walk in the opposite direction. This process repeated, typically for four to eight lengths of the parallel bars, at which point the subject sat (in his wheelchair, by issuing a “sit” voice command), so that data from the walking trial could be recorded (i.e., uploaded and saved to the host computer). A video depicting a lap of walking is provided in the supplemental material that accompanies this paper. Data indicating hip and knee joint angles and electrical power consumption corresponding to over ground walking are given in the following subsections.



Figure 2-6. Subject with T10 complete spinal cord injury walking wearing the powered orthosis.

Gait Kinematics

Figure 2-7 shows measured joint angle data from 23 right steps and 23 left steps, overlaid onto the same plot. Note that an approximate one-second delay exists between each right and left step, during which time the subject adjusted his upper body in preparation for commanding the next step. Figure 2-8 shows the same data shown in Fig. 2-7, but with the delay between steps replaced with a vertical dashed line (which indicates a discontinuity in time), with the time base replaced with a percent stride base, and with the left and right joint angles overlaid onto the same plots. In this manner, the knee and hip joint angles can be qualitatively compared to standard joint kinematics during walking, which is typically represented as a function of stride. These normal biomechanical trajectories (taken from [34]) are also plotted in Fig. 2-8 as dashed lines. The repeatability of the

joint angle data over these 23 strides, and the similarity of such data to normal biomechanics (particularly with respect to the amplitude of knee flexion, and the amplitude of hip flexion and extension), indicate that the powered orthosis is able to provide appropriate and repeatable gait assistance to the user during walking. The gait represented by this data is characterized by an average overground walking speed of 0.22 m/s (0.8 km/hr or 0.5 mi/hr).

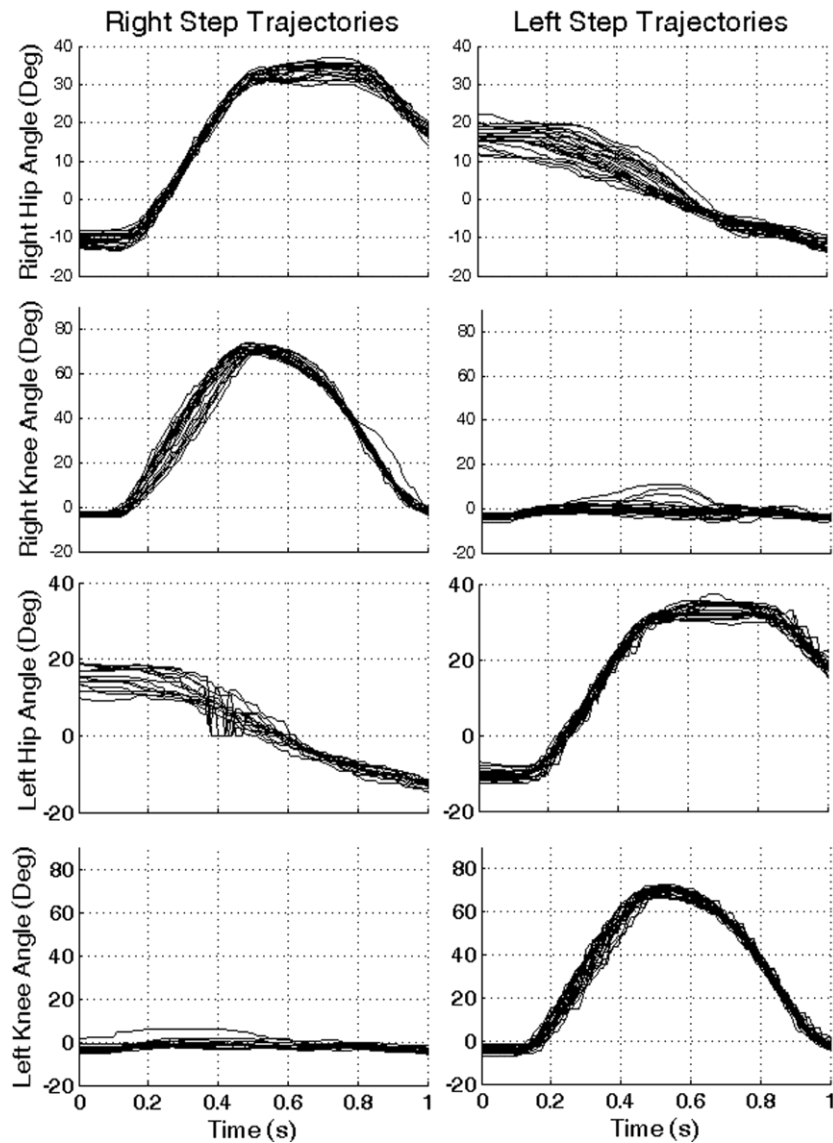


Figure 2-7. Measured joint angles during 23 right steps and 23 left steps.

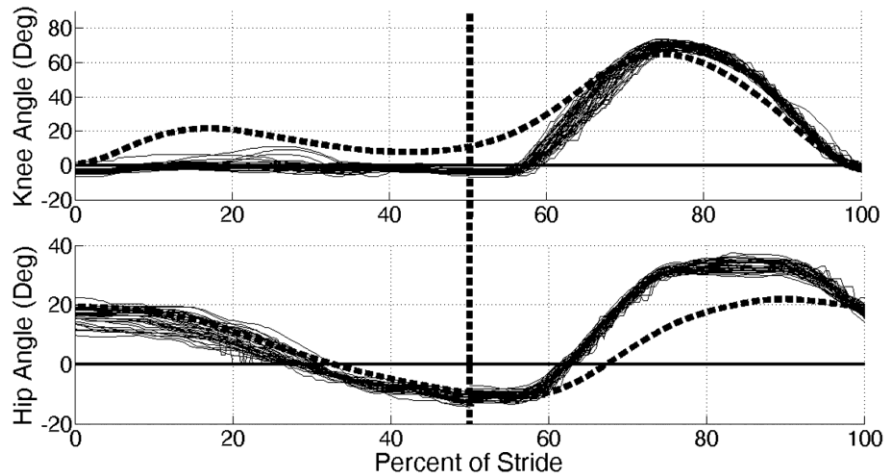


Figure 2-8. Overlaid joint angles for 23 gait cycles. The dashed vertical line represents an approximately one-second pause taken by the subject between steps. The dashed trajectories represent normal biomechanical data for level ground walking at a medium cadence.

Electrical Power Consumption

Electrical power consumption was recorded during the walking represented by Figs. 2-7 and 2-8. The electrical power required by the servoamplifiers, corresponding to the data shown in Fig. 2-8, is shown averaged over all 46 steps (or 23 strides) in Fig. 2-9, which represents an average power consumption of approximately 35 W for each knee actuator (during the active stride), and approximately 22 W for each hip actuator (during the stride). In addition to requiring electrical power during right and left steps, the joint actuators also used power to maintain joint stiffness in the double support states (i.e., while the subject shifted his weight to prepare for the next step). For the 46 step sequence previously described, the total electrical power required by each actuator was 27 W on average for each knee motor and 21 W on average for each hip motor during the swing phase of gait, and 26 W and 29 W of average power for the knee and hip motors, respectively, during the stance phase of gait. The knee brakes additionally required on average approximately 7 W of electrical power during swing, but did not require any power during stance (i.e., they are normally locked brakes). Finally, the average electrical power required by the remainder of the distributed embedded system was measured as 7.2 W. The average measured electrical power consumption

for each component and each phase of the walking cycle is summarized in Table 2-2. With a one-second average pause between steps (corresponding to the 0.22 m/s walking data represented by Fig. 2-8), the total electrical power required by the system was 117 W. Recall that the battery pack included in the powered orthosis prototype described herein is a 680 g lithium polymer battery with a 115 W-hr capacity. Based on the walking data of Fig. 2-9 and Table 2-2, the battery would provide approximately one hour of continuous walking between charges. At the previously stated (measured) average overground speed of 0.8 km/hr (0.5 mi/hr), the powered orthosis would provide a range of approximately 0.8 km (0.5 mi) between battery charges. Note that the range could be easily increased, if desired, without incurring a significant mass penalty, by increasing the size of the battery, which currently constitutes 6% of the system mass (see Table 2-1). For example, doubling the size of the battery pack would double the range and result in an overall device mass of 12.7 kg, as opposed to 12 kg, as implemented here.

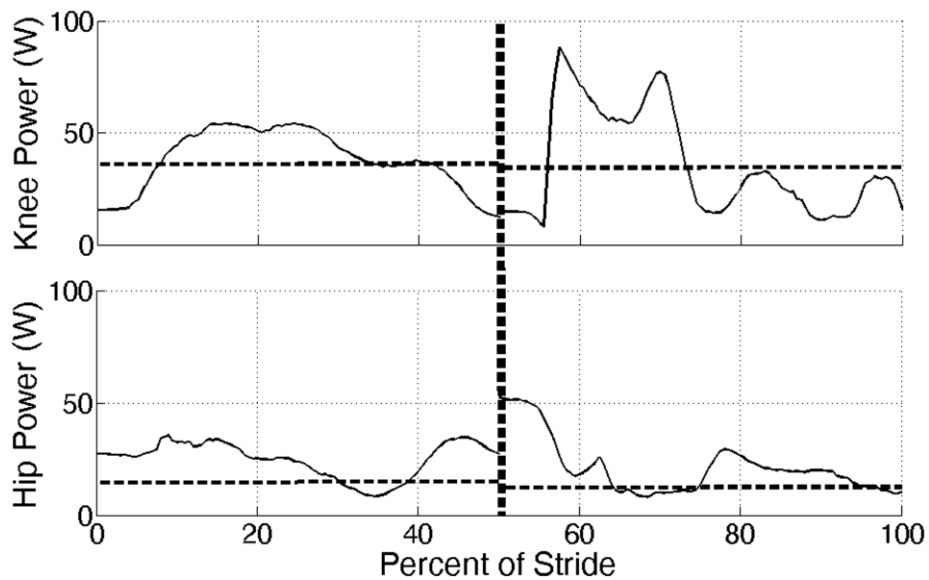


Figure 2-9. Average measured electrical power at the knee and hip joints over one gait cycle (average taken from 23 gait cycles). *The dashed vertical line represents a pause of approximately a second which the subject would take in between steps. The dashed horizontal lines represent average electrical power within one gait cycle.

Component	Power During Stepping (W)	Power Between Steps (W)	*Average Power During Walking (W)
Swing Knee Motor	34.8	19.6	27.2
Stance Knee Motor	35.6	16.5	26.1
Swing Hip Motor	21.4	19.8	20.6
Stance Hip Motor	23.9	34.0	29.0
Embedded Electronics Boards	7.2	7.2	7.2
Swing Knee Brake	13.5	0	6.7
Stance Knee Brake	0	0	0
Total	136.4	97.1	116.8

*Average power assumes a 1 second pause in between steps (i.e., steps are being taken during 50% of the time during "walking")

Table 2-2. Vanderbilt Orthosis electrical power consumption

Audible Sound Level

A digital sound level meter was used while walking with the orthosis. The average sound level, as measured one meter away from the orthosis, was 55 ± 2 dBA (with an ambient noise level of 38 dBA).

Discussion

The powered orthosis has been developed with a strong focus on ergonomics and user acceptance. High priority was given to low mass and minimal body coverage. Additionally, the authors have attempted to minimize the profile of the orthosis in the frontal plane, which adds 3.2 cm at the hip and knee joint, and 4.8 cm at mid-thigh, such that a user is able to sit in an armchair or wheelchair. Similarly, the hip segment protrudes approximately 3.2 cm posteriorly from the user's lower back, such that it should not significantly interfere with a seat back. The orthosis does not extend above mid-abdomen and requires nothing to be worn over the shoulders and nothing above the lower back, which presumably renders the device less noticeable when sitting at a desk or table. The compact design of the orthosis is greatly facilitated by the integration of the distributed embedded system within the orthosis structure. With quick disconnects at each hip joint, the

orthosis is easily separated into three modular components – right leg, left leg, and hip segment – for ease of donning and doffing and also for increased portability. An important aspect of the device is the normally locked knee brakes, which presumably provide a fail-safe in the event of power loss (e.g., a fully depleted battery). The combination of low joint impedances at the hip in the absence of control, along with locked knees, renders the device the essential equivalent of a pair of long-leg braces in the event of power loss, such that the user is neither in danger, nor completely immobilized by such an unplanned occurrence.

One trade-off associated with the design of the orthosis is the need for custom fitting relative to users of different sizes. Of particular importance is that the sagittal plane centers of rotation of the orthosis joints be concentric with the approximate corresponding centers of rotation of the user's physiological hip and knee joints, and the width of the hip piece correspond to the width of the user's hips. In the absence of shoulder straps or structure under the shoes, the orthosis must fit the wearer well in order to effectively support the weight of the orthosis and provide the desired functionality.

Conclusion

This paper describes a powered lower limb orthosis developed to assist gait in spinal cord injured individuals. Experimental results from walking trials with a T10 complete paraplegic indicate that the orthosis is capable of providing a repeatable gait with knee and hip joint amplitudes that are similar to those observed during non-SCI walking. Electrical power measurements with the current battery pack and control algorithms indicate a battery life of approximately an hour, and a corresponding walking range of approximately 0.8 km. The authors expect this range to increase with efficiency in enhancements in the control algorithms, and can of course be most easily increased with a larger battery pack, which (given the size of the current battery pack), is unlikely to significantly increase the mass or size of the device. Future work includes the addition of automated, sensor-based gait mode transitions, such that the device can operate without voice commands.

References

- [1] (2010). Spinal Cord Injury Facts and Figures at a Glance. Available: <https://www.nscisc.uab.edu>
- [2] R. W. Hanson and M. R. Franklin, "Sexual loss in relation to other functional losses for spinal cord injured males," *Archives of Physical Medicine and Rehabilitation*, vol. 57, pp. 291-293, 1976.
- [3] D. L. Brown-Triolo, M. J. Roach, K. Nelson, and R. J. Triolo, "Consumer perspectives on mobility: implications for neuroprosthesis design," *Journal of Rehabilitation Research and Development*, vol. 39, pp. 659-669, 2002.
- [4] L. Phillips, M. Ozer, P. Axelson, and H. Chizek, *Spinal cord injury: A guide for patient and family*: Raven Press, 1987.
- [5] A. M. Dollar and H. Herr, "Lower Extremity Exoskeletons and Active Orthoses: Challenges and State-of-the-Art," *Robotics, IEEE Transactions on*, vol. 24, pp. 144-158, 2008.
- [6] H. Herr, "Exoskeletons and orthoses: classification, design challenges and future directions," *Journal of NeuroEngineering and Rehabilitation*, vol. 6, p. 21, 2009.
- [7] R. Bogue, "Exoskeletons and robotic prosthetics: a review of recent developments," *Industrial Robot: An International Journal*, vol. 36, pp. 421-427, 2009.
- [8] K. T. Ragnarsson, "Functional electrical stimulation after spinal cord injury: current use, therapeutic effects and future directions," *Spinal Cord*, vol. 46, pp. 255-274, April 2008 2008.
- [9] P. B. Butler, R. E. Major, and J. H. Patrick, "The technique of reciprocal walking using the hip guidance orthosis (hgo) with crutches," *Prosthetics and Orthotics International*, vol. 8, pp. 33-38, 1984.
- [10] R. E. Major, J. Stallard, and G. K. Rose, "The dynamics of walking using the hip guidance orthosis (hgo) with crutches," *Prosthetics and Orthotics International*, vol. 5, pp. 19-22, 1981.
- [11] G. K. Rose, "The principles and practice of hip guidance articulations," *Prosthetics and Orthotics International*, vol. 3, pp. 37-43, 1979.
- [12] G. Baardman, et al., "The influence of the reciprocal hip joint link in the Advanced Reciprocating Gait Orthosis on standing performance in paraplegia," *Prosthetics and Orthotics International*, vol. 21, pp. 210-221, 1997.
- [13] J. Beillot, et al., "Energy consumption of paraplegic locomotion using reciprocating gait orthosis," *European Journal of Applied Physiology and Occupational Physiology*, vol. 73, pp. 376-381, 1996.
- [14] M. Bernardi, I. Canale, L. D. F. Castellano, F. Felici, and M. Marchetti, "The efficiency of walking of paraplegic patients using a reciprocating gait orthosis.," *Paraplegia*, vol. 33, pp. 409-415, 1995.
- [15] L. A. Harvey, G. M. Davis, M. B. Smith, and S. Engel, "Energy expenditure during gait using the walkabout and isocentric reciprocal gait orthoses in persons with paraplegia," *Archives of Physical Medicine and Rehabilitation*, vol. 79, pp. 945-949, 1999.

- [16] L. A. Harvey, T. Newton-John, G. M. Davis, M. B. Smith, and S. Engel, "A comparison of the attitude of paraplegic individuals to the walkabout orthosis and the isocentric reciprocal gait orthosis," *Spinal Cord*, vol. 35, pp. 580-584, 1997.
- [17] M. J. Ijzerman, et al., "The influence of the reciprocal cable linkage in the advanced reciprocating gait orthosis on paraplegic gait performance," *Prosthetics and Orthotics International*, vol. 21, pp. 52-61, 1997.
- [18] C. Scivoletto, M. I. Mancini, B. Fiorelli, B. Morganti, and M. Molinari, "A prototype of an adjustable advanced reciprocating gait orthosis (ARGO) for spinal cord injury (SCI)," *Spinal Cord*, vol. 41, pp. 187-191, 2003.
- [19] S. Tashman, F. E. Zajac, and I. Perakash, "Modeling and Simulation of Paraplegic Ambulation in a Reciprocating Gait Orthosis," *Journal of Biomechanical Engineering*, vol. 117, pp. 300-308, 1995.
- [20] C. S. To, R. Kobetic, J. R. Schnellenger, M. L. Audu, and R. J. Triolo, "Design of a variable constraint hip mechanism for a hybrid neuroprosthesis to restore gait after spinal cord injury," *IEEE/ASME Transactions on Mechatronics*, vol. 13, pp. 197-205, 2008.
- [21] M. L. Audu, C. S. To, R. Kobetic, and R. J. Triolo, "Gait evaluation of a novel hip constraint orthosis with implication for walking in paraplegia," *IEEE Transactions on Neural Systems and Rehabilitation Engineering*, vol. 18, pp. 610-618, 2010.
- [22] J. E. Beard, J. C. Conwell, D. S. Rogers, and H. Lamousin, "Design of a powered orthotic device to aid individuals with a loss of bipedal locomotion," in *Second National Applied Mechanisms and Robotics*, 1991.
- [23] M. Townsend and R. Lepofsky, "Powered walking machine prosthesis for paraplegics," *Medical and Biological Engineering and Computing*, vol. 14, pp. 436-444, 1976.
- [24] M. Vukobratovic, D. Hristic, and Z. Stojiljkovic, "Development of active anthropomorphic exoskeletons," *Medical and Biological Engineering and Computing*, vol. 12, pp. 66-80, 1974.
- [25] B. J. Ruthenberg, N. A. Wasylewski, and J. E. Beard, "An experimental device for investigating the force and power requirements of a powered gait orthosis," *Journal of Rehabilitation Research and Development*, vol. 34, pp. 203-213, 1997.
- [26] N. Kawashima, Y. Sone, K. Nakazawa, M. Akai, and H. Yano, "Energy expenditure during walking with weight-bearing control (WBC) orthosis in thoracic level of paraplegic patients," *Spinal Cord*, vol. 41, pp. 506-510, 2003.
- [27] Y. Ohta, et al., "A two-degree-of-freedom motor-powered gait orthosis for spinal cord injury patients," *Proceedings of the Institution of Mechanical Engineers, Part H: Journal of Engineering in Medicine*, vol. 221, pp. 629-639, 2007.
- [28] H. Yano, S. Kaneko, K. Nakazawa, S.-I. Yamamoto, and A. Bettouh, "A new concept of dynamic orthosis for paraplegia: The weight bearing control (WBC) orthosis," *Prosthetics and Orthotics International*, vol. 21, pp. 222-228, 1997.
- [29] Y. Hasegawa, J. Jang, and Y. Sankai, "Cooperative walk control of paraplegia patient and assistive system," in *IEEE/RSJ International Conference on Intelligent Robots and Systems*, 2009, pp. 4481-4486.

- [30] K. Suzuki, G. Mito, H. Kawamoto, Y. Hasegawa, and Y. Sankai, "Intention-based walking support for paraplegia patients with Robot Suit HAL," *Advanced Robotics*, vol. 21, pp. 1441-1469, 2007.
- [31] A. Tsukahara, Y. Hasegawa, and Y. Sankai, "Standing-up motion support for paraplegic patient with Robot Suit HAL," in *IEEE International Conference on Rehabilitation Robotics*, 2009, pp. 211-217.
- [32] A. Tsukahara, R. Kawanishi, Y. Hasegawa, and Y. Sankai, "Sit-to-Stand and Stand-to-Sit Transfer Support for Complete Paraplegic Patients with Robot Suit HAL," *Advanced Robotics*, vol. 24, pp. 1615-1638, 2010.
- [33] D. A. Winter, *The biomechanics and motor control of human gait: normal, elderly and pathological*, 2nd ed.: University of Waterloo Press, 1991.

CHAPTER III

Manuscript 2: A Method for the Autonomous Control of Lower Limb Exoskeletons for Persons with Paraplegia

Hugo A. Quintero, Ryan J. Farris, and Michael Goldfarb

Vanderbilt University

Nashville, TN

Submitted as a Regular Paper to the

ASME Journal of Medical Devices

(In Review)

Abstract

Efforts have recently been reported by several research groups on the development of computer-controlled lower limb orthoses to enable legged locomotion in persons with paraplegia. Such systems must employ a control framework that provides essential movements to the paraplegic user (i.e., sitting, standing, and walking), and ideally enable the user to autonomously command these various movements in a safe, reliable, and intuitive manner. This paper describes a control method that enables a paraplegic user to perform sitting, standing, and walking movements, which are commanded based on postural information measured by the device. The proposed user interface and control structure was implemented on a powered lower limb orthosis, and the system was tested on a paraplegic subject with a T10 complete injury. Experimental data is presented that indicates the ability of the proposed control architecture to provide appropriate user-initiated control of sitting, standing, and walking. The authors also provide a link to a video that qualitatively demonstrates the user's ability to independently control basic movements via the proposed control method.

Introduction

One of the most significant impairments resulting from paraplegia is the loss of mobility, particularly given the relatively young age at which such injuries occur [1-3]. In addition to diminished mobility, the inability to stand and walk entails significant physiological impairments, including muscular atrophy, loss of bone mineral content, frequent skin breakdown problems, increased incidence of urinary tract infection, muscle spasticity, impaired lymphatic and vascular circulation, impaired digestive operation, and reduced respiratory and cardiovascular capacities [4].

In an effort to facilitate legged locomotion in individuals with paraplegia, several computer-controlled lower limb orthosis systems have been, and are being, developed and described in the research literature. Some of these include hybrid FES-systems, which combine a computer-controlled orthosis with computer-controlled functional electrical stimulation (FES) of leg muscles, such as the systems described by [5-9]. Recently, a number of powered lower limb orthoses, or exoskeletons, have also been described for purposes of gait assistance for persons

with paraplegia, including those described by [10-16]. In addition to these systems, two other exoskeleton systems, developed by commercial entities, are those by Argo Medical Technologies (ReWalk) and Berkeley Bionics (eLEGS). Technical information regarding these two systems have not yet appeared in the engineering literature. In the aforementioned publications describing computer-controlled orthoses (i.e., [5-16]), the authors focus on the capacity of their respective systems to provide legged mobility, but do not focus on specifically on control methods that enable the user to autonomously command various movements. In order to demonstrate mobility, these approaches have either incorporated push-button controls on the stability aid, or have incorporated a system operator, who operates the system (e.g., from a host computer) on behalf of the paraplegic individual. The emerging commercial systems, ReWalk and eLEGS, presumably provide for autonomous user control. To the authors' knowledge, however, no information has been published in the engineering literature regarding the control methods incorporated by either of these systems. Based on product information available from the respective companies, the ReWalk exoskeleton appears to utilize a tilt-sensor on the torso to gate subsequent steps while walking, and utilizes a wrist-mounted keypad to select between other types of movements. The eLEGS exoskeleton reportedly utilizes instrumentation on the forearm crutches or walker to gate subsequent steps while walking.

To the authors' knowledge, no publication in the engineering literature has described and demonstrated a method that enables a paraplegic user to intuitively and autonomously control (i.e., without push-button controls or the assistance of a system operator) the basic movements associated with legged mobility (i.e., sitting, standing, and walking). As such, this paper presents a control architecture for a powered lower limb orthosis (or exoskeleton) designed to enable a paraplegic user to autonomously navigate through these movements, without the use of their hands or the aid of an external operator. Specifically, the control architecture enables the user to switch between sitting, standing, and walking, based on the user's upper body movement. The control architecture was implemented on a powered lower limb orthosis and evaluated on a paraplegic subject with a T10 motor and sensory complete injury (i.e., American Spinal Injury

Association, ASIA, A classification). The ability of the user to autonomously control the system was assessed by having the paraplegic user repeatedly perform a timed-up-and-go (TUG) test, which is a standard clinical measure of legged mobility [17]. The paper describes the control architecture and its implementation, and presents experimental results of the TUG tests. The test results support the ability of the proposed control architecture to enable user-autonomous control of the basic movements associated with legged mobility.

Powered Orthosis Prototype

Although the proposed control interface is generally applicable to a number of computer-controlled lower limb orthoses (such as those previously described), for purposes of this paper, the architecture was implemented on the powered lower limb orthosis shown in Fig. 3-1. Specifically, the orthosis shown in Fig. 3-1 incorporates four motors, which impose sagittal plane torques at each hip and knee joints. As seen in the figure, the orthosis contains five segments, which are: two shank segments, two thigh segments, and one hip segment. Each thigh piece contains two brushless DC motors which are used to drive the hip and knee articulations through a speed-reduction transmission. Each joint can provide up to 12 Nm of continuous torque and 40 Nm for shorter (i.e., 2-sec) durations. As a safety measure, both knee joints include normally locked brakes, in order to preclude knee buckling in the event of a power failure. The system does not contain foot or ankle components, but is designed to be used in conjunction with a standard ankle foot orthosis (AFO) to provide stability for the ankle, and to preclude foot drop during the swing phase of gait. Physical sensing in the orthosis consists of Hall-effect-based angle and angular velocity sensing in each hip and knee joint, and 3-axis accelerometers and single-axis gyroscopes in each thigh segment. A pair of microcontrollers located in the thigh segments, provide low-level control of the orthosis. In the current implementation, the microcontrollers communicate with a host computer via a data tether, which facilitates controller development and data visualization. All power on the orthosis is provided by a lithium polymer battery located in the hip segment (see Fig. 3-1). A functional schematic of the embedded system on the orthosis is shown in Fig. 3-2.

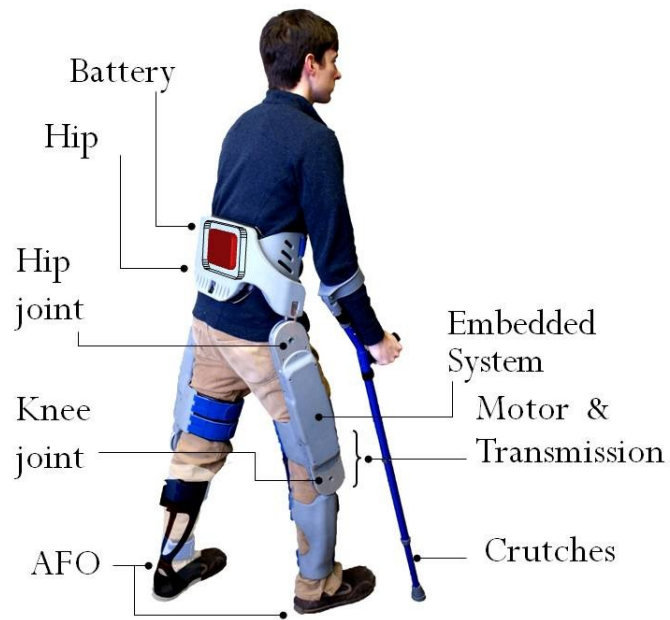


Figure 3-1. Powered lower limb orthosis.

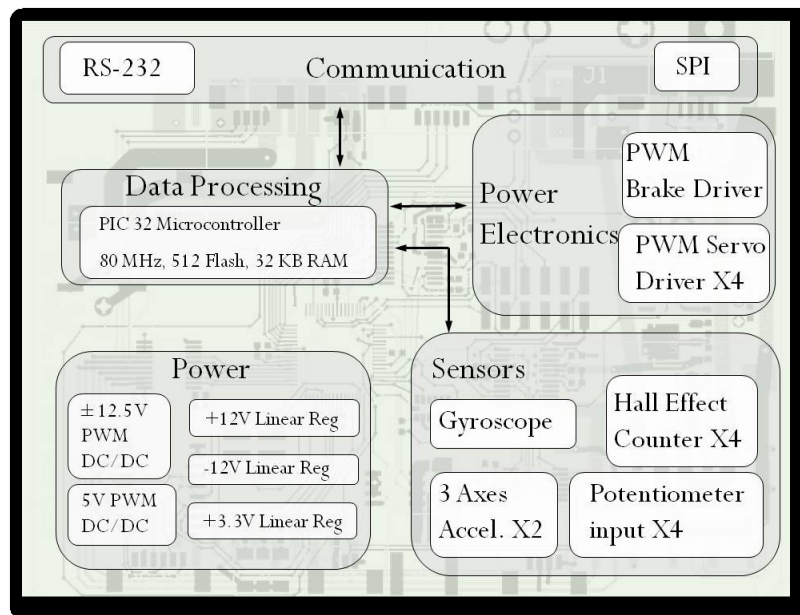


Figure 3-2. Functional schematic of embedded system.

Joint-Level Controllers

The general control structure of the orthosis consists of variable-impedance joint-level controllers, the behavior of which is supervised by an event-driven finite-state controller. The joint-level controllers consist of variable-gain proportional-derivative (PD) feedback controllers around each (hip and knee) joint, where at any given time, the control inputs into each controller consists of the joint angle reference, in addition to the proportional and derivative gains of the feedback controller. Note that the latter are constrained to positive values, in order to ensure stability of the feedback controllers. With this control structure, in combination with the open-loop low output impedance of the orthosis joints, the joints can either be controlled in a high-impedance trajectory tracking mode, or in a (relatively) low-impedance mode, by emulating physical spring-damper couples at each joint. The former is used where it may be desirable to enforce a predetermined trajectory (e.g., during the swing phase of gait), while the latter is used when it may be preferable not to enforce a pre-determined joint trajectory, but rather to provide assistive torques that facilitate movement toward a given joint equilibrium point (as in transitioning from sitting to standing), or to impose dissipative behavior at the joint (as in transitioning from standing to sitting).

Finite-State Control Structure

The joint-level controller receives trajectory commands, as well as PD gains, from a supervisory finite-state machine (FSM), which (for sitting, standing, and walking) consists of 12 states, as shown in Fig. 3-3. The FSM consists of two types of states: static states and transition states. The static states consist of sitting (S1), standing (S2), right-leg-forward (RLF) double support (S3), and left-leg-forward (LLF) double support (S4). The remaining 8 states, which transition between the four static states, include sit-to-stand (S5), stand-to-sit (S6), stand-to-walk with right half step (S7), stand-to-walk with left half step (S11), walk-to-stand with left half step (S10), walk-to-stand with right half step (S12), right step (S9), and left step (S8).

Each state in the FSM is fully defined by the combination of a set of trajectories, and a set of

joint feedback gains. In general, the latter are either high or low. The set of trajectories utilized in six of the eight transition states are shown in Fig. 3-4. For all the trajectories shown in Fig. 3-4, the joint feedback gains are set high. The final angles of the trajectories shown in Fig. 4 for the various joints define the constant joint angles that correspond to the static states of RLF double support (S3), LLF double support (S4), and standing (S2). Three states remain, which are the static state of sitting and the two transition states of sit-to-stand and stand-to-sit. The static state of sitting (S1) is defined by zero gains, and therefore the joint angles are unimportant. The transition from stand-to-sit (S6) consists of a zero proportional gain and a high derivate gain (i.e., damping without stiffness). Thus, the joint angles are also immaterial for this state, assuming they are constant. Finally, the sit-to-stand (S5) state is defined by standing (S2) joint angles, and utilizes a set of PD gains that ramp up from zero to a value that corresponds to a high impedance state. Table 3-1 and Fig. 3-4 summarize the trajectories and nature of the feedback gains that together define completely the behavior in all states of the FSM shown in Fig. 3-3.

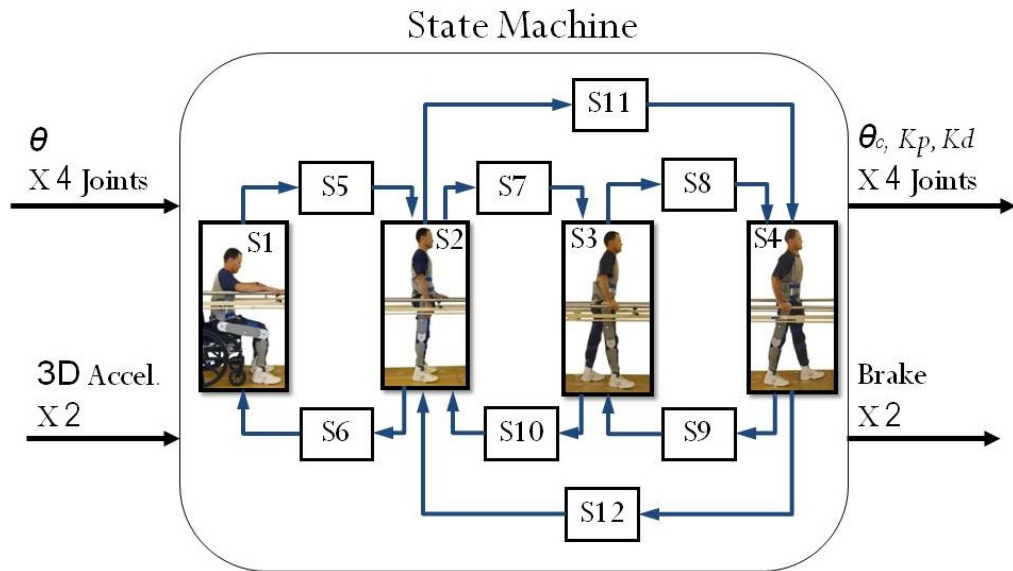
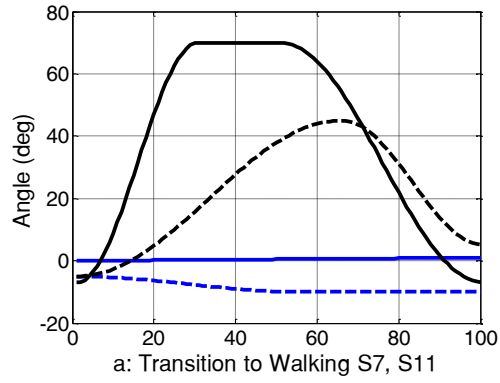


Figure 3-3. Finite state machine for sitting, standing, and walking.



Swing Hip - - - -
 Swing Knee ————
 Stance Hip - - - -
 Stance Knee ————

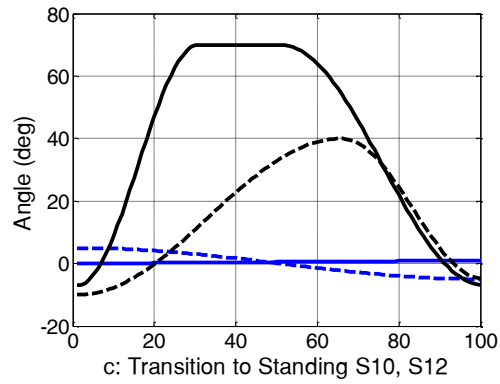
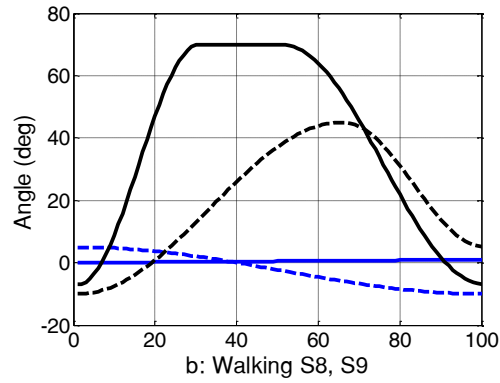


Figure 3-4. Walking trajectories corresponding to finite states as indicated.

CONTROL CHARACTERISTICS IN EACH STATE

State	Type	Gains	Control Priority
S1- Sitting	Static	Low	NA
S2- Standing	Static	High	Position
S3- Right Forward	Static	High	Position
S4- Left Forward	Static	High	Position
S5- 1 to 2	Transition	N.A	Gain
S6- 2 to 1	Transition	N.A	Gain
S7- 2 to 3	Transition	High	Trajectory
S8- 3 to 4	Transition	High	Trajectory
S9- 4 to 3	Transition	High	Trajectory
S10- 3 to 2	Transition	High	Trajectory
S11- 2 to 4	Transition	High	Trajectory
S12- 4 to 2	Transition	High	Trajectory

Table 3-1. Joint controller characteristics within each state.

Switching Between States

The volitional command of the basic movements in the FSM is based on the location of the (estimated) center of pressure (CoP), defined for the (assumed quasistatic user/orthosis) system as the center of mass projection onto the (assumed horizontal) ground plane. This notion is illustrated in Fig. 3-5, which indicates the approximate location of the CoP, relative to the forward-most heel. It is assumed that, with the use of the stability aid, the user can affect the posture of his or her upper body, and thus can affect the location of the CoP. By utilizing the accelerometers in the orthosis, which provide a measure of the thigh segment angle (α in Fig. 3-5) relative to the inertial reference frame (i.e., relative to the gravity vector), in combination with the joint angle sensors (which provide a measure of the configuration of the orthosis and user), the orthosis controller can estimate the location of the CoP (in the sagittal plane). More specifically, in this estimation, the authors assume level ground; that the heels remain on the ground; that the head, arms, and trunk (HAT) can be represented as a single segment with fixed inertial properties;

and that out-of-sagittal-plane motion is small. Given these assumptions, along with estimates of the length, mass and location of center of mass of each segment (right and left shank, right and left thigh, and HAT), the controller can estimate the projection of the CoP on the ground. Let the distance from the forward-most heel to the CoP be X_c , where a positive value indicates that the CoP lies anterior to the heel, and a negative number indicates the CoP lies posterior to the heel (see Fig. 3-5). From a state of double support (S3 or S4), the user commands the next step by moving the CoP forward, until it meets a prescribed threshold, at which point the FSM will enter either the right step or left step states, depending on which foot started forward. From a standing position (S2), the user commands a step by similarly moving the CoP forward until it meets a prescribed threshold, but also leaning to one side in the frontal plane (as indicated by the 3-axis accelerometers in the thigh segments), which indicates that the orthosis should step with the leg opposite the direction of frontal plane lean (i.e., step forward with the presumably unweighted leg). That is, leaning to the right (and moving the CoP forward) will initiate a left step, while leaning to the left (and moving the CoP forward) will initiate a right step. In order to transition from a standing state (S2) to a sitting state, the user shifts the CoP rearward, such that the CoP lies behind the user. Finally, to transition from a sitting to a standing state (S1 to S2), the user leans forward (as illustrated in Fig. 3-6a), which shifts the CoP forward to a predetermined threshold, which initiates the transition from sitting to standing. Note that the right portion of Fig. 3-6 shows the case where the user's CoP is not sufficiently forward to initiate a transition from sitting to standing. Finally the transition from (either case of) double support to standing (i.e., from either S3 or S4, to S2) is based on the timing associated with crossing the CoP threshold. That is, if the CoP does not cross the CoP threshold within a given time following heel strike (i.e., if the controller remains in either state S3 or S4 for a given duration), subsequent crossing of the CoP threshold will transition to standing (S2) rather than to the corresponding double support configuration. That is, a sufficient pause during gait indicates to the system that the user wishes to stand, rather than continue walking forward. A summary of all switching conditions, governing the user interface with the FSM controller, is given in Table 3-2.

The previous discussion indicates that the user-initiated right and left steps occur when the estimated location of the CoP (relative to the forward heel) exceeds a given threshold. The authors have found that this approach provides enhanced robustness when this threshold is a function of the step length. That is, despite high-gain trajectory control in the joints of the orthosis during swing phase, scuffing of the foot on the ground, as occasionally occurs, in combination with compliance in the orthosis structure, can alter the step length during walking. In the case of a small step length, the forward thigh is nearly vertical, and the user is more easily able to move the CoP forward of the forward heel. In the case of a large step length, the forward thigh is forms a larger angle with the vertical, and moving the CoP forward is more difficult. As such, the CoP threshold during walking was constructed as a linear function, where the CoP threshold (i.e., the amount the CoP must lie ahead of the forward heel) decreases with increasing step size.

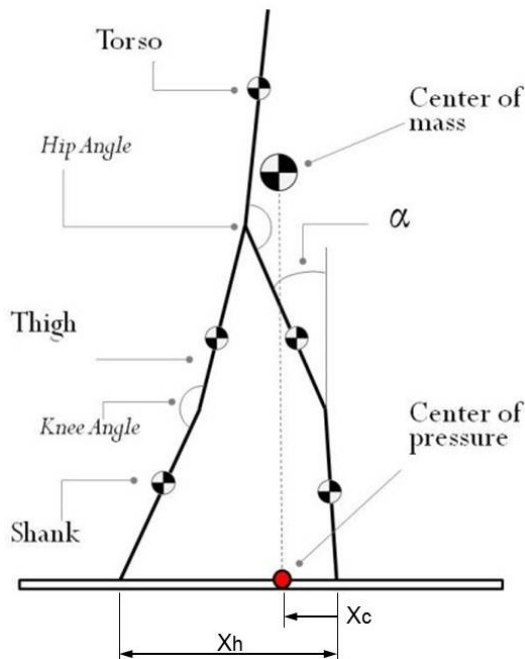


Figure 3-5. Schematic indicating estimated stride length (X_h) and center of pressure (X_c), both estimated based on the configuration of the orthosis.

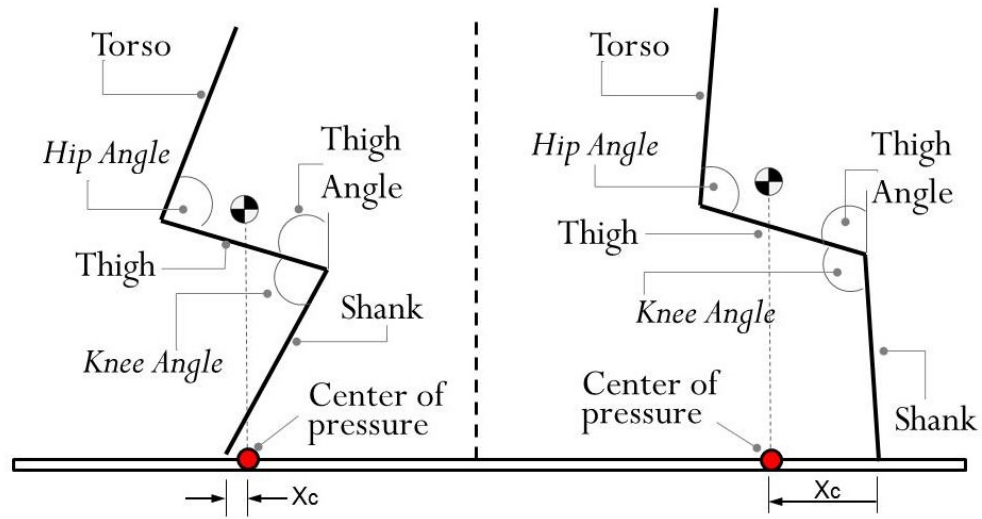


Figure 3-6. Schematic indicating the use of center of pressure (X_c) estimate for purposes of sit-to-stand and stand-to-sit transitions.

STATE MACHINE SWITCHING CONDITIONS

Transition	Condition
S1 to S5	The user leans forward and pushes up.
S5 to S2	Hip and knee joints meet the Standing (S2) configuration.
S2 to S7	The user leans forward and left.
S7 to S3	Hip and knee joints meet the Right Forward (S3) configuration.
S3 to S8	The user leans forward.
S8 to S4	Hip and knee joints meet the Left Forward (S4) configuration.
S4 to S9	The user leans forward.
S9 to S3	Hip and knee joints meet the Right Forward (S3) configuration.
S3 to S10	The user pauses for a predetermined period prior to leaning forward.
S10 to S2	Hip and knee joints meet the Standing (S2) configuration.
S2 to S6	The user leans backward.
S6 to S1	A predetermined time has lapsed.
S2 to S11	The user leans forward and right.
S11 to S4	Hip and knee joints meet the Left Forward (S4) configuration.
S4 to S12	The user pauses for a predetermined period prior to leaning forward.
S12 to S2	Hip and knee joints meet the Standing (S2) configuration.

Table 3-2. Walking trajectories corresponding to finite states as indicated.

Experimental Implementation

The proposed control architecture (defined by Fig. 3-3, Table 3-1, and Table 3-2) was implemented on the previously described powered lower limb orthosis, and the ability of the system to enable a user to autonomously perform the basic movements associated with legged mobility (i.e., sitting, standing, and level walking) was assessed in preliminary trials conducted with a paraplegic subject. The subject was a 35-year-old male (1.85 m, 73 kg) with a T10 motor and sensory complete injury (i.e., ASIA A), 9 years post injury. The evaluations were conducted at the Shepherd Center (Atlanta GA, USA), a rehabilitation hospital specializing in spinal cord injury. The testing was approved by both the respective Vanderbilt University and Shepherd Center Institutional Review Boards. All data presented here corresponds to walking conducted using a walker as a stability aid. The subject is shown wearing the orthosis and using the walker in Fig. 3-7.

The ability of the powered orthosis and control architecture to provide autonomously commanded sitting, standing, and walking was assessed by having the subject autonomously perform a timed-up-and-go (TUG) test. The TUG test is a standard clinical measure for assessing legged mobility [35]. In this test the subject starts seated in a chair, and given a start command, stands up, walks forward three meters, turns around in place, walks back to the starting point, and sits down in the chair. In order to assess the ability of the subject to autonomously control movements of the orthosis, this test was repeated a number of times, until the subject was comfortable performing the test. Once comfortable with the task, the subject was asked to repeat the TUG test three times. The set of data that corresponds to the third of these three TUG tests is shown in Fig. 3-8. Specifically, the figure shows the right and left hip and knee joint angles corresponding to this TUG test, along with the corresponding states of the FSM. In the sequence, the user starts in the sitting state (S1), after which the system enters the sitting to standing mode (S5), in which both hips and both knees provide torques to facilitate joint extension. Following S5, the state history depicts a series of consecutive steps, followed by a period of standing (S2), during which the subject turned in place, with the aid of the walker. The first series of steps is then followed by a second series, during which the subject returned to the chair. Once at the chair, the subject

again entered standing mode (S2), allowing the subject to turn in place, prior to returning to a seated position in the chair. A video of actual TUG test corresponding to this data can be viewed at: <http://research.vuse.vanderbilt.edu/cim/quinteroetal.wmv>.

Recall that the threshold for the CoP during walking is function of the step length. Figure 3-9 shows the system state, the estimated CoP (X_c), and the CoP switching threshold (X_e) for several steps (of slightly varying length). As seen in the figure, the CoP threshold (X_e) varies with step length (X_n). In general, when the CoP (X_c) exceeds the threshold at the end of the swing phase trajectory, the controller will switch immediately to the contralateral swing phase (i.e., switching between S8 and S9). If the CoP does not cross the CoP threshold at the end of swing phase, the controller will remain in the respective double support phase (S3 or S4) until the user shifts the CoP to cross the CoP threshold.

Figure 3-10 presents the sequences of finite states corresponding to each of the three TUG tests. The subject completed the three tests in 103, 128, and 112 s, respectively. The average time to complete the sequence was 114 s, with a standard deviation of 8.6 s (7.5%). The consistency between trials (i.e., standard deviation of $\pm 7.5\%$) indicates that the control approach appeared to provide a repeatable means for the subject to control the basic movements associated with legged mobility.

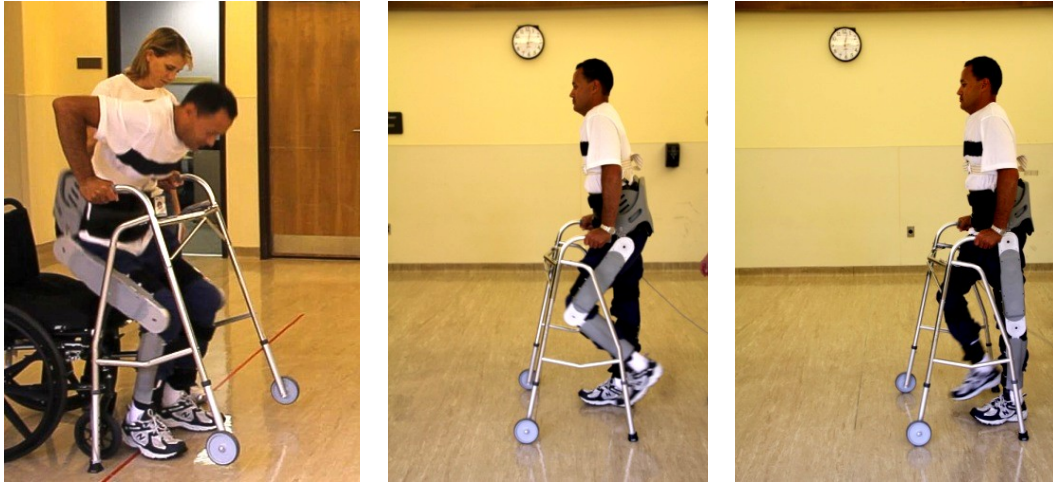


Figure 3-7. Photographic sequence showing standing, a left step, and a right step.

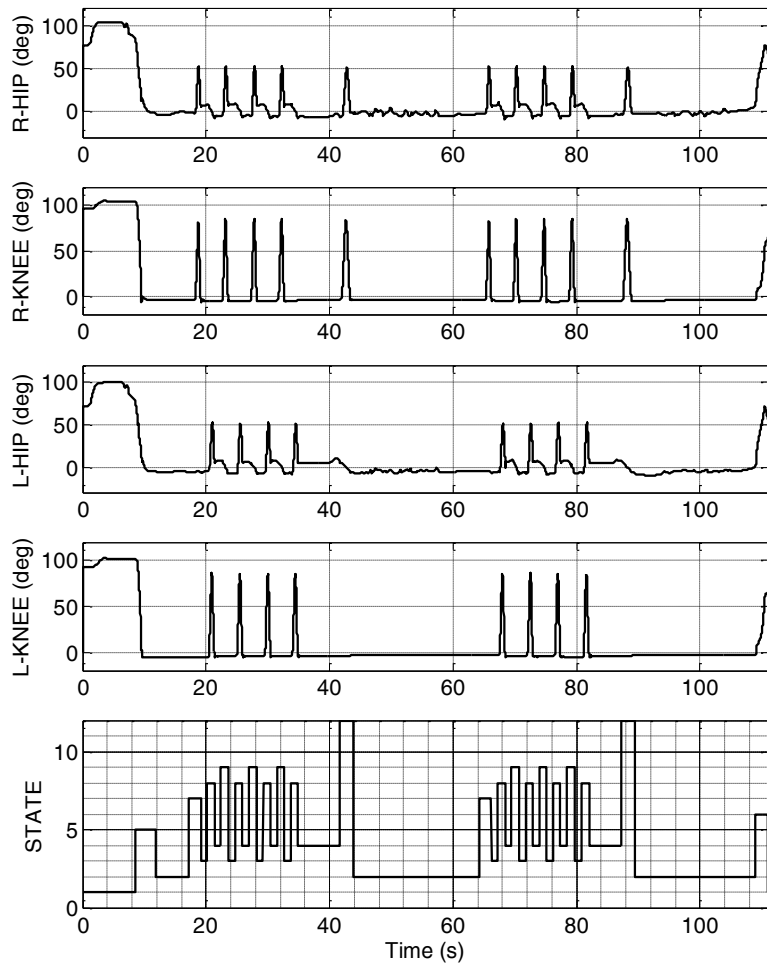


Figure 3-8. Joint angles and controller state during the third TUG test.

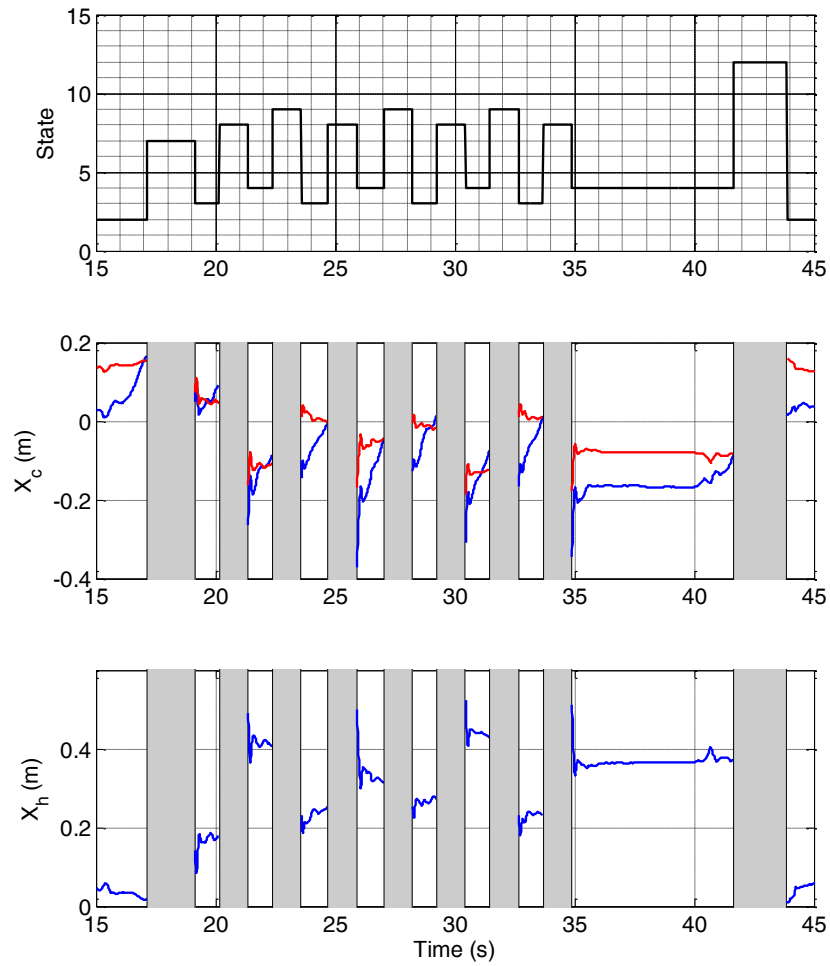


Figure 3-9. Data excerpted from Fig. 3-8. Top row: finite state corresponding to a sequence of steps. Middle row: center of pressure estimate (X_c , blue) and center of pressure threshold (X_c , red). Bottom row: step length estimate (X_h).

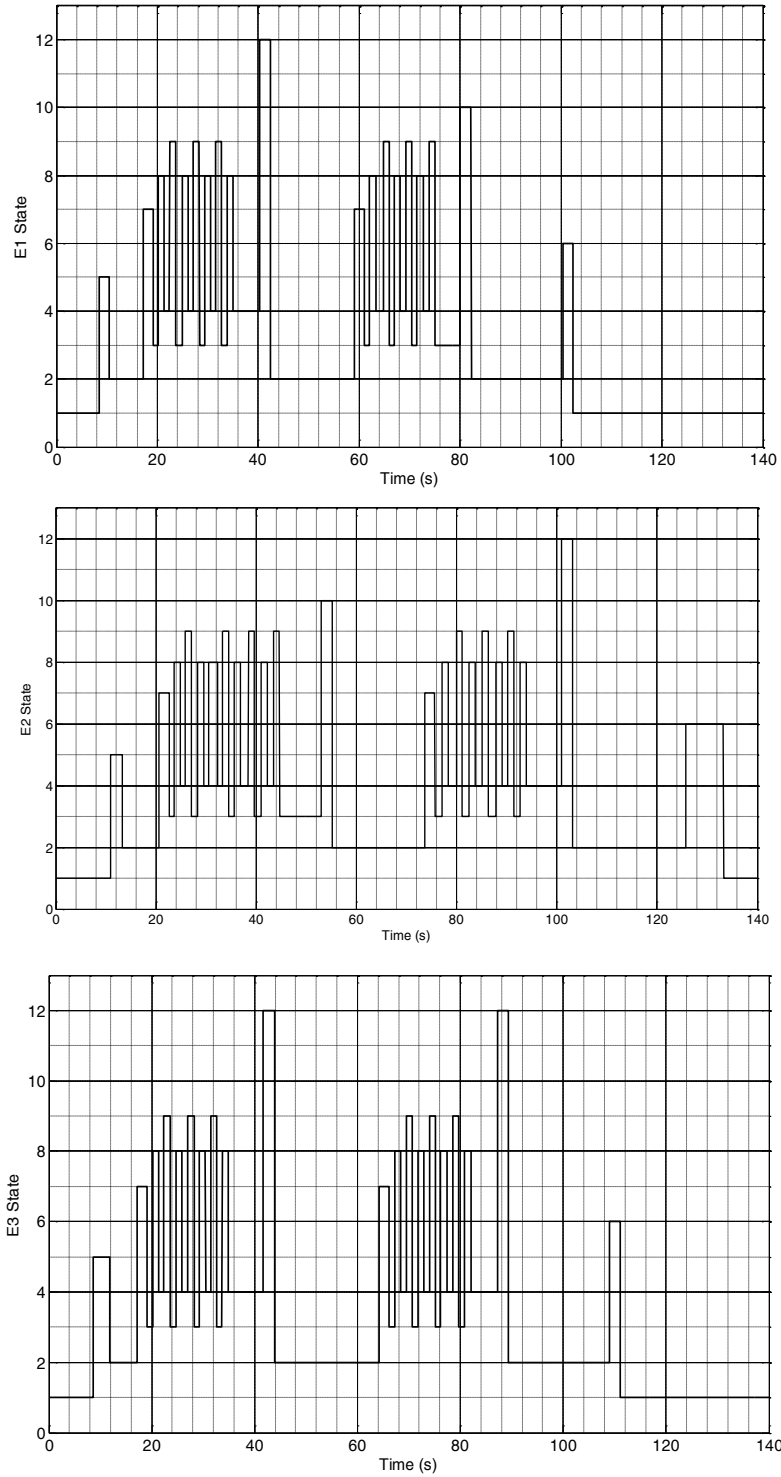


Figure 3-10. Finite states corresponding to each of the three TUG tests.

Conclusion

This paper presents a method for the control of a powered orthosis that enables autonomous (user-controlled) basic legged mobility, including sitting, standing, and walking, for persons with paraplegia (i.e., enables the user to autonomously navigate through these movements, without the aid of push-buttons or an external operator). The architecture, summarized by Fig. 3-3 and Tables 3-1 and 3-2, incorporates a finite state structure, in which the joints assume either high or low output impedance, depending on the current finite state. Switching between finite states is largely dependent on an estimate of the location of the CoP relative to the forward heel. The approach was implemented on a powered lower limb orthosis and was assessed by having a subject with a T10 complete injury autonomously perform a series of timed-up-and-go tests. The ability of the subject to perform these tests, and the consistency of the movement between tests, indicate that the control methodology was effective in enabling the user to autonomously perform the basic movements associated with legged mobility (i.e., sitting, standing, and walking).

References

- [1] "Spinal Cord Injury Facts and Figures at a Glance," <https://www.nscisc.uab.edu>, 2011.
- [2] Brown-Triolo, D. L., Roach, M. J., Nelson, K., and Triolo, R. J., 2002, "Consumer perspectives on mobility: implications for neuroprosthesis design," *Journal of Rehabilitation Research and Development*, pp. 659-669.
- [3] Hanson, R. W., and Franklin, M. R., 1976, "Sexual loss in relation to other functional losses for spinal cord injured males," *Archives of Physical Medicine and Rehabilitation*, 57, pp. 291-293.
- [4] Phillips, L., Ozer, M., Axelson, P., and Fonseca, J., 1987, *Spinal cord injury: A guide for patient and family*, Raven Press.
- [5] Audu, M. L., To, C. S., Kobetic, R., and Triolo, R. J., 2010, "Gait evaluation of a novel hip constraint orthosis with implication for walking in paraplegia," *IEEE Transactions on Neural Systems and Rehabilitation Engineering*, 18(6), pp. 610-618.
- [6] Kobetic, R., To, C. S., Schnellenberger, J. R., Audu, M. L., Bulea, T. C., Gaudio, R., Pinault, G., Tashman, S., and Triolo, R. J., 2009, "Development of hybrid orthosis for standing, walking, and stair climbing after spinal cord injury," *Journal of Rehabilitation Research & Development*, 43(3), pp. 447-462.
- [7] To, C. S., Kobetic, R., Schnellenberger, J. R., Audu, M. L., and Triolo, R. J., 2008,

- "Design of a variable constraint hip mechanism for a hybrid neuroprosthesis to restore gait after spinal cord injury," *IEEE/ASME Transactions on Mechatronics*, 13(2), pp. 197-205.
- [8] Durfee, W. K., and Rivard, A., 2005, "Design and Simulation of a Pneumatic, Stored-energy, Hybrid Orthosis for Gait Restoration," *Journal of Biomechanical Engineering*, 127(6), pp. 1014-1019.
- [9] Goldfarb, M., Korkowski, K., Harrold, B., and Durfee, W., 2003, "Preliminary evaluation of a controlled-brake orthosis for FES-aided gait," *IEEE Transactions on Neural Systems and Rehabilitation Engineering*, 11(3), pp. 241-248.
- [10] Ohta, Y., Yano, H., Suzuki, R., Yoshida, M., Kawashima, N., and Nakazawa, K., 2007, "A two-degree-of-freedom motor-powered gait orthosis for spinal cord injury patients," *Proceedings of the Institution of Mechanical Engineers, Part H: Journal of Engineering in Medicine*, 221(6), pp. 629-639.
- [11] Kwa, H. K., Noorden, J. H., Missel, M., Craig, T., Pratt, J. E., and Neuhaus, P. D., 2009, "Development of the IHMC mobility assist exoskeleton," *Proceedings of the 2009 IEEE international conference on Robotics and Automation*, IEEE Press, Kobe, Japan, pp. 1349-1355.
- [12] Neuhaus, P. D., Noorden, J. H., Craig, T. J., Torres, T., Kirschbaum, J., and Pratt, J. E., 2011, "Design and Evaluation of Mina: a Robotic Orthosis for Paraplegics," *International Conference on Rehabilitation Robotics*, IEEE Press, Zurich, Switzerland, pp. 870-877.
- [13] Tsukahara, A., Hasegawa, Y., and Sankai, Y., 2009, "Standing-up motion support for paraplegic patient with Robot Suit HAL," *IEEE 11th International Conference on Rehabilitation Robotics*, IEEE Press, Kyoto, Japan, pp. 211-217.
- [14] Hasegawa, Y., Jang, J., and Sankai, Y., 2009, "Cooperative walk control of paraplegia patient and assistive system," *IEEE/RSJ International Conference on Intelligent Robots and Systems*, IEEE Press, St. Louis, USA, pp. 4481-4486.
- [15] Suzuki, K., Mito, G., Kawamoto, H., Hasegawa, Y., and Sankai, Y., 2007, "Intention-based walking support for paraplegia patients with Robot Suit HAL," *Advanced Robotics*, 21(12), pp. 1441-1469.
- [16] Tsukahara, A., Kawanishi, R., Hasegawa, Y., and Sankai, Y., 2010, "Sit-to-Stand and Stand-to-Sit Transfer Support for Complete Paraplegic Patients with Robot Suit HAL," *Advanced Robotics*, 24(11), pp. 1615-1638.
- [17] Podsiadlo, D., and Richardson, S., 1991 "The timed "Up & Go": a test of basic functional mobility for frail elderly persons," *J Am Geriatr Soc*, 39(2), pp. 142-148.

CHAPTER IV

Manuscript 3: A Preliminary Assessment of Mobility and Exertion in a Lower Limb Exoskeleton for Persons with Paraplegia

Ryan J. Farris, Hugo A. Quintero, Clare Hartigan, and Michael Goldfarb

Vanderbilt University

Nashville, TN

Submitted as a Regular Paper to the

IEEE/ASME Transactions on Neural Systems and Rehabilitation Engineering

(In Review)

Abstract

This paper describes a functional assessment of a powered lower limb exoskeleton designed to provide gait assistance to persons with paraplegia. The authors propose an assessment protocol for assessing the mobility and exertion associated with systems that provide legged mobility assistance for persons with SCI. The mobility aspect of the assessment protocol is based on two well-established assessment tools in the clinical community, which are the timed-up-and-go test and the ten meter walk test. The exertion aspect of the assessment is based on the change in heart rate entailed in the two standard tests, in addition to the Borg rating of perceived exertion. The proposed assessment protocol was implemented on a single SCI subject, and the mobility and exertion associated with four cases of mobility and stability aids was assessed. The results indicate that the powered exoskeleton affords similar mobility and requires a somewhat lower level of exertion relative to long-leg braces with a swing-through gait, and affords significantly improved mobility with significantly less exertion relative to long-leg braces with a reciprocal gait.

Introduction

One of the most significant impairments resulting from paraplegia is the loss of mobility [1]. In addition to diminished mobility, the inability to stand and walk entails significant physiological impairments, including loss of bone mineral content, frequent skin breakdown problems, increased incidence of urinary tract infection, muscle spasticity, impaired lymphatic and vascular circulation, impaired digestive operation, and reduced respiratory and cardiovascular capacities [2].

In an effort to facilitate legged locomotion in individuals with paraplegia, several computer-controlled lower limb orthosis systems have been, and are being, developed and described in the research literature. Such orthoses include hybrid FES-systems, which supplement functional electrical stimulation (FES) of leg muscles with a computer-controlled orthosis; and fully powered orthoses (or exoskeletons), which utilize electric motors as the primary form of motive assistance. Recent examples of the former include those described in [3-7], while recent examples of the latter include those described in [8-14], in addition to the ReWalk (Argo Medical

Technologies) and eLEGS (Berkeley Bionics) systems, two emerging commercial systems that have not yet been described in the engineering literature.

Despite the number of emerging systems designed to provide legged mobility assistance for individuals with paraplegia, there is currently a lack of published data by which the capabilities of each can be comparatively assessed. That is, although several such mobility assistance systems have been characterized, each system has generally used different metrics. The absence of standardized metrics is a significant impediment in uniformly and comparatively assessing the capabilities provided by a given system. This paper proposes an assessment method, and uses it to assess the mobility and level of exertion associated with the legged mobility provided by a powered lower limb exoskeleton, relative to two cases of legged mobility afforded by long-leg braces (considered as the standard current intervention for legged mobility).

A Proposed Set of Assessment Metrics

Metrics Used in Prior Publications

In [4], the authors indicate ability of the hybrid-FES system to provide legged mobility to an SCI subject by showing the variation in knee joint angle kinematics over a number of strides. In [7], the authors indicate the efficacy of the hybrid-FES system in providing legged mobility, relative to other legged mobility interventions, on four paraplegic subjects using as primary measures the average walking speed; percent increase in heart rate and blood pressure; oxygen uptake and carbon dioxide exhalation; and variation in hip and knee joint angle kinematics over a number of strides. In [8], the authors assess the efficacy of a powered orthosis, relative to a passive reciprocating gait orthosis, on four paraplegic subjects by measuring average walking speed; average step length; and the vertical and lateral motion of each subject's head. In [10], the authors quantitatively characterize the efficacy of a powered lower limb exoskeleton primarily by characterizing the walking speed with two paraplegic individuals. In this publication, the authors use heart rate, respiration rate, skin color, and perspiration levels to qualitatively assess level of exertion; the ability to maintain eye contact to qualitatively assess cognitive effort; and the ability to catch a ball

to qualitatively assess standing stability. In [11] and [14], the authors evaluated the ability of a powered lower limb exoskeleton to provide sit-to-stand and stand-to-sit maneuvers to a paraplegic user by reporting the hip and knee joint angles during these maneuvers, and also by reporting the force exerted by the user's arms on a horizontal bar. In [13], the authors assess the ability of a powered exoskeleton to assist persons with incomplete SCI by comparing hip and knee joint angles and stride length for walking with and without the exoskeleton. Finally, in [15], the authors demonstrated the ability of a powered exoskeleton to provide walking by comparing hip and knee joint kinematics to healthy kinematics, and by reporting average walking speed.

A Standardized Set of Metrics

Although the metrics utilized in the aforementioned publications provide insight into the efficacy of each respective system, these measures in general lack uniformity and standardization, and none collectively characterize the basic functionality of a lower limb exoskeleton, which consists of standing, walking, turning, and sitting. As such, the authors propose the use of standardized walking tests that collectively characterize the degree of mobility provided by, and level of exertion associated with, a lower limb exoskeleton system for spinal cord injured persons.

A recent survey of outcome measures for persons with SCI identifies seven primary measures associated with functional ambulation [16], which include the Timed Up and Go (TUG) test, the Ten Meter Walk Test (10MWT), the Six Minute Walk Test (6MWT), the Spinal-Cord Injury Functional Ambulation Inventory (SCI-FAI), the Functional Independence Measure (FIM), the Spinal Cord Independence Measure (SCIM), and the Walking Index for Spinal Cord Injury (WISCI-II). Of these, the first three are timed measures, the latter three are categorical assessments of ambulation, and the SCI-FAI has components of both. For purposes of assessing the efficacy of mobility systems for providing legged assistance to individuals with SCI, a measurable standardized metric is preferred relative to a classification, since it largely removes subjectivity from the assessment, and further provides a means of characterizing exertion in addition to mobility. As such, for purposes of this paper, the measurable assessments (TUG, 10MWT, and 6MWT) were favored over the observational assessments (SCI-FAI, FIM, SCIM, and WISCI). With regard to the first of these

measurable assessments, the TUG test measures the time required for a subject to stand from a seated position, walk three meters, turn, walk back three meters, turn, and return to the seated position. This test, which was originally proposed in [17], has been shown to have high test-retest reliability as a mobility measure across a wide spectrum of patient populations, including persons with stroke impairment, Parkinson's disease, arthritis, cerebellar disorders, and unilateral lower limb amputation [17-22]. The Ten Meter Walk Test (10MWT) measures the time for a patient to walk ten meters, not including any acceleration or deceleration phases. Like the TUG test, the 10MWT has also been shown to have a high degree of validity and test-retest reliability in assessing the functional mobility of persons with neurological mobility impairment [23-26]. Finally, the Six Minute Walk Test (6MWT) measures the distance a person can walk in six minutes. This test is ideally performed using a straight walkway approximately 30 m long (e.g., a hallway), where the subject turns around a marker following every 30 m length. This measure was originally proposed to assess cardiovascular and respiratory capacity in persons with heart or lung diseases[26, 27], but has also been utilized as a functional mobility assessment for persons with neurologically impaired mobility [28-30].

Since the TUG test is the only one of the aforementioned timed assessments that encompasses sit-to-stand, stand-to-sit, turning, and walking; since these movements constitute the basic set of legged mobility functionality; and since the TUG test has been shown to have a test-retest reliability correlation coefficient of 0.98 among the SCI population [26], the TUG test was selected as an obvious independent measure for characterizing legged mobility systems for SCI. Further, since the TUG test is used across a wide range of impairments, it offers the added benefit of comparison of the SCI target population to a much broader patient population.

While the TUG test largely characterizes the ability of a subject to perform functional transitions (sit-to-stand, stand-to-walk, walk-to-stand, turn in place, and stand-to-sit), the 6MWT and the 10MWT largely characterize a person's (essentially steady state) walking speed. Accordingly, the two measures have been shown to have a strong correlation (i.e., a correlation coefficient of 0.95) in the SCI population [26]. Further, like the TUG test, both measures have been

demonstrated to have a high test-retest correlation coefficient (both approximately 0.98) [26].

Despite the high degree of correlation between the 10MWT and the 6MWT, it has been suggested that the 6MWT can provide a measure of endurance (or exertion) that is not as well captured by the 10MWT, and it has been suggested that to “provide the most comprehensive battery [of testing] it will be important to include a measure of endurance such as the 6MWT” [31]. The authors agree with this assertion; however, the 6MWT is more difficult to administer than the 10MWT, since it requires ambulation over a 30 m walkway. Since an effective standardized assessment procedure should be administered in as universal a setting as possible, and in as short a period as possible; since both the 10MWT and 6MWT assess average walking speed, and since both demonstrate similar reliability; since the two measures are strongly correlated; and since the 10MWT is more easily administered and requires far less space than the 6MWT, the authors propose the use of the 10MWT to characterize the steady-state walking functionality of the lower limb exoskeleton systems. Note that use of the 10MWT, in lieu of the 6MWT, is further supported by [31], who suggest that the 10MWT provides “the most valid measure of improvement in gait and ambulation” for the SCI population, and [30], who assert that “the 10MWT appears to be the best tool to assess walking capacity in SCI subjects.” As such, the TUG and 10MWT assessments are utilized herein to characterize the efficacy of a lower limb exoskeleton system in providing legged mobility to a person with paraplegia, and the basic transitions associated with it. The authors acknowledge, however, that supplementing these outcome measures with the 6MWT would provide a more complete assessment of the efficacy of this and other lower limb gait assistance systems.

A gait assistance system should provide effective mobility without an undue level of exertion. The single measure typically utilized in both the TUG and 10MWT is the time required to complete each respective test. This measure provides a quantitative measure of mobility (the former largely characterizing the efficacy of gait transitions, the latter characterizing primarily the efficacy of steady-state walking), but neither characterizes the level of exertion associated with these activities. In order to characterize the level of exertion, the time to complete these tests is

supplemented with measurement of the pre- and post-test heart rate, which is commonly used to measure physical exertion. This physiological measure of exertion is further supplemented by rating each test with the Borg Rating of Perceived Exertion (RPE) Scale, as proposed in [32], which is well-validated and widely used indication of perceptual effort, in which a subject rates his or her level of exertion on a scale of 6 to 20, where 6 corresponds to “no exertion at all” and 20 corresponds to “maximal exertion.” On this scale, casual healthy walking corresponds to a rating of 9.

Thus, the proposed assessment of a powered legged assistance system for persons with SCI consists of the combination of a TUG test and a 10MWT, where the mobility provided by the system is characterized by the time required to complete each test, and the exertion required by the system is characterized by the change in pre- and post-test heart rate, and by the Borg Rating of Perceived Exertion associated with each test.

Comparative Assessment of Two Mobility Aids

The previously discussed assessment procedure was utilized to comparatively assess the efficacy of a powered lower limb exoskeleton system in providing legged mobility to a paraplegic subject with a T10 motor and sensory complete injury (i.e., American Spinal Injury Association, ASIA, A classification). Specifically, this paper presents the aforementioned mobility and exertion measures for the TUG and 10MW tests for four mobility aid combinations, which include 1) the Vanderbilt powered lower limb exoskeleton with a walker; 2) the Vanderbilt powered lower limb exoskeleton with forearm crutches; 3) a set of long-leg braces with a walker, using a swing-through type gait; and 4) a set of long-leg braces with a walker, using a reciprocal type gait. A video is included with the supplemental material that shows the subject walking with each of the four methods.

Vanderbilt Lower Limb Exoskeleton

The Vanderbilt lower limb exoskeleton, shown in Fig. 4-1, provides powered assistance in the

sagittal plane at both hip and knee joints. The exoskeleton consists of a hip segment, a right and left thigh segment, and a right and left shank segment. The hip segment contains a lithium polymer battery which powers the exoskeleton, of which each thigh segment contains a pair of brushless DC motors, which actuate the hip and knee joints respectively through speed reduction transmissions. The knee joints are additionally equipped with normally-locked brakes, in order to preclude knee buckling in the event of a power failure. Although the exoskeleton does not explicitly contain a foot segment or ankle joint, it is designed to be used in conjunction with a standard ankle foot orthosis (AFO), which provides stability at the ankle, and precludes foot drop during the swing phase of gait. The total mass of the exoskeleton, including the battery, is 12 kg (26.4 lb). A more detailed description of the exoskeleton design, including a description of the embedded electronics system, is given in [15].

As required by the assessment procedures previously described, the powered lower limb exoskeleton enables sit-to-stand transitions, standing, stand-to-walk transitions, walking, walk-to-stand transitions, and stand-to-sit transitions. In order to enable the user to have autonomous control of these maneuvers, a user interface approach was developed based on the user's ability to affect his or her center of pressure via the use of his or her upper body, in combination with a stability aid. Specifically, based on sensors embedded in the exoskeleton, the control system estimates the location of the user's center of pressure (CoP), defined as the user's center of mass projection onto the (assumed horizontal) ground plane, and uses the distance between the CoP and the location of the forward ankle joint as the primary command input. Thus, the user transitions out of a given activity (sitting, standing, or walking) by leaning forward or back, such that the CoP moves in an anterior or posterior direction, which commands the controller to transition to a different activity mode. This approach enables the user to autonomously perform the TUG test and 10MWT presented here, without the assistance of an external operator. A more detailed description of the exoskeleton control architecture and user interface, which discusses more specifically the conditions required to move between activities, is given in [33]. Finally, note that the turning maneuver (performed twice in each TUG test) does not entail a separate control

mode, but rather is performed in the standing activity mode, with the use of the stability aid, by incrementally twisting the upper body and turning in place. This follows the typical turning methodology utilized with long-leg braces (see discussion below).



Figure 4-1. Vanderbilt lower limb exoskeleton.

Long-leg Braces

The mobility and level of exertion associated with the powered exoskeleton were compared to the respective mobility and level of exertion associated with long-leg brace ambulation. Long-leg

braces are the most common legged mobility aids used by persons with paraplegia. The braces used in this case study, which are representative of this type of mobility aid, are shown in Fig. 4-2. These braces consist of a thigh segment, shank segment, and integrated shoe for each leg. The knee joint of each leg consists of a latching hinge joint, such that the joint can remain flexed while donning or sitting, but mechanically locks at full extension, and remains locked during use. Following use, the user can unlatch the knee joints with the posterior lever, which facilitates a more natural seated posture, and simplifies the doffing procedure. Most long-leg braces incorporate posterior bail locks, which release the knees as the metal bail (located behind and slightly above the knee) is forced upward by the edge of a seat as the user leans backwards. In addition to locking knee joints, each leg of the long-leg braces incorporates an articulated ankle joint, which allows limited ankle dorsiflexion, but precludes ankle plantarflexion.

Long leg braces such as those shown in Fig. 4-2 require the use of a stability aid, and are typically used with either a swing-through or reciprocal method of ambulation. The reciprocal method is an approximation of healthy gait, in which the subject alternatively takes left and right steps. Specifically, the subject uses the stability aid to alternately lean left and right, which unweights the swing leg, while simultaneously leaning forward, such that gravity can act to swing the leg forward. This method tends to be slower and more laborious than the swing-through method, in which the subject moves the stability aid forward, resulting in a forward leaning posture, and unweights both legs simultaneously, such that gravity acts to swing both legs through together. This method does not require leaning side-to-side, and since one leg need not remain on the ground while the other is in swing, it generally affords greater ground clearance and larger strides. Note that the swing-through method is typically used with a “spreader bar,” as shown in Fig. 4-2, which mechanically couples both legs together near the ankle joints.

A typical sit-to-stand maneuver with braces starts with the subject seated in a chair, with the knee joints fully extended and locked, with the legs fully extended in front of the user, and the heels of the shoes in contact with the ground. Using a walker as a stability aid, as was the case with the assessments reported here, the user pushes upward in the walker, such that his or her legs are

drawn up through the walker, until in a fully upright position. A typical stand-to-sit maneuver requires that the user position himself or herself in front of a chair, then bending forward at the waist, and essentially falling backward into the chair as the chair lifts the bail locks, unlocking the knees. Finally, turning in place is afforded by incrementally rotating the stability aid by twisting the upper body, then unweighting the legs to reorient them with the upper body and stability aid. Using this method, a user can typically turn 180 deg in three or four increments with a walker, and approximately twice as many increments with forearm crutches.



Figure 4-2. Long-leg braces used in assessments (shown with spreader bar attached for swing-through gait).

Assessment Methodology

The mobility and level of exertion associated with the powered lower limb exoskeleton was

assessed with the previously described metrics, and compared to the respective mobility and level of exertion associated with long leg brace ambulation. These assessments were performed on a single paraplegic subject with a T10 motor and sensory complete injury (ASIA A classification). The subject was 35 year of age, 9 years post-injury, 1.85 m (6 ft) tall, and with a body mass at the time of testing of 73 k (160 lb). The subject is shown wearing the lower limb exoskeleton and long leg braces in Figs. 4-3 and 4-4, respectively.



Figure 4-3. T10 complete paraplegic subject wearing Vanderbilt exoskeleton.



Figure 4-4. Subject wearing long-leg braces.

TUG Test Protocol

For the TUG test, the (lightly-colored) floor was marked with two lengths of dark tape placed 3 m (10 ft) apart, which designated the starting position and turning position, respectively. A wheelchair with locked wheels and footrests removed was used as the chair for the TUG test, and was positioned fully behind the starting position. The subject was instructed to wait for the verbal cue to start, then stand, walk until his body crossed the turning mark, turn, walk back to the chair, turn, and sit. The total time was recorded from the initial verbal cue, to the time the subject returned to a seated position in the wheelchair.

In order to standardize exertion measurement, the subject's heart rate was taken exactly one minute prior to the start of each TUG test, and exactly 30 sec following each TUG test. The heart rate measurement was taken with an automated monitor (Dynamap V100 by General Electric), which required approximately 20 sec from initiation (i.e., donning of finger clip) to measurement. Specifically, the TUG test was initiated 60 sec after reporting the subject's heart rate, while heart rate measurement was initiated 30 sec after TUG test completion (and as such the heart rate

measurement following each TUG test was reported approximately 50 sec after completion of the test). The subject was allowed to practice the TUG test until he felt comfortable performing it. Once the subject was comfortable performing the TUG test, the test and associated heart rate and perceived exertion measurements were performed three consecutive times. The subject was allowed a period of rest between each test, until he felt rested and ready to perform the next test.

10MWT Protocol

For the 10MWT, the floor was marked with two lengths of dark tape placed 10 m (33 ft) apart. In this test, the subject ambulated at a steady-state through the 10 m walkway (i.e., the subject starting walking several meters prior to the first mark, and continued to walk through the second mark. The starting and ending times were recorded based on the subject's body crossing the respective marks. As with the TUG test, the subject's heart rate was taken approximately 60 sec prior to and 60 sec following each test. Since the 10MWT does not start and end in a seated position, however, and since these measurements were taken in a seated position, the intervals between heart rate measurement and the start and end of the 10MWT were somewhat more approximate than during the TUG test. As with the TUG test, the subject completed the 10MWT three consecutive times, and was allowed to rest between tests until he felt ready to perform the next.

Mobility Aid and Stability Aid Combinations

Four cases of ambulation were assessed. The subject was able to independently perform both the TUG test and 10MWT with both a walker and with forearm crutches, and therefore both cases were assessed. When using the long-leg braces, the subject was able to independently perform these tests using a walker as a stability aid, but was not able to perform these tests with forearm crutches. As such, ambulation with the long-leg braces was conducted with a walker as stability aid, for the cases of reciprocal and swing-through ambulation.

For both cases using the exoskeleton, the TUG test started and ended in a seated position with both knees flexed. For both cases using the long-leg braces, the TUG test started in a seated

position with both knees fully extended and locked (i.e., the time required to extend and lock the knees prior to standing, was not included in the TUG test times). Although no assistance was provided to the subject during any of the tests, all tests involved the use of a gait belt and close monitoring by a trained physical therapist, as per the Institutional Review Board approval corresponding to these assessments.

Borg Rating of Perceived Exertion

Rather than rate each trial individually, the subject was asked to rate the collective battery of tests (i.e., three trials of a TUG test, and three trials of a 10MWT) for each combination of mobility and stability aid, using the Borg scale of perceived exertion. As such, each mobility and stability aid combination was assessed by the subject with a single Borg score.

Results and Discussion

The results of the assessment for each the four cases of ambulation are summarized in Table 4-1. Additionally, a video is provided with the supplemental material that provides a qualitative understanding of the legged mobility provided in each case. For each of the four cases of ambulation, the table lists the average TUG test time (in seconds) and corresponding standard deviation (in parentheses) for the three TUG trials; the average 10MWT time and corresponding standard deviation for the three 10MWT trials; the average change in pre- and post-test heart rate, and associated standard deviation across the three trials for each test type; and the subject's rating of perceived exertion corresponding to the battery of assessments for each ambulation case. A single-degree-of-freedom analysis of variance (ANOVA) was conducted to assess the extent to which the mean measurement of each test type was significantly different from each of the other test types. The mobility and exertion measures, and the extent to which they are different, are discussed in the sections below. Note that the ANOVA was conducted using a confidence level of 90%, unless otherwise noted in the discussion.

Walking Method	TUG Time (seconds)	Heart Rate Change (%)	10MWT Time (seconds)	Heart Rate Change (%)	BORG Perceived Exertion
LL Braces + Walker (Reciprocal)	178 (14)	41.8 (17.1)	109 (7)	18.4 (5.9)	16
LL Braces + Walker (Swing-Through)	118 (3)	19.0 (7.2)	89 (17)	16.1 (2.9)	13
Exoskeleton + Walker	107 (5)	10.1 (4.6)	81 (10)	5.4 (9.5)	12
Exoskeleton + Forearm Crutches	120 (4)	3.9 (5.4)	89 (4)	-1.2 (10.7)	10

*Results are average and (standard deviation) of three trials.

Table 4-1. Summary of Assessment Data.

Mobility

The principal measures of mobility consist of the average TUG test time and the average 10MWT time. The average TUG times for each mobility aid case, bracketed by plus and minus one standard deviation, are shown graphically in Fig. 4-5. As reported in Table 4-1, the exoskeleton with walker provided the fastest average TUG test time (107 sec), followed by the long-leg braces with a swing-through gait (118 sec), the exoskeleton with forearm crutches (120 sec), and lastly by the long-leg braces with reciprocal gait (178 sec). Based on the ANOVA, however, the difference in means between the exoskeleton and swing-through cases is not significant, while the difference between these means and the mean of the reciprocal gait with braces is significant by a substantial margin. The 10MWT times showed a similar trend, as shown graphically in Fig. 4-6. Specifically, the exoskeleton with walker provided the fastest average 10MWT time (81 sec), followed by the long-leg braces with a swing-through gait and exoskeleton with forearm crutches (each of which had an average time of 89 sec), and lastly by the long-leg braces with reciprocal gait (109 sec). As with the TUG times, based on the ANOVA, the difference in means between the former three cases is not significant, while the difference in means between the slowest of the first set (i.e., long-leg braces with swing-through gait) and the long-leg braces with reciprocal gait is significantly different (with a confidence level of 83%). Therefore, the mobility component of the assessment indicates that the exoskeleton (with either walker or forearm crutches) provides similar mobility to a

swing-through gait with braces and a walker, while all of these provide significantly improved mobility relative to the reciprocal gait afforded by the braces with a walker.

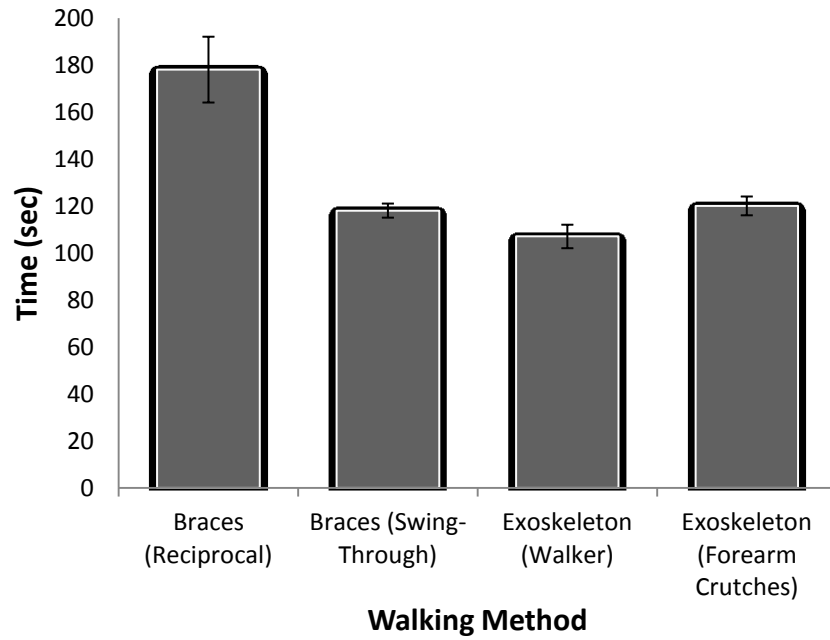


Figure 4-5. Graph of TUG test completion times in each walking method

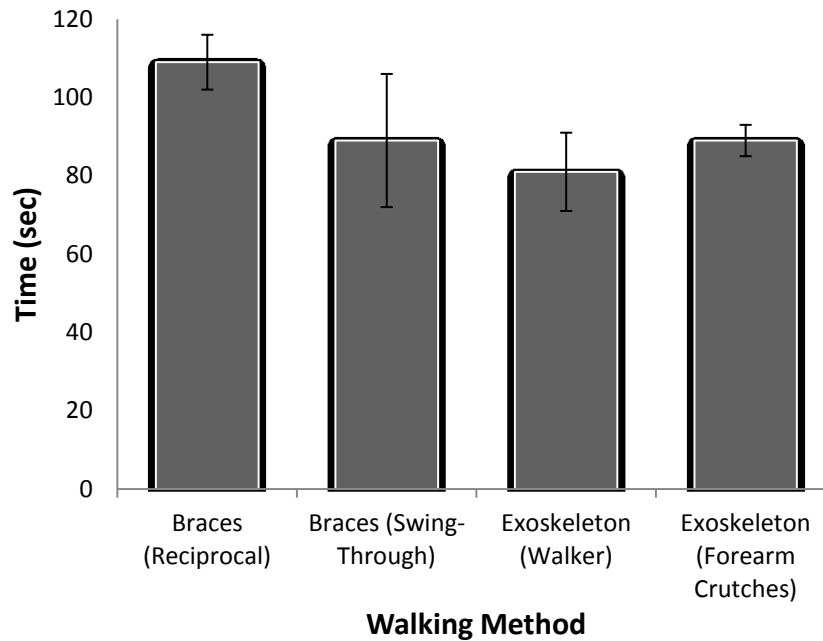


Figure 4-6. Graph of TMWT completion times in each walking method.

Exertion

The principal measures of exertion are the percent change in heart rate during the TUG and 10MWT tests, in addition to the Borg perceived exertion ratings. The percent change in heart rate is defined as the difference between the post and pre-test heart rates, divided by the pre-test heart rate (multiplied by 100). The average change in heart rate for both TUG and 10MWT is summarized graphically in Figs. 4-7 and 4-8. For both the TUG and 10MWT, the average change in heart rate was the smallest for the case of walking with the exoskeleton with forearm crutches (3.9% and -1.2%, respectively, where the latter indicates that on average, the heart rate decreased during the 10MWT). The other cases of walking were similarly ordered for both the TUG and 10MWT. In order of increasing average heart rate for the TUG and 10MWT, the remaining cases were ordered as the exoskeleton with walker (10.1% and 5.4%, respectively), the swing-through gait with the braces and walker (19.0% and 16.1%, respectively), and the reciprocal gait with the braces and walker (41.8% and 18.4%, respectively). Despite the fact that the average change in heart rate was much

lower for the exoskeleton with crutches and walker, respectively, relative to the braces with swing-through gait, the ANOVA indicates that the difference in means is not always statistically significant. Specifically, for the TUG test, the difference in means for the three lower average changes in heart rate is not statistically significant; these are, however, all statistically significantly lower than the case of reciprocal walking with braces. For the 10MWT, the difference in means of the two exoskeleton cases are not statistically different; the difference in means of the two cases with braces are also not statistically different; while the difference in means between these two groups are significantly different (but with the variance in data, only with a 61% confidence level). As such, for the TUG test, the exoskeleton (with both walker and crutches) and the swing-through gait with braces and walker required statistically similar levels of exertion, while the reciprocal gait with the braces and walker required a significantly greater level of exertion. With the 10MWT, both cases with the exoskeleton required similar levels of exertion, while both cases with the braces required significantly increased exertion.

The aforementioned measurements are reinforced by the Borg perceived exertion ratings. As previously mentioned, the subject provided a single, collective Borg perceived exertion rating for each mobility case, as graphically depicted in Fig. 4-9. The subject's ratings of perceived exertion correlates strongly with the order of mean changes in heart rate indicated in Figs. 4-7 and 4-8. That is, in order of increasing effort, the subject rated the exoskeleton with crutches as the least taxing (RPE of 10, which is slightly more than equivalent to healthy casual walking); followed by the exoskeleton with walker (RPE of 12); braces and walker with a swing-through gait (RPE of 13); and braces and walker with a reciprocal gait (RPE of 16). Thus, legged mobility with the exoskeleton was generally considered as "light exercise" while legged mobility with the braces was considered as "hard (heavy) exercise," according to the Borg scale [32].

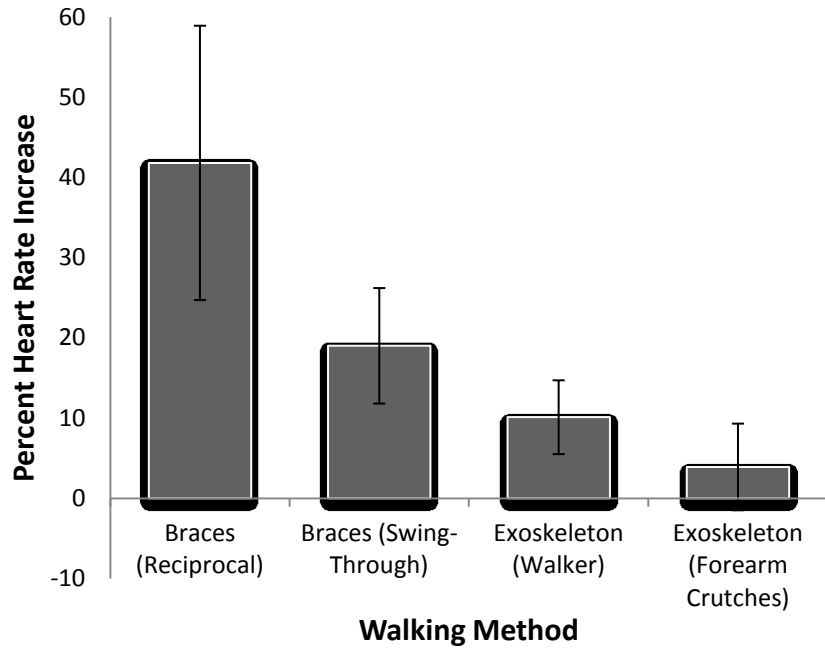


Figure 4-7. Graph of user exertion during TUG test in each walking method.

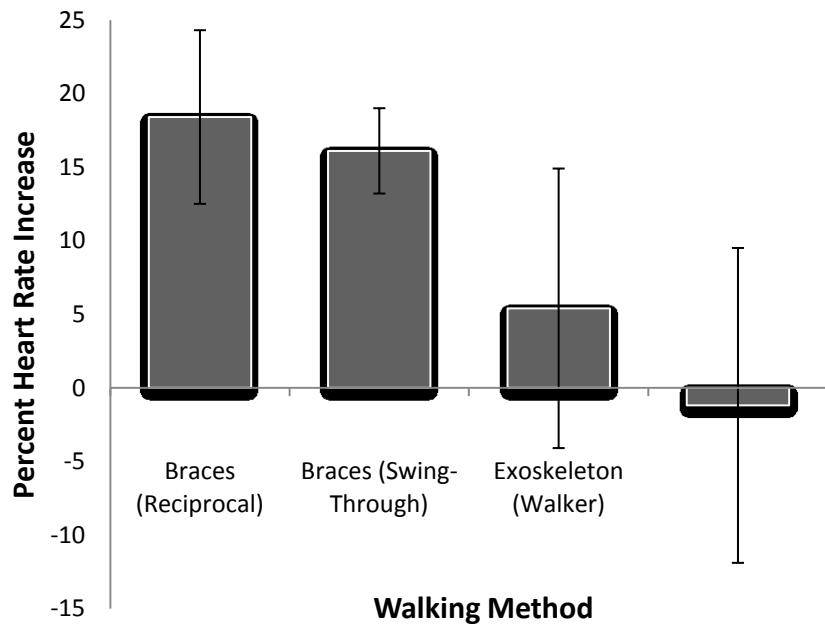


Figure 4-8. Graph of exertion during TMWT in each walking method.

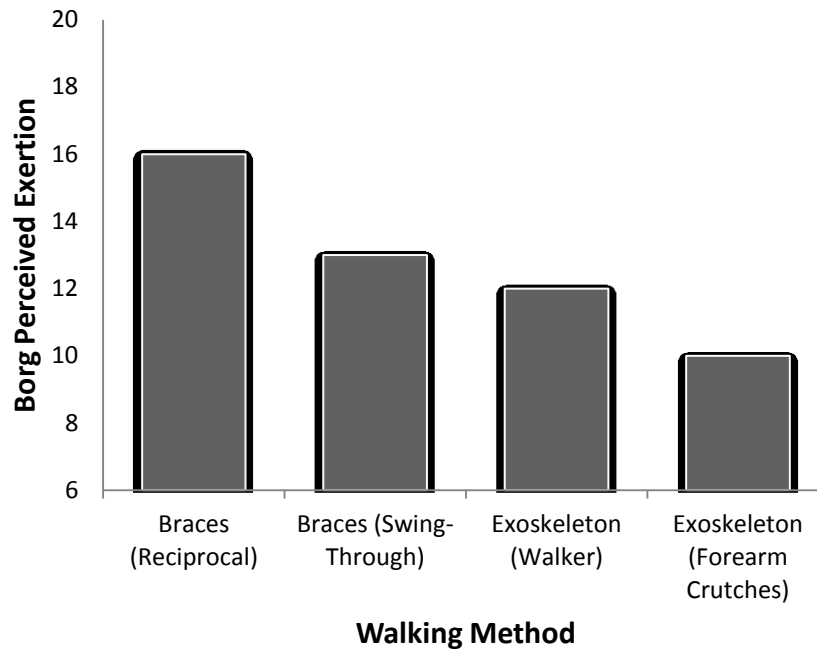


Figure 4-9. Graph of user-perceived exertion during standardized walking tests in each walking method. Note that the Borg Scale ranges from 6 ("no exertion") to 20 ("maximal exertion").

Consideration of Walking as a Fundamentally Reciprocal Activity

For purposes of completeness, the authors included the case of swing-through gait in the assessment and discussion presented here. One can legitimately argue, however, that “legged mobility” as applied to human subjects implies walking; walking fundamentally entails a reciprocal movement of the legs; and therefore, a swing-through gait should not be included in assessing the efficacy of a mobility aids for facilitating legged mobility in persons with SCI. If one therefore considers only the three cases of mobility aids that provide a reciprocal gait (i.e., the two exoskeleton cases and the reciprocal gait with braces and walker), then in all cases, the exoskeleton (with either stability aid) provides significantly faster TUG and 10MWT times, with significantly lower levels of exertion, relative to the braces. Specifically, the exoskeleton provides on average 37% faster TUG times and 22% faster 10MWT times, and concomitantly entails an 83% lower change in heart rate for the TUG test, and an 89% lower change in heart rate for the 10MWT

(note here that the two exoskeleton cases were averaged together, since as previously discussed, these cases are statistically similar). As such, based on the previously discussed measures of mobility and exertion in legged mobility aids, the exoskeleton provides significantly improved mobility, and concomitantly provides significantly less exertion, relative to the reciprocal walking enabled by long-leg braces and a walker.

Conclusion

Systems have started to emerge that provide legged mobility for persons with paraplegia. In this paper, the authors propose an assessment methodology to assess the efficacy of such systems, specifically with regard to mobility and exertion, based on the TUG test and 10MWT (two well-established assessments in the clinical community). Using this assessment methodology, the authors assessed four cases of legged mobility on a single paraplegic subject. Specifically, legged mobility was assessed with long-leg braces and a walker, with both a reciprocal and swing-through gait, and was also assessed with a powered lower limb exoskeleton, with both a walker and forearm crutches as a stability aid. The assessments suggest that the degree of mobility provided by the exoskeleton was statistically similar to the degree of mobility afforded by long-leg braces with a swing-through gait, while the level of exertion was similar to the swing-through gait for the TUG test, and significantly lower than the swing-through gait for the 10MWT. The assessments further suggest that the degree of mobility provided by the exoskeleton was significantly better than the degree of mobility provided by long-leg braces with a reciprocal gait, while the level of exertion required by the former was significantly lower than that required by the latter.

References

- [1] D. L. Brown-Triolo, M. J. Roach, K. Nelson, and R. J. Triolo, "Consumer perspectives on mobility: implications for neuroprosthesis design," presented at the Journal of Rehabilitation Research and Development, 2002.
- [2] L. Phillips, M. Ozer, P. Axelson, and J. Fonseca, *Spinal cord injury: A guide for patient and family*: Raven Press, 1987.
- [3] M. L. Audu, C. S. To, R. Kobetic, and R. J. Triolo, "Gait evaluation of a novel hip constraint orthosis with implication for walking in paraplegia," *IEEE Transactions on Neural Systems and Rehabilitation Engineering*, vol. 18, pp. 610-618, 2010.
- [4] R. Kobetic, C. S. To, J. R. Schnellenger, M. L. Audu, T. C. Bulea, R. Gaudio, G. Pinault, S. Tashman, and R. J. Triolo, "Development of hybrid orthosis for standing, walking, and stair climbing after spinal cord injury," *Journal of Rehabilitation Research & Development*, vol. 43, pp. 447-462, 2009.
- [5] C. S. To, R. Kobetic, J. R. Schnellenger, M. L. Audu, and R. J. Triolo, "Design of a variable constraint hip mechanism for a hybrid neuroprosthesis to restore gait after spinal cord injury," *IEEE/ASME Transactions on Mechatronics*, vol. 13, pp. 197-205, 2008.
- [6] W. K. Durfee and A. Rivard, "Design and Simulation of a Pneumatic, Stored-energy, Hybrid Orthosis for Gait Restoration," *Journal of Biomechanical Engineering*, vol. 127, pp. 1014-1019, 2005.
- [7] M. Goldfarb, K. Korkowski, B. Harrold, and W. Durfee, "Preliminary evaluation of a controlled-brake orthosis for FES-aided gait," *IEEE Transactions on Neural Systems and Rehabilitation Engineering*, vol. 11, pp. 241-248, 2003.
- [8] Y. Ohta, H. Yano, R. Suzuki, M. Yoshida, N. Kawashima, and K. Nakazawa, "A two-degree-of-freedom motor-powered gait orthosis for spinal cord injury patients," *Proceedings of the Institution of Mechanical Engineers, Part H: Journal of Engineering in Medicine*, vol. 221, pp. 629-639, 2007.
- [9] H. K. Kwa, J. H. Noorden, M. Missel, T. Craig, J. E. Pratt, and P. D. Neuhaus, "Development of the IHMC mobility assist exoskeleton," presented at the Proceedings of the 2009 IEEE international conference on Robotics and Automation, Kobe, Japan, 2009.
- [10] P. D. Neuhaus, J. H. Noorden, T. J. Craig, T. Torres, J. Kirschbaum, and J. E. Pratt, "Design and Evaluation of Mina: a Robotic Orthosis for Paraplegics," in *International Conference on Rehabilitation Robotics*, ed. Zurich, Switzerland: IEEE Press, 2011, pp. 870-877.
- [11] A. Tsukahara, Y. Hasegawa, and Y. Sankai, "Standing-up motion support for paraplegic patient with Robot Suit HAL," presented at the IEEE 11th International Conference on Rehabilitation Robotics, Kyoto, Japan, 2009.
- [12] Y. Hasegawa, J. Jang, and Y. Sankai, "Cooperative walk control of paraplegia patient and assistive system," presented at the IEEE/RSJ International Conference on

- Intelligent Robots and Systems, St. Louis, USA, 2009.
- [13] K. Suzuki, G. Mito, H. Kawamoto, Y. Hasegawa, and Y. Sankai, "Intention-based walking support for paraplegia patients with Robot Suit HAL," *Advanced Robotics*, vol. 21, pp. 1441-1469, 2007.
 - [14] A. Tsukahara, R. Kawanishi, Y. Hasegawa, and Y. Sankai, "Sit-to-Stand and Stand-to-Sit Transfer Support for Complete Paraplegic Patients with Robot Suit HAL," *Advanced Robotics*, vol. 24, pp. 1615-1638, 2010.
 - [15] H. A. Quintero, R. J. Farris, and M. Goldfarb, "Control and implementation of a powered lower limb orthosis to aid walking in paraplegic individuals," in *Rehabilitation Robotics (ICORR), 2011 IEEE International Conference on*, 2011, pp. 1-6.
 - [16] T. Lam, V. K. Noonan, and J. J. Eng, "A systematic review of functional ambulation outcome measures in spinal cord injury," *Spinal Cord*, vol. 46, pp. 246-254, 2007.
 - [17] D. Podsiadlo and S. Richardson, "The timed "Up & Go": a test of basic functional mobility for frail elderly persons," *J Am Geriatr Soc*, vol. 39, pp. 142-148, 1991.
 - [18] C. Hughes, C. Osman, and A. K. Woods, "Relationship among performance on stair ambulation, functional reach, and Timed Up and Go tests in older adults," *Issues on Aging*, vol. 21, pp. 18-22, 1998.
 - [19] S. Morris, M. E. Morris, and R. Iansek, "Reliability of Measurements Obtained With the Timed "Up & Go" Test in People With Parkinson Disease," *Physical Therapy*, vol. 81, pp. 810-818, February 2001 2001.
 - [20] T. Schoppen, A. Boonstra, J. W. Groothoff, J. de Vries, L. N. H. Göeken, and W. H. Eisma, "The timed "up and go" test: Reliability and validity in persons with unilateral lower limb amputation," *Archives of physical medicine and rehabilitation*, vol. 80, pp. 825-828, 1999.
 - [21] A. Shumway-Cook, S. Brauer, and M. Woollacott, "Predicting the Probability for Falls in Community-Dwelling Older Adults Using the Timed Up & Go Test," *Physical Therapy*, vol. 80, pp. 896-903, September 2000 2000.
 - [22] M. Thompson and A. Medley, "Performance of individuals with Parkinson's disease on the Timed Up & Go," *Neurology Report*, vol. 22, pp. 16-21, 1998.
 - [23] P. Rossier and D. T. Wade, "Validity and reliability comparison of 4 mobility measures in patients presenting with neurologic impairment," *Arch Phys Med Rehabil*, vol. 82, pp. 9-13, 2001.
 - [24] M. Schenkman, T. M. Cutson, M. Kuchibhatla, J. Chandler, and C. Pieper, "Reliability of impairment and physical performance measures for persons with Parkinson's disease," *Physical Therapy*, vol. 77, pp. 19-27, 1997.
 - [25] M. T. Smith and G. D. Baer, "Achievement of simple mobility milestones after stroke," *Arch Phys Med Rehabil*, vol. 80, pp. 442-447, 1999.
 - [26] H. J. van Hedel, M. Wirz, and V. Dietz, "Assessing walking ability in subjects with spinal cord injury: Validity and reliability of 3 walking tests," *Archives of physical medicine and rehabilitation*, vol. 86, pp. 190-196, 2005.
 - [27] J. Roomi, M. M. Johnson, K. Waters, A. Yohannes, A. Helm, and M. J. Connolly,

- "Respiratory rehabilitation, exercise capacity and quality of life in chronic airways disease in old age," *Age Ageing*, vol. 25, pp. 12-16, 1996.
- [28] J. J. Eng, K. S. Chu, A. S. Dawson, C. M. Kim, and K. E. Hepburn, "Functional Walk Tests in Individuals With Stroke," *Stroke*, vol. 33, pp. 756-761, March 1, 2002.
- [29] N. D. Harada, V. Chiu, and A. L. Stewart, "Mobility-related function in older adults: Assessment with a 6-minute walk test," *Archives of physical medicine and rehabilitation*, vol. 80, pp. 837-841, 1999.
- [30] H. J. A. van Hedel, M. Wirz, and V. Dietz, "Standardized assessment of walking capacity after spinal cord injury: the European network approach," *Neurological Research*, vol. 30, pp. 61-73, 2008.
- [31] A. B. Jackson, C. T. Carnel, J. F. Ditunno, M. S. Read, M. L. Boninger, M. R. Schmeler, S. R. Williams, and W. H. Donovan, "Outcome Measures for Gait and Ambulation in the Spinal Cord Injury Population," *Journal of Spinal Cord Medicine*, vol. 31, pp. 487-499, 2008.
- [32] G. A. V. Borg, "Psychophysical bases of perceived exertion," *Medicine and Science in Sports and Exercise*, vol. 14, pp. 377-381, 1982.
- [33] H. A. Quintero, R. J. Farris, C. Hartigan, I. Clesson, and M. Goldfarb, "A Powered Lower Limb Orthosis for Providing Legged Mobility in Paraplegic Individuals," *Topics in Spinal Cord Injury Rehabilitation*, vol. 17, pp. 25-33, 2011.

CHAPTER V

Manuscript 4: Joint Torque and Power Requirements during Stair Ascent and Descent in a Lower Limb Exoskeleton for Persons with Paraplegia

Ryan J. Farris, Hugo A. Quintero, and Michael Goldfarb

Vanderbilt University

Nashville, TN

Submitted as a Regular Paper to the

ASME Journal of Medical Devices

(In Review)

Abstract

This paper presents experimental data characterizing the joint torque and power required to provide stair ascent and descent functionality to a person with paraplegia. The authors briefly describe stair ascent and descent functionality in a powered lower limb exoskeleton, and present hip and knee joint angles resulting from (multiple trials of) stair ascent and descent maneuvers, in addition to the hip and knee joint torque and power required to perform this functionality. Joint torque and power requirements are summarized, including peak hip and knee joint torque requirements of 0.75 Nm/kg and 0.87 Nm/kg, respectively, and peak hip and knee joint power requirements of approximately 0.65 W/kg and 0.85 W/kg, respectively.

Introduction

In an effort to facilitate legged locomotion in individuals with paraplegia, several computer-controlled lower limb orthoses and exoskeletons have been, and are being, developed and described in the research literature. These include hybrid FES-systems, which supplement functional electrical stimulation (FES) of leg muscles with a computer-controlled orthosis; and fully powered lower limb exoskeletons, which utilize electric motors as the primary form of motive assistance. Recent examples of the former include those described in [1-5], while recent examples of the latter include those described in [6-12], in addition to the commercially emerging powered lower limb exoskeletons being developed by Argo Medical Technologies and Ekso Bionics, respectively.

Among the important criteria in the design of such gait assistance exoskeletons (and computer-controlled orthoses) is the amount of torque and power required at the enabling joints (which are typically the hip and knee joints). In fact, it can be argued that the joint torque and power requirements in a lower limb exoskeleton are the single most important design specifications in such systems, since nearly all other design decisions propagate from these considerations (e.g., actuator type and size, transmission type and size, power system type and

size, structural considerations, etc.). Further, one can reasonably assert that, of all the movements that such systems should enable, stair ascent and descent is the most demanding with regard to hip and knee joint torque and power. That is, since the gait associated with such systems is generally quasistatic in nature (partly due to the nature of walking with a stability aid), the loading in such systems is generally governed by gravitational (rather than inertial) effects. The movements most directly associated with gravitational loads are sit-to-stand and stand-to-sit transitions, and stair ascent and descent. Since sit-to-stand and stand-to-sit maneuvers utilize the left and right legs in parallel, however, the loading in such movements is typically much smaller than in stair ascent and descent. The latter movements require a single leg to either lift or lower the center of mass of the body a significant distance. As such, one would expect the joint torque and power required for stair ascent and descent to define the joint torque and power requirements for such systems.

Measurements of hip and knee joint torque and power during for healthy stair ascent and descent have been published in the biomechanics literature [13-15]. The nature of stair ascent and descent in exoskeleton systems for persons with paraplegia, however, is quite different from the nature of stair ascent and descent in healthy individuals. First, lower limb exoskeletons for persons with paraplegia typically do not include actuated ankle joints. Second, the nature of movement in such systems, as it pertains to the SCI population, is altered by the need for a stability aid. Specifically, the use of a stability aid will generally require a step-to (as opposed to a step-over) method of stair ascent and descent, and as previously stated, body movement is more likely to be characterized as quasistatic, relative to stair ascent and descent in the healthy population. Third, data from a healthy population does not reflect the passive loading imposed by the inactive legs of an SCI individual in the lower limb exoskeleton (including the joint and tissue stiffness and damping characteristics).

In this paper, the authors have implemented stair ascent and descent capability in a lower limb exoskeleton, and tested the functionality of the system on a paraplegic individual with a T10 complete injury. A series of trials was conducted, and experimental data is presented that

describes the body-mass-normalized hip and knee joint torque and power required by the exoskeleton during stair ascent and descent. The hip and knee joint requirements are summarized, and contrasted with data previously published for healthy subjects. To the authors' knowledge, no similar data has previously appeared in the engineering literature.

Hardware and Implementation

The Vanderbilt lower limb exoskeleton, shown in Fig. 5-1, provides powered assistance in the sagittal plane at both hip and knee joints. The exoskeleton consists of a hip segment, a right and left thigh segment, and a right and left shank segment. The hip segment contains a lithium polymer battery which powers the exoskeleton, while each thigh segment contains a pair of brushless DC motors, which actuate the hip and knee joints respectively through speed reduction transmissions. The knee joints are additionally equipped with normally-locked brakes, in order to preclude knee buckling in the event of a power failure. Although the exoskeleton does not explicitly contain a foot segment or ankle joint, it is designed to be used in conjunction with a standard ankle foot orthosis (AFO), which provides stability at the ankle and precludes foot drop during the swing phase of gait. The total mass of the exoskeleton, including the battery, is 12.3 kg (27.0 lb). A more detailed description of the exoskeleton design, including a description of the embedded electronics system, is given in [16].



Fig. 5-1. Vanderbilt lower limb exoskeleton.

The powered lower limb exoskeleton enables sit-to-stand transitions, stand-to-sit transitions, standing, stand-to-walk transitions, walking, walk-to-stand transitions, and stair ascent and descent. Details regarding the control structure and approach are given in [16], although a brief overview is given here. In order to enable the user to have autonomous control of these maneuvers, a user interface approach was developed based on the user's ability to affect his or her center of pressure via the use of his or her upper body, in combination with a stability aid. Specifically, based on sensors embedded in the exoskeleton, the control system estimates the location of the user's center of pressure (CoP), defined as the user's center of mass projection onto the (assumed horizontal) ground plane, and uses the distance between the CoP and the location of the forward ankle joint as the primary command input. As such, the act of leaning forward or backward at various points in the gait cycle indicates user intent to perform the next

movement in a given activity. In the case of stair ascent, each step is ascended in a two-stage sequence. In the first part of the sequence, a forward shift in the CoP estimate lifts the right leg to the subsequent stair tread; in the second part of the sequence, a forward shift in the CoP estimate brings the (lagging) left leg onto the same tread as the (leading) right leg. At this point, a subsequent forward shift in the CoP will repeat the sequence, thus enabling the user to ascend the next stair tread. Figure 5-2 illustrates the sequence of movement during stair ascent, including the starting posture (Fig. 5-2a); leaning forward for the first CoP trigger (Fig. 5-2b); lifting of right leg to subsequent stair tread (Fig. 5-2c), leaning forward for the second CoP trigger (Fig. 5-2d); and lifting of body and placement of left foot on subsequent stair tread, next to right (Fig. 5-2e). Unlike the stair ascent procedure, the stair descent procedure requires only an initial CoP trigger. Figure 5-3 illustrates the sequence of movement involved in stair descent, including the starting posture (Fig. 5-3a); leaning forward for the CoP trigger (Fig. 5-3b); extension of right leg over subsequent stair tread (Fig. 5-3c); lowering of body and right foot to subsequent stair tread (Fig. 5-3d); and movement of left foot onto subsequent stair tread, next to right foot (Fig. 5-3e).



Fig. 5-2. Stair ascent sequence, including a) starting posture, b) leaning forward for initial CoP trigger, c) lifting of right leg to subsequent stair tread, d) leaning forward for second CoP trigger, and e) lifting of body and placement of left foot on subsequent stair tread, next to right foot.



Fig. 5-3. Stair descent sequence, showing a) starting posture, b) leaning forward for CoP trigger, c) extension of right leg over subsequent stair tread, d) lowering of body and right foot to subsequent stair tread, and e) movement of left foot to subsequent stair tread.

Data Collection

The stair ascent and descent functionality was implemented in the Vanderbilt lower limb exoskeleton, and trials were conducted on a paraplegic subject. The subject was a 36-year-old male, 1.85 m (6 ft, 2 in) tall, body mass of 73 kg (160 lb), with a T10 motor and sensory complete injury (i.e., American Spinal Injury Association, ASIA, A classification), 9 years post injury. Testing was performed at the Shepherd Center (Atlanta, GA, USA), a rehabilitation hospital specializing in spinal cord injury. A physical therapist was present for all trials, in accordance with the approved Institutional Review Board protocol. All trials were performed on a standard staircase, characterized by a step height 15 cm (6 in) of and a step depth of 29 cm (11.5 in). All tests were performed with a handrail support on the right side, and a forearm crutch on the left side. The subject was allowed to practice stair ascent and descent until he felt accustomed to and comfortable with the respective movements, and until the therapist reported that the subject was able to complete the respective movements without assistance from her (i.e., which she classified as contact guard assist). Following this practice, the exoskeleton hip and knee joint angles and torques, as measured by instrumentation on the exoskeleton, were recorded during 12 successive stair ascent movements, and 12 successive stair descent movements.

Results and Discussion

Stair Ascent

The averaged right and left hip and knee joint angles, torques, and power from the stair ascent trials are shown in Figs. 5-4, 5-5, and 5-6, respectively. Specifically, Fig. 5-4 shows the averaged measured joint angles for the right and left hip and knee joints for 12 successive stair ascent movements, where each averaged trajectory is bracketed by plus and minus one standard deviation across the 12 trials. Note that a positive angle represents joint flexion (relative to a nominal standing posture), while a negative angle represents joint extension. The right leg led the movement in all stair ascent movements, with the left leg thus trailing. Time $t=0$ represents the

start of the movement, as triggered by the first CoP shift. The dashed vertical line in the figure represents the time between the completion of the first phase of movement, and the initialization of the second phase of movement, as triggered by a second forward shift in the CoP. The average duration of this pause during these 12 stair ascent movements was 2.9 s, with a standard deviation of 0.9 s. Therefore, although the second phase of the stair ascent movement is shown to begin at 2.0 s, in fact the second phase started on average 4.9 s after the initial trigger, with a standard deviation of 0.9 s. Thus, the data to the left of the dashed line in the figure depicts the measured joint trajectories during the process of lifting the right leg from the starting stair tread, and planting the right foot on the successive stair tread, while the data to the right of the dashed line depicts the measured joint trajectories during the process of lifting the body onto the successive stair tread, and subsequently planting the left foot on the stair tread next to the right. Since the controlled portion of the movement requires 4 s, and the average duration of the pause for the CoP trigger was 2.9 s (with a standard deviation of 0.9 s), the average time required to complete the stair ascent movement was 6.9 s (with a standard deviation of 0.9 s). During the 12 stair ascent movements, the average time between successive ascents was 11.2 s (with a standard deviation of 1.2 s). As such, the approximate duty cycle of exoskeleton movement was approximately 62%.

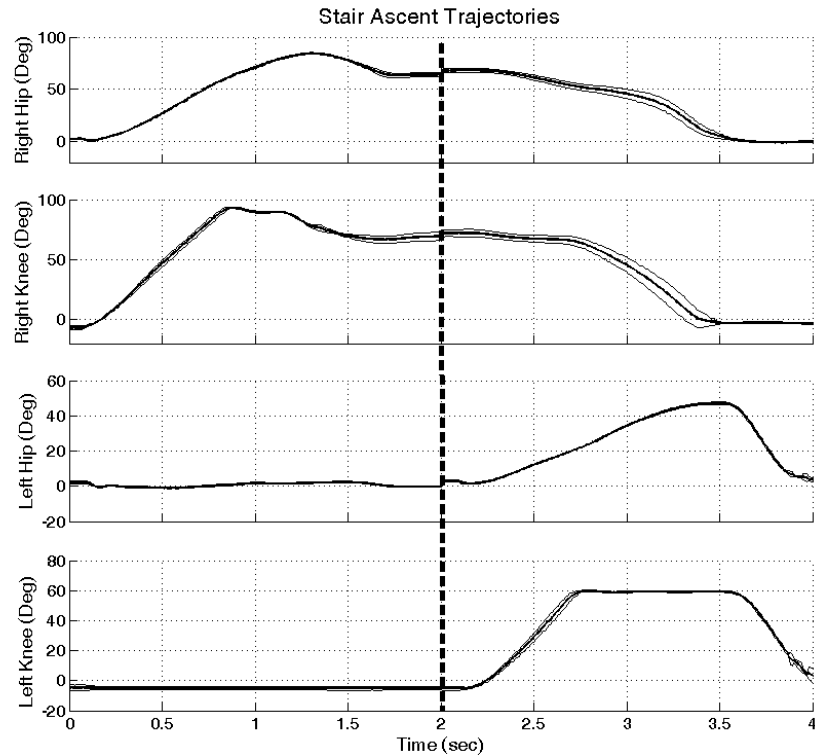


Fig. 5-4. Measured joint angles averaged from 12 stair ascent movements, along with plus and minus one standard deviation, all with the right leg leading the movement (and left leg trailing). The dashed vertical line represents a discontinuity in time (of approximately 3 s), during which the subject shifted his CoP forward to trigger the next phase of the movement.

Figure 5-5 shows the averaged measured body-mass-normalized joint torque for the right and left hip and knee joints for 12 successive stair ascent movements, where each averaged torque profile is bracketed by plus and minus one standard deviation across the 12 trials. Note that the torques are positive in flexion and negative in extension. Based on the averaged torques across these trials, the largest knee joint torque required during the stair ascent movement was 0.87 Nm/kg (in extension), required at the right knee joint during the process of lifting the body up to the next stair tread, while the largest hip joint torque was approximately 0.75 Nm/kg (in flexion), required during the process of lifting the right leg onto the successive stair tread.

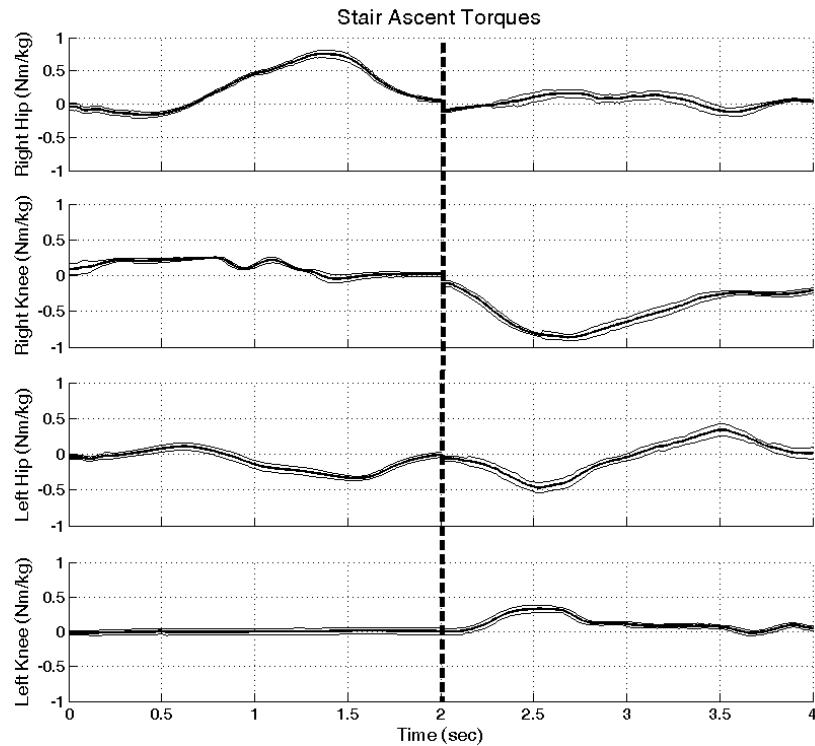


Fig. 5-5. Measured body-mass-normalized joint torques averaged over 12 stair ascent movements, along with plus and minus one standard deviation, all with the right leg leading the movement (and left leg trailing). The dashed vertical line represents a discontinuity in time (of approximately 3 s), during which the subject shifted his CoP forward to trigger the next phase of the movement.

Figure 5-6 shows the averaged body-mass-normalized joint power for the right and left hip and knee joints for 12 successive stair ascent movements, where each averaged power profile is bracketed by plus and minus one standard deviation across the 12 trials. Note that positive power represents exoskeleton power generation, while negative power represents exoskeleton power absorption (or dissipation). Based on the measured data, the peak knee joint power is approximately 0.85 W/kg (power generation), required while lifting the body, while the peak hip joint power is approximately 0.65 W/kg (power generation), required while lifting the leg up to the next stair tread. Additionally, the maximum root-mean-square (RMS) power during a movement is

0.43 W/kg at the knee joint, sustained for a 2-s period while lifting the body, and 0.33 W/kg at the hip joint, also sustained for a 2-s period, while lifting the leading leg onto the next stair tread. Note that the power required during the approximately 3-s duration of the intermediate CoP trigger is essentially zero.

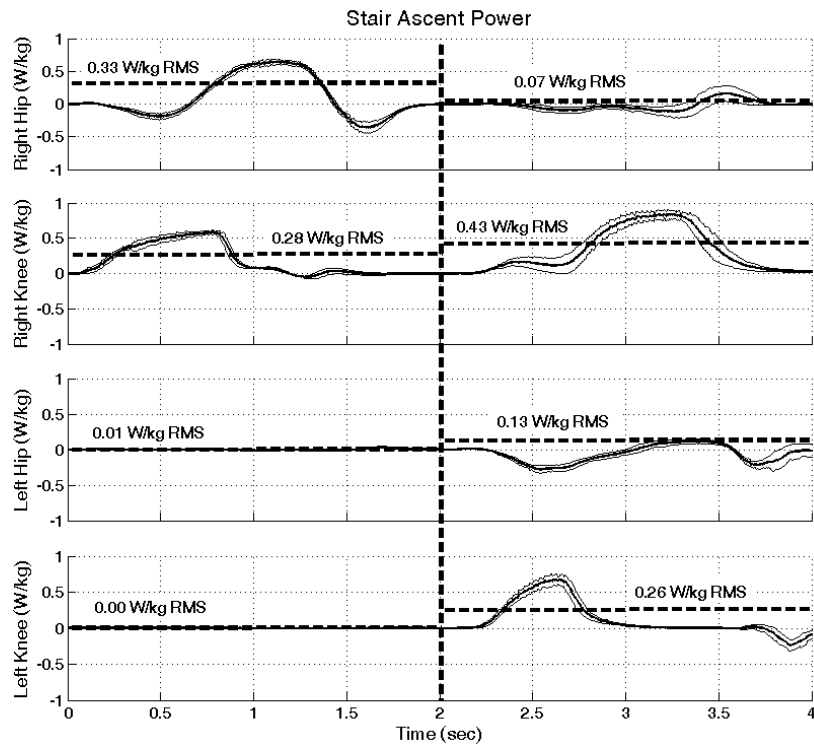


Fig. 5-6. Body-mass-normalized power averaged over 12 stair ascents movements, along with plus and minus one standard deviation, all with the right leg leading the movement (and left leg trailing). The dashed vertical line represents a discontinuity in time (of approximately 3 s), during which the subject shifted his CoP forward to trigger the next phase of the movement. The dashed horizontal line indicates RMS averaged power during each of the two phases of ascent for each joint.

Stair Descent

The averaged right and left hip and knee joint angles, torques, and power from the stair descent trials are shown in Figs. 5-7, 5-8, and 5-9, respectively. Specifically, Fig. 5-7 shows the averaged measured joint angles for the right and left hip and knee joints for 12 successive stair descent movements, where each averaged trajectory is bracketed by plus and minus one standard deviation across the 12 trials. As in ascent, the right leg led the movement in all stair descent movements, with the left leg thus trailing. Time $t=0$ represents the start of the movement, as triggered by the CoP shift. The average time required to complete the stair descent movement was 3.7 s (with a standard deviation of 0.1 s). During the 12 stair descent movements, the average time between successive descents was 8.0 s (with a standard deviation of 1.1 s). As such, the approximate duty cycle of exoskeleton movement was 46%.

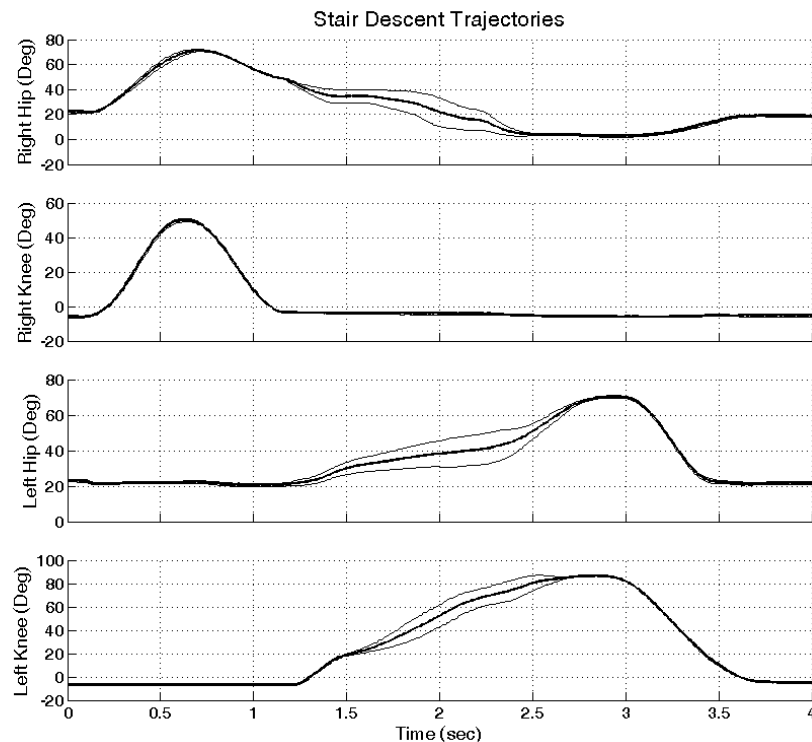


Fig. 5-7. Measured joint angles averaged from 12 stair descent movements, along with plus and minus one standard deviation, all with the right leg leading the movement (and left leg trailing).

Figure 5-8 shows the averaged measured body-mass-normalized joint torque for the right and left hip and knee joints for 12 successive stair descent movements, where each averaged torque profile is bracketed by plus and minus one standard deviation across the 12 trials. Based on the averaged torques across these trials, the largest knee joint torque required during the stair descent movement was 0.35 Nm/kg (in extension), required at the left knee joint during the process of lowering the body and the right foot to the subsequent stair tread, while the largest hip joint torque was approximately 0.57 Nm/kg (in extension), required during the process of lowering the lagging (left) foot onto the successive stair tread next to the right.

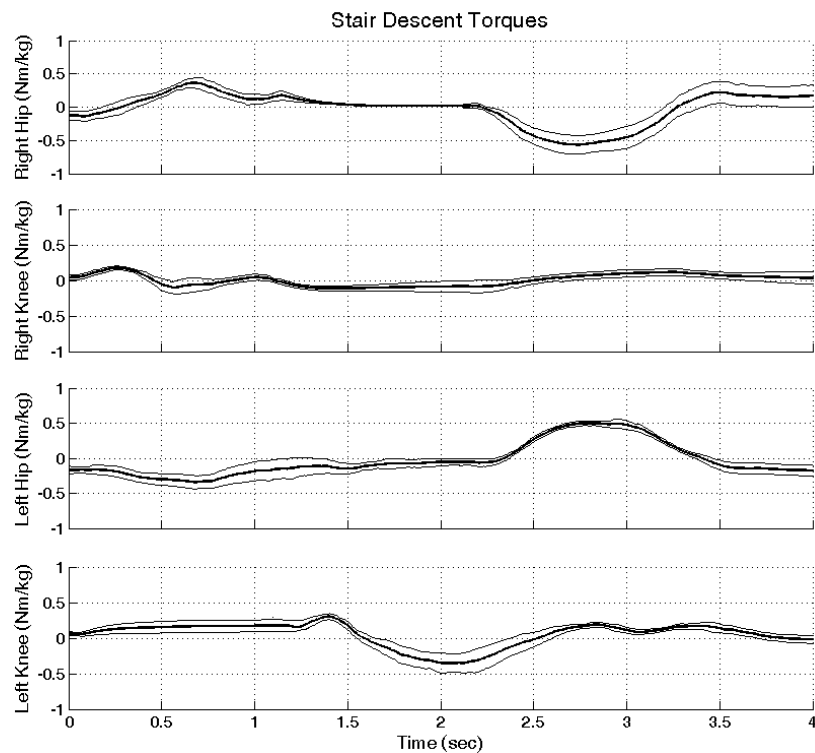


Fig. 5-8. Measured body-mass-normalized joint torques averaged over 12 stair ascents movements, along with plus and minus one standard deviation, all with the right leg leading the movement (and left leg trailing).

Figure 5-9 shows the averaged body-mass-normalized joint power for the right and left hip and knee joints for 12 successive stair descent movements, where each averaged power profile is bracketed by plus and minus one standard deviation across the 12 trials. Based on the measured data, the peak knee joint power is approximately 0.55 W/kg (power dissipation), required while lowering the body, while the peak hip joint power is approximately 0.5 W/kg (power generation), required while extending the right leg over the subsequent stair tread and also while lowering the left leg down to the subsequent tread. Additionally, the maximum root-mean-square (RMS) power during the descent movement is 0.22 W/kg at the knee joint, and 0.15 W/kg at the hip joint, both occurring over the 4-s period required for the stair descent maneuver.

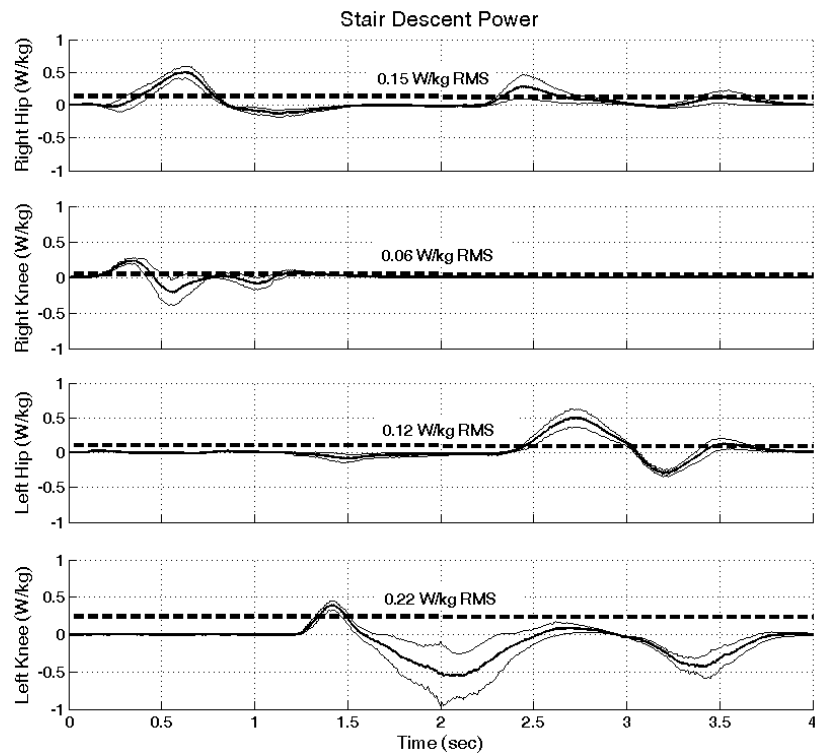


Fig. 5-9. Body-mass-normalized power averaged over 12 stair ascents movements, along with plus and minus one standard deviation, all with the right leg leading the movement (and left leg trailing). The dashed horizontal line indicates RMS averaged power during descent for each joint.

Comparing to Healthy Subject Data

Comparable torque and power data for stair ascent and descent with non-disabled subjects is presented in [16]. In ascent, and for a similar stair riser height, the maximum joint torques are 0.47 Nm/kg (extensive) at the hip and 1.05 Nm/kg (extensive) at the knee, both occurring while lifting the body, as opposed to the 0.75 Nm/kg and 0.87 Nm/kg, respectively, required for exoskeleton ascent. The maximum joint powers for able bodied ascent, 0.85 W/kg (power generation) at the hip, and 2.3 W/kg (power generation) at the knee, also occur while lifting the body mass. These values are considerably larger than the values reported for ascent with the exoskeleton (0.65 W/kg and 0.85 W/kg, respectively), due both to lower required joint torques, and to the fact that stair ascent with the exoskeleton occurs at a significantly lower rate, relative to able-bodied subjects.

In descent, the maximum able-bodied joint torques at the hip and knee were approximately 0.62 Nm/kg (flexive), and 1.25 Nm/kg (extensive), respectively. As with ascent, able-bodied joint torques are greater than the corresponding maximum exoskeleton hip and knee torques of 0.57 Nm/kg and 0.35 Nm/kg, respectively. Hip joint power between able-bodied and exoskeleton descent are comparable, with 0.4 W/kg required during able-bodied descent at the hip (power generation), and 0.5 W/kg required during SCI descent. The peak power of 3.8 W/kg (power dissipation) required at the knee joint for able-bodied descent, however, is substantially higher than that required for SCI descent, which was 0.55 W/kg.

In summary, the exoskeleton requires a maximum torque of 0.75 Nm/kg at the hip joint (as opposed to 0.62 Nm/kg in able-bodied data), and a maximum torque of 0.87 Nm/kg at the knee joint (as opposed to 1.25 Nm/kg in able-bodied data). Further, the exoskeleton requires peak powers of 0.65 W/kg at the hip joint (as opposed to 0.85 W/kg in able-bodied data), and 0.85 W/kg at the knee joint (as opposed 3.8 W/kg in able-bodied data).

Nominal Lower Limb Torque and Power Requirements

Having obtained repeatable stair ascent and descent with a paraplegic individual by means of a powered exoskeleton, it is reasonable to consider the reported normalized torque and power

demands as they relate to absolute system performance requirements. The maximum hip and knee joints torques required for stair ascent and descent with the exoskeleton were shown to be 0.75 Nm/kg and 0.87 Nm/kg, respectively. The peak hip and knee joint power was shown to be 0.65 W/kg and 0.85 W/kg, respectively. Considering a reasonable upper bound for subject body mass as 90 kg (~200 lbs), a gait assistance exoskeleton with stair ascent and descent capability would need to provide maximum absolute joint torques of 68 Nm and 78 Nm at the hip and knee joints, respectively, and peak joint powers of 59 W and 77 W at the hip and knee joints, respectively.

Conclusion

Measured data characterizing the joint torque and power requirements for a lower limb exoskeleton has not previously been published. This paper addresses these issues based on the premise that the largest torque and power requirements on these systems will occur during stair ascent and descent. Averaged results from 12 stair ascents and descents are presented, including joint trajectories, body-mass-normalized joint torques, and body-mass-normalized joint power. The peak torque requirement at the hip is 0.75 Nm/kg and at the knee is 0.87 Nm/kg, both occurring during ascent. The peak hip joint power is approximately 0.65 W/kg (power generation), required while lifting the leg up to the next stair tread, while the peak knee joint power is approximately 0.85 W/kg (power generation), required while lifting the body mass. This knowledge of joint torque and power requirements should provide improved specifications for purposes of designing lower limb exoskeleton systems for facilitating legged locomotion in individuals with paraplegia.

References

- [1] Audu, M. L., To, C. S., Kobetic, R., and Triolo, R. J., "Gait evaluation of a novel hip constraint orthosis with implication for walking in paraplegia," *IEEE Transactions on Neural Systems and Rehabilitation Engineering*, vol. 18, pp. 610-618, 2010.
- [2] Durfee, W. K. and Rivard, A., "Design and Simulation of a Pneumatic, Stored-energy, Hybrid Orthosis for Gait Restoration," *Journal of Biomechanical Engineering*, vol. 127, pp. 1014-1019, 2005.
- [3] Goldfarb, M., Korkowski, K., Harrold, B., and Durfee, W., "Preliminary evaluation of a controlled-brake orthosis for FES-aided gait," *IEEE Transactions on Neural Systems and Rehabilitation Engineering*, vol. 11, pp. 241-248, 2003.
- [4] Kobetic, R., To, C. S., Schnellenberger, J. R., Audu, M. L., Bulea, T. C., Gaudio, R., Pinault, G., Tashman, S., and Triolo, R. J., "Development of hybrid orthosis for standing, walking, and stair climbing after spinal cord injury," *Journal of Rehabilitation Research & Development*, vol. 43, pp. 447-462, 2009.
- [5] To, C. S., Kobetic, R., Schnellenberger, J. R., Audu, M. L., and Triolo, R. J., "Design of a variable constraint hip mechanism for a hybrid neuroprosthesis to restore gait after spinal cord injury," *IEEE/ASME Transactions on Mechatronics*, vol. 13, pp. 197-205, 2008.
- [6] Hasegawa, Y., Jang, J., and Sankai, Y., "Cooperative walk control of paraplegia patient and assistive system," in *IEEE/RSJ International Conference on Intelligent Robots and Systems*, St. Louis, USA, 2009, pp. 4481-4486.
- [7] Kwa, H. K., Noorden, J. H., Missel, M., Craig, T., Pratt, J. E., and Neuhaus, P. D., "Development of the IHMC mobility assist exoskeleton," in *Proceedings of the 2009 IEEE international conference on Robotics and Automation*, Kobe, Japan, 2009, pp. 1349-1355.
- [8] Neuhaus, P. D., Noorden, J. H., Craig, T. J., Torres, T., Kirschbaum, J., and Pratt, J. E., "Design and Evaluation of Mina: a Robotic Orthosis for Paraplegics," in *International Conference on Rehabilitation Robotics*, ed. Zurich, Switzerland: IEEE Press, 2011, pp. 870-877.
- [9] Ohta, Y., Yano, H., Suzuki, R., Yoshida, M., Kawashima, N., and Nakazawa, K., "A two-degree-of-freedom motor-powered gait orthosis for spinal cord injury patients," *Proceedings of the Institution of Mechanical Engineers, Part H: Journal of Engineering in Medicine*, vol. 221, pp. 629-639, 2007.
- [10] Suzuki, K., Mito, G., Kawamoto, H., Hasegawa, Y., and Sankai, Y., "Intention-based walking support for paraplegia patients with Robot Suit HAL," *Advanced Robotics*, vol. 21, pp. 1441-1469, 2007.
- [11] Tsukahara, A., Hasegawa, Y., and Sankai, Y., "Standing-up motion support for paraplegic patient with Robot Suit HAL," in *IEEE 11th International Conference on Rehabilitation Robotics*, Kyoto, Japan, 2009, pp. 211-217.
- [12] Tsukahara, A., Kawanishi, R., Hasegawa, Y., and Sankai, Y., "Sit-to-Stand and Stand-to-Sit Transfer Support for Complete Paraplegic Patients with Robot Suit HAL,"

Advanced Robotics, vol. 24, pp. 1615-1638, 2010.

- [13] McFadyen, B. J. and Winter, D. A., "An integrated biomechanical analysis of normal stair ascent and descent," *Journal of Biomechanics*, vol. 21, pp. 733-744, 1988.
- [14] Nadeau, S., McFadyen, B. J., and Malouin, F., "Frontal and sagittal plane analyses of the stair climbing task in healthy adults aged over 40 years: what are the challenges compared to level walking?," *Clinical Biomechanics*, vol. 18, pp. 950-959, 2003.
- [15] Riener, R., Rabuffetti, M., and Frigo, C., "Stair ascent and descent at different inclinations," *Gait & Posture*, vol. 15, pp. 32-44, 2002.
- [16] Quintero, H. A., Farris, R. J., and Goldfarb, M., "Control and implementation of a powered lower limb orthosis to aid walking in paraplegic individuals," in *Rehabilitation Robotics (ICORR), 2011 IEEE International Conference on*, 2011, pp. 1-6.

Addendum: Curbs and Slopes

Curb Ascent and Descent

Curb ascent and descent are regarded as subsets of stair ascent and descent as far as control is concerned. That is, ascent of a curb is accomplished through the same control paths as ascent of a single step, and descent of a curb is accomplished similarly through the same paths as descent of a single step. Postural control and forearm crutch placement differ, however, from stairs due to the absence of a handrail. This lack of a handrail for support and especially front-to-back stability necessitates a specific coordination of crutch placement for safe and reliable curb ascent/descent. The sequence of motions and the corresponding crutch placements for curb ascent are illustrated in Fig. 5-10. Represented in the figure are the starting posture (Fig. 5-10a), leaning forward for the first CoP trigger (Fig. 5-10b), completion of the first leg lift (Fig. 5-10c), leaning forward for the second CoP trigger (Fig. 5-10d), completion of the final motion up onto the curb (Fig. 5-10e), and shifting of weight and crutches forward (Fig. 5-10f). A sequence of images showing the corresponding progression for curb descent is provided in Fig. 5-11. Represented in this figure are the starting posture (Fig. 5-11a), leaning forward for the CoP trigger (Fig. 5-11b), completion of the first motion (leg lifted off curb) (Fig. 5-11c), completion of the second motion (front leg lowered to ground) (Fig. 5-11d), and completion of the final motion (collecting the rear leg down to the ground) (Fig. 5-11e).



Fig. 5-10. Curb ascent sequence. (a) Starting posture, (b) Leaning forward for CoP trigger, (c) First motion completed, (d) Leaning forward for CoP trigger, (e) Second motion completed, (f) Weight shifted forward with crutches.

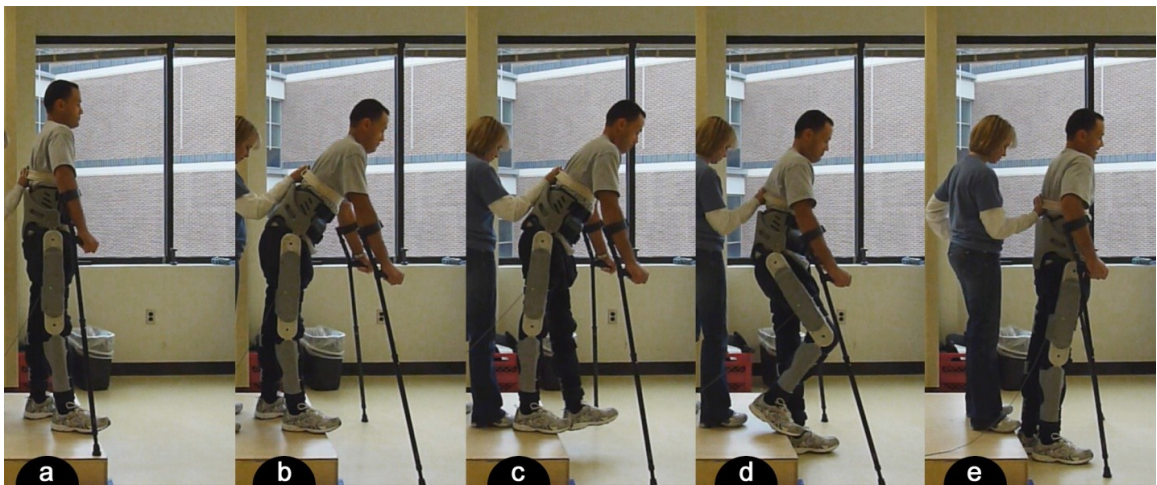


Fig. 5-11. Curb descent sequence. (a) Starting posture, (b) Leaning forward for CoP trigger, (c) First motion completed, (d) Second motion completed, (e) Third motion completed.

Control Strategy for Walking on Slopes

Data from able-bodied slope walking experiments show that hip flexion values increase as much as 10 degrees and knee flexion values as much as 5 degrees for upslope walking on a 5 degree incline [1]. Much greater increases in hip and knee flexion are seen as the incline is increased to 10 degrees: 25 degrees and 26 degrees, respectively. Due to the relative similarity between joint trajectories for level-ground walking and slope walking on a 5 degree incline, and the ADA (Americans with Disabilities Act) standard of an approximately 5 degree maximum allowable slope for handicap accessible ramps [2], no changes were made to modify exoskeleton control explicitly for slope walking. That is, the slope walking tests described subsequently were performed with the same control structure and the same parameters used in the exoskeleton for level ground walking, such that the user could walk from level ground to a 5 degree slope (incline or decline) seamlessly.

Metrics for Assessing Slope Walking Capability

Since no widely accepted metric exists for characterizing a person's ability to traverse slopes, the authors have adapted the standard Timed Up and Go (TUG) test for slope walking. The TUG test measures the time required for a subject to stand from a seated position, walk three meters, turn, walk back three meters, turn, and return to the seated position. It has been identified as one of seven primary measures associated with functional ambulation in a recent survey of outcome measures for persons with SCI [3]. Originally proposed in [4], the test has been shown to have high test-retest reliability as a mobility measure across a wide spectrum of patient populations, including persons with stroke impairment, Parkinson's disease, arthritis, cerebellar disorders, and unilateral lower limb amputation [5-9].

The modified version of the TUG test for characterizing slope walking, hereafter referred to as the Sloped TUG test, measures the time required for a subject to stand from a seated position on

level ground, walk one meter on level ground, walk three meters up a 5 degree slope onto another level surface, turn, walk back down the 3 meter slope and onto the level surface in front of the chair, turn, and return to the seated position. As important as the speed of completion in this test is the ability of the user to complete the test without an undue level of exertion. In order to characterize the level of exertion, the time to complete this test is supplemented with measurement of the pre- and post-test heart rate, which is commonly used to measure physical exertion. This physiological measure of exertion is further supplemented by rating each test with the Borg Rating of Perceived Exertion (RPE) Scale, as proposed in [10], which is well-validated and widely used indication of perceptual effort, in which a subject rates his or her level of exertion on a scale of 6 to 20, where 6 corresponds to —no exertion at all and 20 corresponds to —maximal exertion. On this scale, casual healthy walking on level ground corresponds to a rating of 9.

The setup used for the Sloped TUG experiments is shown in Fig. 5-12. In order to best qualify the performance of the exoskeleton in providing mobility on slopes, this paper presents the aforementioned mobility and exertion measures for slopes for four mobility aid combinations, which include 1) the Vanderbilt powered lower limb exoskeleton with a walker; 2) the Vanderbilt powered lower limb exoskeleton with forearm crutches; 3) a set of long-leg braces with a walker, using a swing-through type gait; and 4) a set of long-leg braces with a walker, using a reciprocal type gait. Long-leg braces are the most common legged mobility aids used by persons with paraplegia. These braces consist of a thigh segment, shank segment, and integrated shoe for each leg. The knee joint of each leg consists of a latching hinge joint, such that the joint can remain flexed while donning or sitting, but mechanically locks at full extension, and remains locked during use.

In order to standardize exertion measurement, the subject's heart rate was taken exactly one minute prior to the start of each TUG test, and exactly 30 sec following each TUG test. The heart rate measurement was taken with an automated monitor (Dynamap V100 by General Electric), which required approximately 20 sec from initiation (i.e., donning of finger clip) to

measurement. Specifically, the TUG test was initiated 60 sec after reporting the subject's heart rate, while heart rate measurement was initiated 30 sec after TUG test completion (and as such the heart rate measurement following each TUG test was reported approximately 50 sec after completion of the test). The subject was allowed to practice the TUG test until he felt comfortable performing it. Once the subject was comfortable performing the TUG test, the test and associated heart rate and perceived exertion measurements were performed three consecutive times. The subject was allowed a period of rest between each test, until he felt rested and ready to perform the next test.



Fig. 5-12. Setup for Sloped TUG Test: a stationary chair followed by one meter of level surface, followed by three meters at 5 degree incline, followed by level surface sufficiently large to allow subject to turn 180 degrees.

Results of Slope Walking Experiments

The results of the slope-walking assessment for each of the four cases of ambulation are summarized in Table 5-1. For each of the four cases of ambulation, the table lists the average Sloped TUG test time (in seconds) and corresponding standard deviation (in parentheses) for the three TUG trials; the average change in pre- and post-test heart rate, and associated standard deviation across the three trials; and the subject's rating of perceived exertion corresponding to the assessment in each ambulation case. The average Sloped TUG completion times for each mobility aid case, bracketed by plus and minus one standard deviation, are shown graphically in Fig. 5-13. The average changes in heart rate for the Sloped TUG tests are summarized graphically in Fig. 5-14. A single-degree-of-freedom analysis of variance (ANOVA) was conducted to assess the extent to which the mean measurement of completion time and percent heart rate change was significantly different (with a 90% confidence level) between the four cases of ambulation. It was shown that slope ambulation with the exoskeleton using forearm crutches for stability was significantly slower than either case of ambulation with long leg braces. Ambulation with the exoskeleton using a walker for stability was significantly faster than with crutches, however, and was not statistically slower than reciprocal walking with long leg braces. Regarding exertion, both cases of slope walking with the exoskeleton were shown to require significantly less exertion than either case of long leg brace walking (with 90% confidence for the exoskeleton/walker combination and 88% confidence for the exoskeleton/crutches combination). These measurements are reinforced by the subject's reported Borg perceived exertion ratings. These ratings are shown graphically in Fig. 5-15 and show that the subject perceived both cases of walking in the exoskeleton to require less exertion than either case of walking with long leg braces. The combination of the exoskeleton with forearm crutches received the lowest exertion rating: 13, which corresponds to "somewhat hard" exercise, but it still feels OK to continue." In contrast, performing the Sloped TUG test with reciprocal walking in long leg braces received the highest exertion rating: 18, which falls between 17 ("Very hard"; very strenuous. A healthy person can still go on, but he or she really has to push him- or herself. It feels very heavy, and the person is very

tired) and 19 (An extremely strenuous exercise level. For most people this is the most strenuous exercise they have ever experienced).

Walking Method	TUG Time (seconds)	Heart Rate Change (%)	BORG Perceived Exertion
LL Braces + Walker (Reciprocal)	139 (8)	31.8 (13.6)	18
LL Braces + Walker (Swing-Through)	117 (6)	28.6 (4.3)	16
Exoskeleton + Walker	147 (10)	-3.1 (5.3)	15
Exoskeleton + Forearm Crutches	173 (7)	11.5 (4.9)	13

Table. 5-1. Summary of slope assessment data. Results are average and (standard deviation) of three trials.

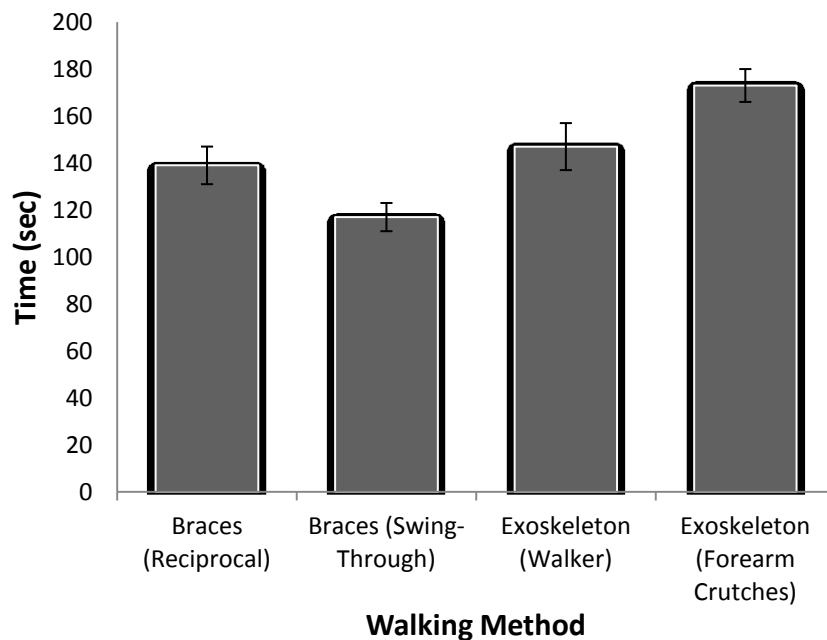


Fig. 5-13. Graph of sloped TUG test completion times in each walking method.

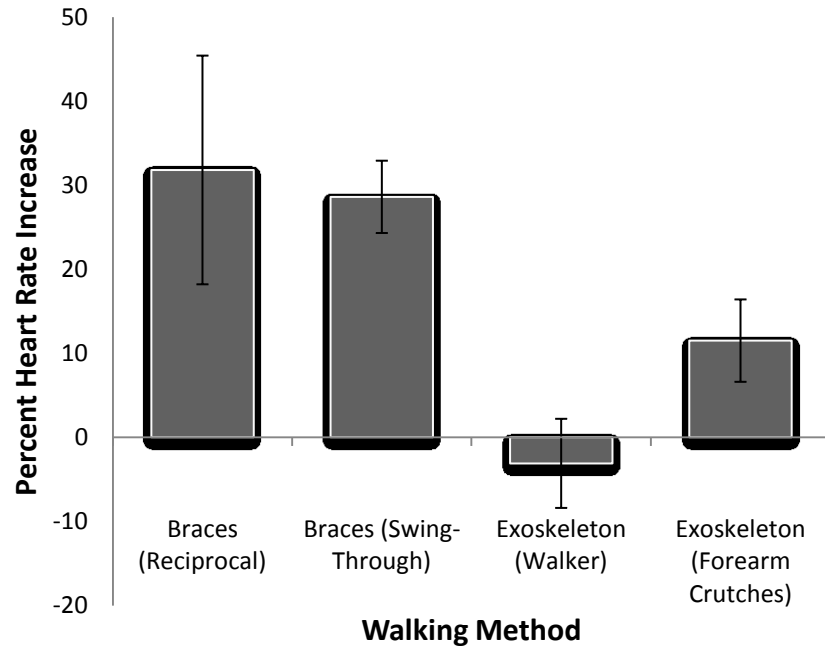


Fig. 5-14. Graph of user exertion during sloped TUG test in each walking method.

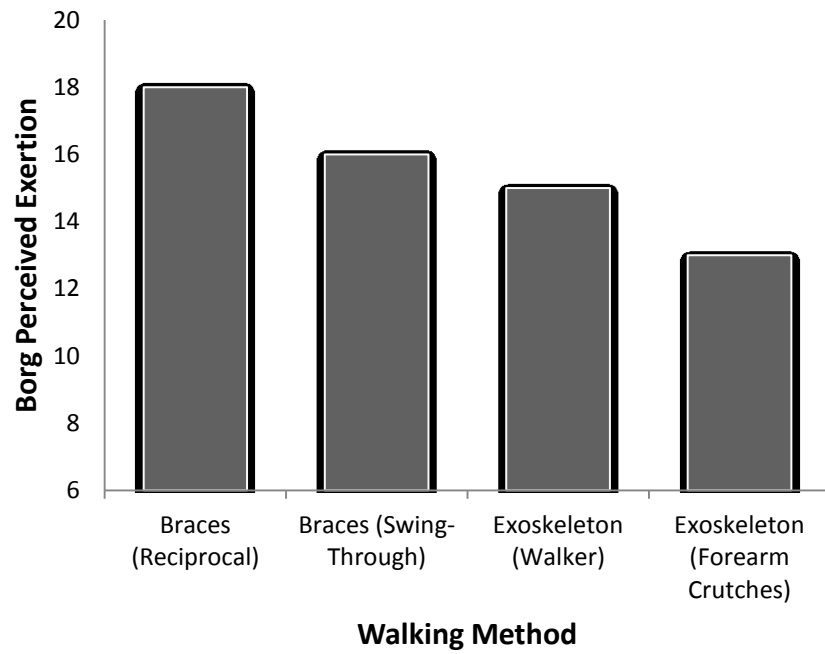


Fig. 5-15. Graph of user perceived exertion during sloped TUG test in each walking method. Note that the Borg Scale ranges from 6 ("no exertion") to 20 ("maximal exertion").

Addendum References

- [1] McIntosh, A. S., Beatty, K. T., Dwan, L. N., and Vickers, D. R., "Gait dynamics on an inclined walkway," *Journal of Biomechanics*, vol. 39, pp. 2491-2502, 2006.
- [2] Slope and Rise, A. A. Guidelines, 2002.
- [3] Lam, T., Noonan, V. K., and Eng, J. J., "A systematic review of functional ambulation outcome measures in spinal cord injury," *Spinal Cord*, vol. 46, pp. 246-254, 2007.
- [4] Podsiadlo, D. and Richardson, S., "The timed "Up & Go": a test of basic functional mobility for frail elderly persons," *J Am Geriatr Soc*, vol. 39, pp. 142-148, 1991
- [5] Hughes, C., Osman, C., and Woods, A. K., "Relationship among performance on stair ambulation, functional reach, and Timed Up and Go tests in older adults," *Issues on Aging*, vol. 21, pp. 18-22, 1998.
- [6] Morris, S., Morris, M. E., and Iansek, R., "Reliability of Measurements Obtained With the Timed "Up & Go" Test in People With Parkinson Disease," *Physical Therapy*, vol. 81, pp. 810-818, February 2001 2001.
- [7] Schoppen, T., Boonstra, A., Groothoff, J. W., de Vries, J., Göeken, L. N. H., and Eisma, W. H., "The timed "up and go" test: Reliability and validity in persons with unilateral lower limb amputation," *Archives of physical medicine and rehabilitation*, vol. 80, pp. 825-828, 1999.
- [8] Shumway-Cook, A., Brauer, S., and Woollacott, M., "Predicting the Probability for Falls in Community-Dwelling Older Adults Using the Timed Up & Go Test," *Physical Therapy*, vol. 80, pp. 896-903, September 2000.
- [9] Thompson, M. and Medley, A., "Performance of individuals with Parkinson's disease on the Timed Up & Go," *Neurology Report*, vol. 22, pp. 16-21, 1998.
- [10] Borg, G. A. V., "Psychophysical bases of perceived exertion," *Medicine and Science in Sports and Exercise*, vol. 14, pp. 377-381, 1982.

CHAPTER VI

Conclusion

This work describes the design and implementation of a powered lower limb orthosis for providing legged mobility to the SCI population. The main contributions of this work, as presented in the four prior manuscripts, are as follows.

Manuscript 1: Preliminary Evaluation of a Powered Lower Limb Orthosis to Aid Walking in Paraplegic Individuals

- A mechanical and electrical design for a light-weight, low-profile, electrically powered lower limb orthosis with onboard power, sensing elements, and DC motor actuated joints.
- The electrical and mechanical power specifications for an active lower limb orthosis that can provide ambulation to a complete paraplegic.
- Validation of the orthosis for over ground walking on a T10 complete paraplegic subject.

Manuscript 2: A Method for the Autonomous Control of a Lower Limb Exoskeleton for Persons with Paraplegia

- An intuitive user control interface for sitting, standing, and walking movements, which are controlled by changes in the user's center of pressure, as determined by on-board sensing.
- An embedded system architecture to enable tethered operation of a lower limb orthosis with onboard computation, signal processing, power management, with high level control handled remotely.
- A general two level control architecture for powered lower limb orthosis. The high level supervisory controller, which is the intent recognizer and state machine, infers the user's intent based on the interaction between the user and the orthosis, and determines the corresponding appropriate state changes. The high level controller also sends the appropriate joint

trajectories and controller gains to the low level controllers. The low level controllers are the closed-loop joint torque controllers.

- Validation of the postural control methodology for sitting, standing, and level-ground walking with a T10 complete paraplegic subject.

Manuscript 3: A Preliminary Assessment of Mobility and Exertion in a Lower Limb Exoskeleton for Persons with Paraplegia

- A proposed assessment protocol for assessing the mobility and exertion associated with systems that provide legged mobility assistance for persons with SCI. This protocol is based on the use of the timed-up-and-go (TUG) test and the ten-meter-walk-test (TMWT) for assessing mobility and percent change in heart rate and Borg rating of perceived exertion for assessing exertion.
- Implementation of the assessment protocol on a single SCI subject with results indicating that the Vanderbilt powered exoskeleton affords similar mobility and requires a somewhat lower level of exertion relative to long-leg braces with a swing-through gain, and affords significantly improved mobility with significantly less exertion relative to long-leg braces with a reciprocal gait.

Manuscript 4: Joint Torque and Power Requirements during Stair Ascent and Descent in a Lower Limb Exoskeleton for Persons with Paraplegia

- Stair ascent and descent functionality demonstrated in a powered lower-limb exoskeleton.
- An analysis of joint torque and power data from paraplegic stair ascent and descent presenting maximum joint torque and power as a design criteria for exoskeletons in general.

All aspects of the exoskeleton have been developed with a focus on user acceptance and commercialization. The mechanical system has been designed to be lightweight and low-profile while still providing the high joint torques necessary for stair climbing and the high joint speeds necessary for natural knee flexion during walking. The control structure provides an intuitive

interface between the user and the exoskeleton for ease of use with a minimal learning curve. It is hoped that this body of work will continue to mature and offer improved quality of life to those who have experienced spinal cord injury.